Quantification of C-type lectin receptors signal transduction

Inaugural-Dissertation

to obtain the academic degree

Doctor rerum naturalium (Dr. rer. nat.)

submitted to the Department of Biology, Chemistry, Pharmacy of

Freie Universität Berlin

by Felix Franz Robert Fuchsberger

from Wien, Austria

March 2021

The majority of experiments described in this thesis was performed at the Max-Planck-Institute of Colloids and Interfaces and a minor part at the University of Vienna, both in the group of Prof. Dr. Rademacher from October 2017 to March 2021. I declare that this dissertation is an original report of my research and has been finished by myself. All contributions from colleagues and collaborators have been indicated clearly and acknowledged.

First Reviewer: Prof. Dr. Christoph Rademacher
Second Reviewer: Prof. Dr. Oliver Daumke

Disputation date: 25.05.2021

Table of Contents

1. Associated Information

1.1 Publications

Parts of this work are or will be published and communicated in the following forms:

Peer-reviewed publications:

Aretz, J., Anumala, U. R., **Fuchsberger, F. F.**, Molavi, N., Ziebart, N., Zhang, H., Nazaré, M., & Rademacher, C. (2018). Allosteric Inhibition of a Mammalian Lectin. Journal of the American Chemical Society. https://doi.org/10.1021/jacs.8b08644

Bachem, G., Wamhoff, E.-C., Silberreis, K., Kim, D., Baukmann, H., **Fuchsberger, F.**, Dernedde, J., Rademacher, C., & Seitz, O. (2020). Amplifying the chelate effect as rational approach to a DNA-scaffolded high affinity binder for Langerin. Angewandte Chemie International Edition. https://doi.org/10.1002/anie.202006880

Bhattacherjee, A., Rodrigues, E., Jung, J., Luzentales-Simpson, M., Enterina, J. R., Galleguillos, D., St. Laurent, C. D., Nakhaei-Nejad, M., **Fuchsberger, F. F.**, Streith, L., Wang, Q., Kawasaki, N., Duan, S., Bains, A., Paulson, J. C., Rademacher, C., Giuliani, F., Sipione, S., & Macauley, M. S. (2019). Repression of phagocytosis by human CD33 is not conserved with mouse CD33. Communications Biology. https://doi.org/10.1038/s42003-019-0698-6

Hendriks, A., van Dalen, R., Ali, S., Gerlach, D., van der Marel, G. A., Fuchsberger, F. F., Aerts, P. C., de Haas, C. J. C., Peschel, A., Rademacher, C., van Strijp, J. A. G., Codée, J. D. C., & van Sorge, N. M. (2021). Impact of Glycan Linkage to Staphylococcus aureus Wall Teichoic Acid on Langerin Recognition and Langerhans Cell Activation. ACS Infectious Diseases, acsinfecdis.0c00822. https://doi.org/10.1021/acsinfecdis.0c00822

Mende, M., Tsouka, A., Heidepriem, J., Paris, G., Mattes, D. S., Eickelmann, S., Bordoni, V., Wawrzinek, R., **Fuchsberger, F. F.**, Seeberger, P. H., Rademacher, C., Delbianco, M., Mallagaray, A., & Loeffler, F. F. (2020). On-Chip Neo-Glycopeptide Synthesis for Multivalent Glycan Presentation. Chemistry - A European Journal. https://doi.org/10.1002/chem.202001291

Schulze, J., Baukmann, H., Wawrzinek, R., **Fuchsberger, F. F.**, Specker, E., Aretz, J., Nazaré, M., & Rademacher, C. (2018). CellFy: A Cell-Based Fragment Screen against C-Type Lectins. ACS Chemical Biology. https://doi.org/10.1021/acschembio.8b00875

van Dalen, R., Diaz, J. S. d. la C., Rumpret, M., **Fuchsberger, F. F.**, van Teijlingen, N. H., Hanske, J., Rademacher, C., Geijtenbeek, T. B. H., van Strijp, J. A. G., Weidenmaier, C., Peschel, A., Kaplan, D. H., &

van Sorge, N. M. (2019). Langerhans cells sense Staphylococcus aureus wall teichoic acid through langerin to induce inflammatory responses. MBio. https://doi.org/10.1128/mBio.00330-19

van Dalen, R., **Fuchsberger, F. F.**, Rademacher, C., Van Strijp, J. A. G., & Van Sorge, N. M. (2020). A Common Genetic Variation in Langerin (CD207) Compromises Cellular Uptake of Staphylococcus aureus. Journal of Innate Immunity. https://doi.org/10.1159/000500547

Wamhoff, E. C., Schulze, J., Bellmann, L., Rentzsch, M., Bachem, G., **Fuchsberger, F. F.**, Rademacher, J., Hermann, M., Del Frari, B., Van Dalen, R., Hartmann, D., Van Sorge, N. M., Seitz, O., Stoitzner, P., & Rademacher, C. (2019). A Specific, Glycomimetic Langerin Ligand for Human Langerhans Cell Targeting. ACS Central Science, 5(5), 808–820. https://doi.org/10.1021/acscentsci.9b00093

Felix F. Fuchsberger, Dongyoon Kim, Marten Kagelmacher, Robert Wawrzinek, Christoph Rademacher. Information transfer in mammalian glycan-based communication. *Submitted*

Mareike Rentzsch, Robert Wawrzinek, Lydia Bellmann, **Felix F. Fuchsberger**, Jessica Schulze, Jil Busmann, Juliane Rademacher, Claudia Zelle-Rieser, Patrizia Stoitzner, Christoph Rademacher. Specific Protein Antigen Delivery to Human Langerhans Cells in Intact Skin. *Submitted*

Mareike Rentzsch, Robert Wawrzinek, Nowras Rahhal, **Felix F. Fuchsberger**, Dongyoon Kim, Jessica Schulze, Christoph Rademacher. Targeted delivery of mRNA via Langerin. *Manuscript in preparation*

Posters:

Eurocarb XX, “A Message-Receiver Model for Glycan Based Cell-Cell Communication” Leiden 2019

7th International mRNA Health Conference, “Targeted delivery of nucleic acids via C-type lectin receptors” Berlin 2019

1.2 Acknowledgements

I thank the ERC for funding this thesis as part of the GLYCONOISE ERC starting grant. I thank the University of Vienna, the Free University Berlin, and the Max-Planck-Institute of Colloids and Interfaces for providing an excellent work environment. I also thank Max Planck Society for support and Prof. Dr. Peter H. Seeberger for helpful discussions and the Deutsches Rheuma Forschungszentrum (DRFZ) for providing access to their cell sorting facility. I further thank Prof. Dr. Bjørn Christensen, Amalie Solberg, and Dr. Ingrid Vikøren Mo for a great collaboration on dectin-1. I thank Prof. Dr. Oliver Seitz and Dr. Gunnar Bachem for collaborating on Langerin. Dr. Matt Macauley and Dr. Abhishek Bhattacherjee I thank for our collaboration on CD33. Dr. Nina van Sorge and Dr. Rob van Dalen have my uttermost gratitude for continued fruitful projects on Langerin. Dr. Robb de Vries and his lab for a cool collaboration on Hemagglutinin. Prof. Dr. Walter Jäger, Dr. Florian Kopp, Dr. Manfreg Ogris, Dr. Haider Sami, Daniela Krizan, Susanne Wiederkum for a warm welcome at the University of Vienna.

I wish to thank all colleagues in these last years, in particular:

Ignacio Alvarez-Martinez, for his friendship and Baba Ghanoush, both excellent eeeeh! Dr. Colin Ruprecht, for his subtitle yet infectious cheerfulness in the lab and beyond. Dr. Marco Mende, for greeting with *Servus!* in a vast sea of *Tag!* and *MoinMoin*. Benjamin König and Grigori Paris for teaching me about polar coordinates. My students that became masters since: Nowras Rahhal and Marten Kagelmacher for their time, energy, and thinking outside of the/my box. Elena Shanina, for her snarky comments and sharp wit. Mareike Rentzsch, for her unwavering stance in the name of science. Dr. Robert *Waffel* Wawrzinek, for being a jolly good chap and blazing the trail. Dr. Maxime Denis, I won't thank for killing Haley's Wolf even if it was *au service de la france*. Dr. Dongyoon Kim, I wish to thank for his deep Einsteinian thinking and sudden dark humour. Dr. Iris Bermejo, for loving cordon bleu and certainly not being the imposter among us. Hen-Xi Zhang, for her refreshing innocence and utter dedication. Jonathan Lefèbre, for his precise and smart questions. I thank Dr. Jonas Aretz, Dr. Jonas Hanske, Dr. Eike Wamhoff, Dr. Jessica Schultze, Hannes Baukmann, and Dr. Natalia Baranova, for their instruction, guidance, and example.

I also wish to thank my family and friends for their support, and Haley Baptist for being a reassuring light in dark times. Finally, I thank Prof. Dr. Christoph Rademacher for his profound guidance, mentor- and leadership in these last few years: "these are the good old days".

2. Summary

Ubiquitous glycans facilitate a plethora of important interactions namely cancer-host, host-pathogen, host-self interactions. Interaction with theses carbohydrates is enabled by lectins and the effects of these interactions can range from redundant to essential. Lectins are exposed on mammalian cell surfaces where they identify the information encoded in glycans and transfer it into signal transduction pathways. Such signal transduction pathways are complex and difficult to analyse. However, quantitative data with single cell resolution provides means to disentangle the associated signalling cascades. C-Type lectin receptors (CLRs) expressed on immune cells were chosen as a model system to study their capacity to transmit information encoded in glycans of incoming particles. To this end, monocytic cell lines cell lines expressing DC-SIGN, MCL, dectin-1, dectin-2, and mincle, as well as TNFAR and TLR-1&2 were established. Based on the study of Cheong *et al.*, 2011 the amount of transmitted information was quantified by following NFκB dependent GFP expression. While most receptors did have a channel capacity of at least 1 bit, it was found that dectin-2 has a lower capacity to transmit information than other lectins. Especially the comparison to the related lectin mincle is interesting, since mincle uses the same pathway effectively. Furthermore, information transmission of dectin-2 could not be enhanced by other lectins or signalling molecules. Yet upon closer analysis it was found that the sensitivity of the dectin-2 signal transduction pathway can be enhanced by overexpression of its co-receptor FcRγ, but surprisingly its transmitted information cannot. Moreover, it was suggested how potential autoimmunity might be a cause for dectin-2's inefficient signalling. The question of signal integration was also approached: How do cells combine the flow of information from multiple receptors? It was shown that the signal of dectin-2 and dectin-1 are being integrated as a compromise between both receptors. The reason for this compromise might be the activity of the phosphoprotein SYK, present in both dectin-1 and dectin-2 signal transduction pathways.

By using the established assays and cell lines, soluble beta glucans (SBGs) were discovered to be potent stimulators of dectin-1, where sensitivity to the SBGs was highly variable and dependent on their β-glucan side chains. Various different ligands for mincle on the other hand resulted in a similar signalling behaviour. Building on insight in targeted delivery to lectins, it was shown how nucleic acids can be delivered to Langerin expressing cells and used to reprogramme the cells, a technology of tremendous potential for vaccination strategies and (non-germline) genetic editing.

Taken together, the concepts of information theory with single cell resolved data enabled the quantification of CLRs signalling behaviour and signal integration. By using dectin-2 and other lectins as example it was demonstrated how the receptor itself determine the efficiency and therefore outcome of the signal transduction pathways. Moreover, the potential to explore glycan lectins interactions in drug targeting was exemplified by delivering mRNA *via* Langerin or demonstrating the dependency of dectin-1 sensitivity upon the β-glucan side chains of its ligands.

2.1 Deutsche Zusammenfassung

Glykane sind allgegenwärtig und in eine Vielzahl wichtiger Interaktionen involviert nämlich Wirt-Pathogen, Wirt-Krebs, sowie Interaktionen innerhalb des Wirtes. Lektine sind Proteine, welche darauf spezialisiert sind, solche Interaktionen durchzuführen. Während manche Lektine essenzielle Rollen innehaben, können andere redundant sein. Lekte werden oftmals als Oberflächenrezeptoren der Zelle exprimiert, hier leiten sie die in Glykanen enthaltenen Information an intrazelluläre Signaltransduktionswege weiter. Diese Signaltransduktionswege sind oft kompliziert und schwer zu analysieren. Doch mit Daten in Einzelzell-Auflösung ist es möglich diese Signaltransduktionswege zu entwirren. Als Modell hierfür wurden in Immunzellen exprimierte C-typ-Lektine gewählt und deren Kapazität die in Glykanen enthaltenen Information zu transferieren analysiert. Die Lektin-Rezeptoren DC-SIGN, MCL, Dectin-1, Dectin-2, Mincle, sowie Rezeptoren TNFAR und TLR-1&2 exprimiert in Monozytischen Zelllinien THP-1 und U937 wurden hierzu verwendet. Basierend auf der Arbeit von Cheong et al., 2011 wurde die transferierte Information mittels NFκB abhängiger GFP Expression quantifiziert. Während die meisten Rezeptoren Kanalkapazitäten von mindestens 1 bit hatten, so transferierte Dectin-2 weniger als 1 bit an maximaler Information. Besonders der Vergleich mit Mincle ist hier interessant, da Dectin-2 und Mincle denselben Signaltransduktionsweg verwenden, jedoch mit unterschiedlicher Kanalkapazität. Weiters wurde entdeckt, dass die von dectin-2 transferierte Information nicht durch die Expression eines Adaptermoleküls oder synergistischer Lektine erhöht werden konnte. Die Sensitivität von dectin-2 konnte dadurch allerdings schon erhöht werden. Eine mögliche Erklärung für die anscheinende Ineffektivität des dectin-2 Lektins konnte in potenzieller Autoimmunität gefunden werden. Die Frage nach dem Mechanismus der Signalintegration wurde auch erforscht: Wie werden mehrere aktivierte Signaltransduktionswege innerhalb einer Zelle kombiniert? In dieser Hinsicht wurde gezeigt, dass die Information von dectin-2 und dectin-1 als Kompromiss zwischen

den beiden aufgenommen wird. Mechanistisch ist es möglich, dass dieser Kompromiss durch das Phosphoprotein SYK vermittelt wird. Weiters wurden lösliche beta-Glukane als potenzielle Liganden für Dectin-1 erforscht. Hier wurde entdeckt, dass die Ligandendichte oder die Länge der beta-Glukan Seitenketten starken Einfluss auf die Sensitivität des Dectin-1 Rezeptors hatte. Außerdem wurde gezeigt, dass es möglich ist Langerin exprimierende Zellen durch die gezielte Gabe von Nukleinsäuren zu reprogrammieren, eine Technologie die viel medizinisches und biotechnologisches Potential hat.

Zusammengefasst ermöglichte die Kombination von Informationstheorie mit Daten in Einzelzell-Auflösung die genaue Quantifikation von Signaltransduktion und Signalintegration. Dectin-2 und weitere Lektine wurden verwendet um zu zeigen, dass der Rezeptor selbst die Effizient des nachgeschalteten Informationskanals bestimmt. Außerdem konnte das Potential in der Erforschung von Glykan-Lektin Interaktionen anhand von Langerin und Dectin-1 für biotechnologische demonstriert werden.

2.2 List of Abbreviations

Alexa647	Alexa Fluor 647 dye
BCR	B-cell receptor
BSA	Bovine serum albumin
CC	Channel capacity
CD	Cluster of differentiation
CLR	C-type lectin receptor
CRD	Carbohydrate recognition domain
CTLD	C-type lectin like domain
Cy5	Cyanin5 Dye
DAMP	Damage associated molecular pattern
DC-SIGN	Dendritic Cell - Specific ICAM3 Grabbing Non-integrin
dectin-1	Dendritic Cell-associated C-type Lectin 1
dectin-2	Dendritic Cell-associated C-type Lectin 2
Dlin	DLin-MC3-DMA
DLS	Dynamic light scattering
DMSO	Dimethylsulfoxid
DNA/cDNA	Deoxyribonucleic acid/ complementary deoxyribonucleic acid
DPBS	Dulbecco's phosphate-buffered saline
ECD	Extra cellular domain
EDEM	ER degradation-enhancing α-mannosidase-like
EDTA	Ethylenediamintetraacetic acid
ERK	Extracellular signal-regulated kinases
FcRγ	Fc Receptor Gamma-Chain
FI	Fluorescence intensity
FP	Fluorescent protein
FSC	Forward scatter
Fuc	Fucose
Gal	Galactose
GalNAc	N-Acetyl galactosamine
GFP	Green fluorescent protein
GlcNAc	N-Acetyl glucosamine
GOI	Gene of interest
GTases	glycosyltransferase
HEK	Human embryonic kidney
ITAM	Immunoreceptor tyrosine-based activation motif
ITIM	Immunoreceptor tyrosine-based inhibition motif
LNPs	Lipid nanoparticles
Man	Mannose
Man-LAM	Mannose-capped LAM

MBL	Mannose binding lectin
MCL	Macrophage inducible C-type lectin
MFI	Mean fluorescence intensity
MGL	Macrophage galactose lectin
MHC	Major histocompatibility complex
mincle	Macrophage inducible C-type lectin
mRNA	Messenger RNA
muLCs	MUTZ-3 Langerhans cells
MW	Molecular weight
NFκB	Nuclear factor 'kappa-light-chain-enhancer' of activated B-cells
PAMP	Pathogen associated molecular pattern
SBG	Soluble β-glucans
SD	Standard deviation
SEC	Size exclusion chromatography
Siglec-3	Sialic acid binding Ig-like lectin 3
SNPs	Single nucleotide polymorphisms
STAT1	Signal transducer and activator of transcription 1
SYK	Spleen tyrosine kinase
TDB	Trehalose-6,6-dibehenate
TDM	Trehalose dimycolate
TLR	Toll-like receptor
TNF-α	Tumour necrosis factor alpha
wt	Wild type
WTA	Wall teichoic acid

3. Introduction

The primary source of information in biology stems from the genetic code, mRNA and proteins are direct products of it. Glycans on the other hand are secondary gene products, they are not directly encoded by DNA, but are made by a multitude of enzymes. The enzymes are in turn proteins directly encoded by the DNA, therefore primary gene products. This makes research in glycobiology very challenging. Glycans are ubiquitous and present on all living cells. They cover the cellular surface in a dense layer, the glycocalyx. While glycans and the glycocalyx also serve structural purposes, they do just as proteins encode for ligands, which are recognized by receptors to trigger specific biochemical reactions. The proteins that are mainly tasked with the recognition of glycans are known as lectins. Glycan lectin interactions transfer a wide range of information. For example, tumour cells can initiate metastasis and promote dissociation from their initial tissue by upregulating sialylated glycans (Fuster and Esko, 2005; Woods *et al.*, 2017). Also a change in N-glycosylation enables recognition by Galectin-1 which then triggers angiogenesis in vascular cells, a mechanism which is also used by tumours (Croci *et al.*, 2014). For a long time, it was thought these tumour associated changes of glycans were a mere by-product of the disease, from the mentioned examples it should however become clear that such changes are driven by purpose.

Glycans also play important roles in protein function and modification. Slight variation in protein glycosylation can enhance or weaken protein-protein as well as protein-drug interactions (Wu *et al.*, 2018). It should therefore not come as a surprise, that the glycosylation of proteins used in biopharmaceutical products are required to be well characterized. Glycan lectin interactions are also essential in various other processes. Mincle for example one of many glycan binding pathogen recognition receptors not only probes for pathogen associated molecular patterns (PAMPs), but also for self-damage in the form of damage associated molecular patters (DAMPs) (Miyake, Oh-hora and Yamasaki, 2015; Williams, 2017). These examples should demonstrate that glycans and their interactions play integral parts in many fields and applications of biology.

How information is encoded in and decoded from glycans as a whole, is however challenging since hundreds of different glycans are present in different forms such as glycoproteins and -lipids. At the same time, the cell cannot alter a single glycoprotein but rather changes the glycosylation machinery, hence affecting multiple parts of the glycome (Cummings, 2009). Moreover, the interplay between glycans and their readers the lectins is complicated by the lack of specificity. There is no glycan being

only recognized by one lectin and there is no lectin that is highly specific for a single given glycan. Additionally, affinities are low and recognition is often dictated by abundancy and multivalency effects. Overall, the change or presence of a single glycan alone will often not lead to massive changes in glycan lectin interactions and its associated cellular signal transduction pathways. Therefore, these interactions should be viewed with single cell resolution of a cellular population to catch smaller effects of mere stochastic rather than deterministic proportions. Suppose a certain glycans is being overexpressed by upregulation of the associated glycosylation machinery. This glycan could then in turn slightly activate a signalling pathway, which would for example only changes the state of 15% of the surrounding cells on average. Such a small effect could only be quantified by a single cell resolved method, which ideally also measures enough cells to have a statistically robust sample size. Thus, the quantification of lectins signalling pathways in particular call for analysis with single cell resolved methods.

3.1 Importance of the glyco-code

Glycans, just like proteins and nucleic acids are carrier of biological information, a fact already noted when the first carbohydrate recognizing lectins were discovered and researched in the 1980s (Drickamer, 1988). Whereas the protein and nucleic acid code is straightforward, linear, clear translation between the two, the glyco-code is much more complex and enigmatic. In a given triplet of either biomolecule for example: the nucleic acid comes with 4^3 possible sequences, due to the four bases. A peptide triplet could come in 20^3 sequences (=8000), assuming the classic 20 amino acids. If the 75 monosaccharides that the consortium for function glycomics currently has a symbol assigned to are considered, the glycan triplet could potentially come with 75^3 different isomers. But this argument is exaggerated since mammals for example only use 10 different monosaccharides: mannose, fucose, glucose, N-acetyl-glucosamine (GlcNAc), glucuronic acid, sialic acid, galactose, N-acetyl-galactosamine (GalNAc), xylose, and iduronic acid (IdoA). However the glyco-code is not limited by being linear, humans for example can link carbohydrates in eight different linkages (Cummings, 2009). Additionally all of these can be α/β isomers (Šebestík, Reiniš and Ježek, 2012). The number of possible isomers of a mammalian trisaccharide was calculated to be 126,080 (Werz *et al.*, 2007). We can therefore confidently judge the glyco-code to have the highest (theoretical) information density. The high density of information potentially encoded within glycans also brings with it a highly complex field to study. Thus, glycobiology and the study of glycoconjugates has been studies less extensively, when compared to

other fields such as proteomics and genomics (Gabius, 2015). In recent years however, a growing interest in the potential of glycans as well as refined techniques have uncovered many exciting findings, in the field of tumour immunology for example:

We now know that during malignant transformation of tumours the many changes in their glycosylation pattern are neither random nor simply a by-product of their transformation. Integrins expressed by tumour cells are often over-glycosylated with branched tetra-antennary N-glycan structures, promoting dissociation of tumours from their current environment, thus helping metastasis (Mehta *et al.*, 2012). Truncated O-glycans as well as increased sialyation are also associated with similar processes (Pinho and Reis, 2015). Three commonly found tumour associated glycans (*e.g.* Sialyl T or Tn antigens, terminal GalNAc glycans, and fucosylated Lewis X or Y antigens) are bound by the Siglec (sialic acid binding Ig-like lectin) family, MGL, and DC-SIGN, respectively (Fig 1). Macrophages, monocytes, and dendritic cells readily express these three lectins. Although it seems counterintuitive, the binding of immune cells to tumour tissue binding can result in secretion of anti-inflammatory cytokines. Thus, this process aids cancer in evasion and manipulation of the immune system (RodrÍguez, Schetters and van Kooyk, 2018).

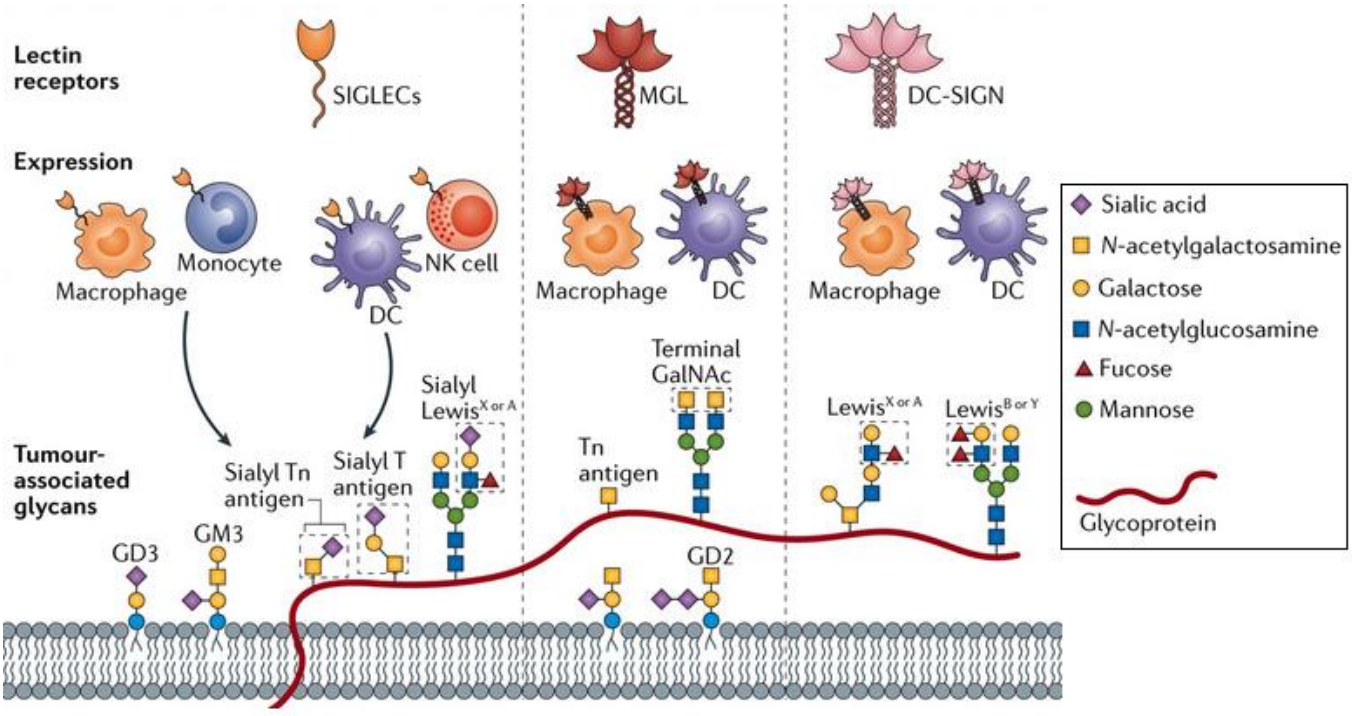

Figure 1: Schematic representation of immune evasion by tumors initiated via glycan-lectin interactions. By expression of specific tumor associated glycans, lectins are thought to attach immune cells to tumors. Shown are subsets of immune cells with lectins relevant to this process and their glycan ligands. Figure adapted from (Rodríguez, Schetters and Van Kooyk, 2018).

Besides the studies on the tumour glyco-code more than 100 gene defects in glycosylation have been found and these help with the uncovering and potential treatment of congenital disorders (Hennet and Cabalzar, 2015). Walker–Warburg syndrome for example, a autosomal-recessive inheritable muscular dystrophy, was shown to be associated with mutations of the mannosyltransferase genes POMPT1 and 2 (Beltrán-Valero de Bernabé *et al.*, 2002; van Reeuwijk, 2005). Along with other mutations these then cause the defect glycosylation of α-dystroglycan resulting in the muscular disease (Roscioli *et al.*, 2012). All of these examples emphasize the importance of glycans in various settings.

The sheer diversity of glycan that eukaryotes can synthesize is sometimes puzzling since this large repertoire of glycans made by a much smaller amount of glycosyltransferase (GTases). Especially when one considers that a given protein is synthesized in various glycoforms in a phenomenon known as microheterogeneity. The different glycoforms are then thought to provide a mean to slightly alter protein-protein affinity and function. Here a given protein is decorated with many different glycoforms, which themselves can modulate protein activity. It is therefore a requirement to determine and document the glycoforms of produced biopharmaceuticals (Stavenhagen *et al.*, 2019). A recent study by (Jaiman and Thattai, 2020) tackles the discrepancy between the glycan repertoire and the synthesising GTases. They show that by splitting up the promiscuous GTases in various Golgi compartments, the cell can generate a high amount of different glycans.

3.2 Messages of glycan-lectin interactions

The actual messages encoded by glycans are vastly different and diverse. Therefore, this section will sort them into three general categories which are 1) binding and attachment factors, 2) guiding moieties 3) signalling moieties.

Binding and attachment factors

Binding and attachment messages include cell-matrix, cell-cell, and inter-matrix interactions. In this case the lectins and glycan are simple connectors. A good example for this is the rolling of leucocytes in the bloodstream: Upon tissue damage, selectins are being expressed by the surrounding endothelial cells. These selectins then bind to ligands expressed by leukocytes, which guides them to their destination and enable their migration (Varki *et al.*, 2017). Another example is the bacterial lectin LecA in *Pseudomonas aeruginosa*, with the bacteria uses to attach and stabilize its own biofilm (Passos da Silva *et al.*, 2019). Interfering with this cell-matrix interaction is therefore a novel approach to target bacterial infections by *pseudomonas*. It should also be pointed out that in these binding processes and also other glycan lectin interactions the isomer can have tremendous impact of the binding. Langerin for example is known to recognize *Staphylococcus aureus* via GlcNAc residues on the wall teichoic acid (WTA) of the bacterium. Recently it was shown via knockout of the relevant genes that specifically the β-isomer is bound by langerin rather than α-GlcNAc (van Dalen *et al.*, 2019).

Guiding messages

In the group of guiding messages, glycans are used as tags and markers for routing in cellular processes or protein complexes. Here, the processing of protein folding is a classic example: N-glycans are being used to sort proteins for either chaperone assisted (re-)folding or mark them for degradation. EDEM (ER degradation-enhancing α-mannosidase-like) proteins are responsible for this process cleaving two mannose residues off the Man9GlcNAc2 structures present on proteins in the ER maturation process. The proteins thus marked with Man7GlcNAc2 are then being routed for degradation (Varki *et al.*, 2017). Similarly, slight differences between glycoforms of a protein can be used to fine tune protein activity in a phenomenon known as microheterogeneity. It was found recently that subtle changes, such as the addition of fucose in the N-glycans of α1-acid glycoprotein (AGP), can change its K_d for Warfarin, an anticoagulant used in vascular disease. They also found that formation of the haptoglobin–haemoglobin complex is affected by microheterogeneity between its glycoforms (Wu *et al.*, 2018).

Signalling moieties

The third category encompasses all moieties that trigger signalling pathways of any kind. Most prominent are pathogen associated signalling patterns such as α-mannans that trigger dectin-2 signal transduction (Fig 2) or β-glucans that trigger the same for dectin-1 (Goodridge, Wolf and Underhill, 2009; Feinberg *et al.*, 2017). Such signal transduction pathways typically consist of signal cascades which activate transcription factors and in turn cytokine secretion.

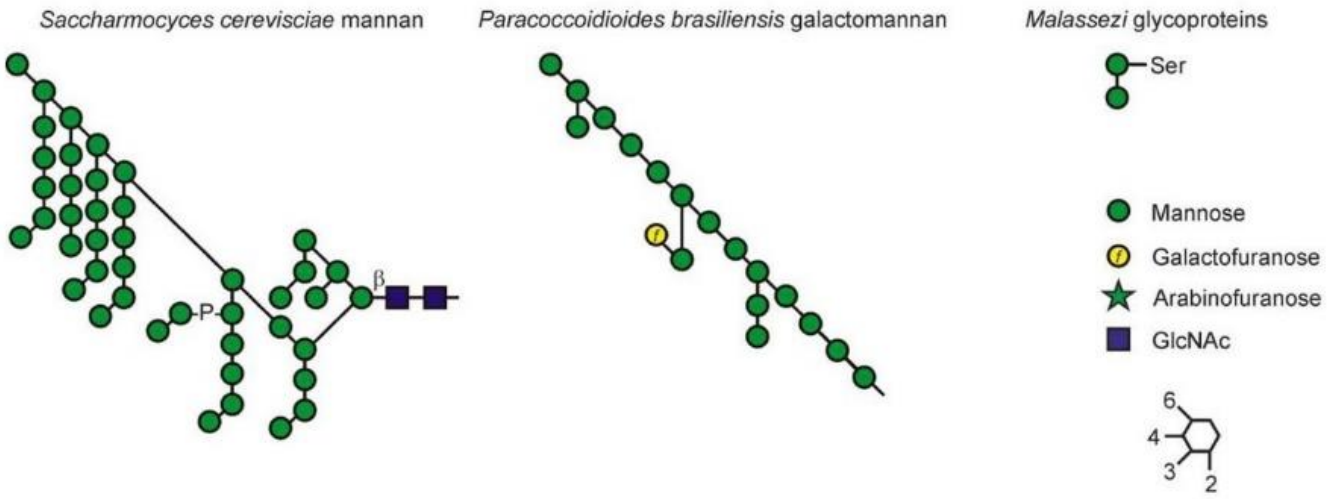

Figure 2: Examples of α-mananns recognized by dectin-2. Mannan extracted from *S. cerevisiae*, and FurFurMan a glycoprotein extract from *Malassezia furfur* are being used in this dissertation for stimulation of dectin-2. Figure adapted from Feinberg et al. 2017.

Yet signalling moieties are not necessarily always pathogen associated. Examples for self-recognition are the functions of galectins, which are multivalent galactose binding lectins, often found in self-recognition processes. Interestingly, while galectins are responsible for signalling pathways in immunity, angiogenesis, development, and apoptosis; all members of this protein family lack classic signalling domains (Varki *et al.*, 2017). However, they do initiate signalling by cross-linking proteins on the cellular surface. Human galectin-1 for example can trigger angiogenesis by cross-linking VEGF2 (Vascular endothelial growth factor receptor 2) (Croci *et al.*, 2014). Since galectin-1 itself could in this case also fall into the category of binding messages, it should be clear, that overlaps between these three categories do exist.

3.3 C-type lectins are important immune cell receptors

Within the lectin receptors, C-type lectins are the most diverse group and due to their important roles in immunology they are of significant interest in academic research and medicinal application (Spaulding *et al.*, 2017; Wamhoff *et al.*, 2019; Girotti *et al.*, 2020). Historically named for their need of Ca^{2+} as a co-factor, members of the C-type lectin family have a characteristic C-type lectin like domain (CTLD), which was first noted in (Drickamer, 1988). The distinct fold present in the carbohydrate recognition domain (CRD) consists of two disulfide bridges between two loops in the protein structure. The classic CTLD in this family of more than 1000 proteins has up to four Ca^{2+} binding sites which form hydrogen bonds with the recognized monosaccharide (Sancho and Reis e Sousa, 2012). Further features of C-type lectin receptors (CLRs) are the EPN (Glu-Pro-Asn) motif associated with binding of mannose-type carbohydrates and the QDP (Gln-Asp-Pro) triplet associated with galactose-type carbohydrates (Zelensky and Gready, 2005). The function of CLRs range from binding and adhesion of *e.g*. selectins, to the opsonization of collectins such as mannose binding lectin (MBL), to the membrane bound pattern recognition receptors (PRRs) (Varki *et al.*, 2017). Interestingly, many of the CLRs that function as PRRs are concomitantly responsible for binding endogenous ligands. DC-SIGN for instance is a PRR that also mediates cell to cell adhesion in humans (Garcia-Vallejo and van Kooyk, 2013). CLRs can be classified into 16 subcategories, according to function and structural features. Due to their expression on dendritic cells the class 2 of these subcategories houses the most prominent examples of CLR such as langerin, DC-SIGN and dectin-2. All of these are thought to have a lot of potential for biomedical applications and therefore their signalling pathways are interesting research topics.

3.3.1 Signalling of C-type lectin receptors

The simplest and quite robust way to classify the signalling of membrane bound CLRs is in three distinct groups: immunoreceptor tyrosine-based activation motif (ITAM) signalling, immunoreceptor tyrosine-based inhibition motif (ITIM) signalling, and ITAM/ITIM independent (Sancho and Reis e Sousa, 2012).

The ITAM and an ITAM-like group signal by phosphorylation of their tyrosine residues. These phosphotyrosines are then bound by signalling kinases, which further propagate the signal. This is usually facilitated by the by spleen tyrosine kinase (SYK) which binds the ITAMs phosphotyrosines residues with its SHP2 domain. Certain CLRs do not contain an ITAM themselves but rather associate with the Fc Receptor Gamma-Chain (FcRγ) to use its ITAM (Mócsai, Ruland and Tybulewicz, 2010). Mincle and dectin-2 are classic representative of this group (Kerscher, Willment and Brown, 2013).

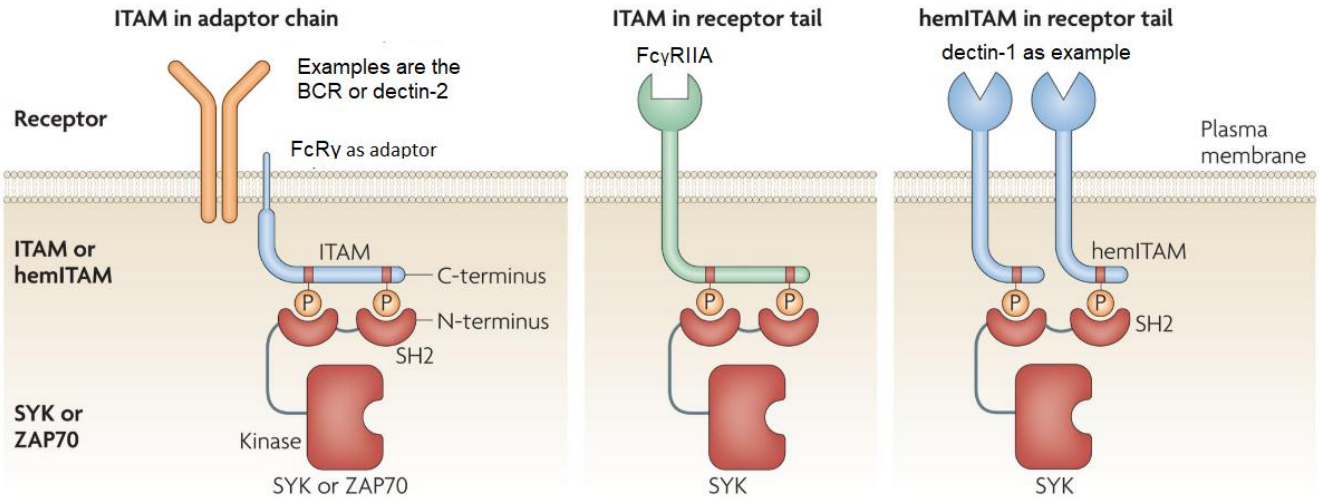

Figure 3: Different ways of ITAM usage, either by an adaptor molecule, ITAM or hemITAM in the receptors intracellular tail. ITAM or hem-ITAM domains then bind SYK or ZAP70 via phospho-tyrosines for further signal transmission. Figure adapted from Mócsai, Ruland and Tybulewicz, 2010.

The ITIM group on the other hand shut down signalling pathways by recruiting phosphatases. Members of this group are then often involved in regulation or modulation of pathways. The third category is ITAM/ITIM independent; these lectins very often do not have signal transduction pathways associated, like Langerin for example. Such lectins are then thought to either only modulate signals from other receptors or purely function as uptake receptors (Sancho and Reis e Sousa, 2012).

Since it is necessary to have an observable cellular reaction to quantify the signal of a signalling pathway, only lectins that trigger or modulate a cellular reaction could be quantified. Since this thesis is focused on signalling and information transfer, the project naturally evolved towards those signalling receptors involved in immunology. It should also be noted that the majority of data available for those lectins are derived from animal usually murine models, lectins however often have different functions in different organisms or in some cases no equivalent receptors can be found in other organisms. Therefore, only human lectins expressed in human cells were used in this thesis.

3.3.2 C-type lectins bearing ITAMs: Dectin-2 and its family

Dendritic Cell-associated C-type Lectin 2 (dectin-2) was first described more than 20 years ago and was at the time named due to an expression pattern similar to dectin-1 (Ariizumi, Shen, Shikano, Ritter, *et al.*, 2000). However, it is clear now that dectin-2 and its associated family of proteins is functionally distinct from dectin-1. While initially thought to be expressed exclusively on Langerhans cells, it is now know to be found on a variety of myeloid cells such as macrophages, neutrophils and various dendritic cell subsets (Kerscher, Willment and Brown, 2013). dectin-2 is a classic Ca^{2+}-dependent EPN containing, mannose binding CLR. It is best described as a fungal PRR for yeast like *C. albicans.* But also mannosylated lipoarabinomannan (Man-LAM) as displayed by mycobacterium tuberculosis or the yeast extract FurFurMan are being recognized by dectin-2 (Ishikawa *et al.*, 2013). Due to these ligands, dectin-2 is thought as a recognition receptor for α-mannans, well characterized ligands are Mannose α1-2 ligands, as was demonstrated in a murine model (Zhou *et al.*, 2018). Here α1-2Mannoses were used to densely decorate polystyrene beads, which could trigger the dectin-2 signalling pathway. Just like mincle dectin-2 does not contain its own signalling domain, but rather associates and uses the ITAM domain of FcRγ (Miyake, Oh-hora and Yamasaki, 2015). FcRγ then leads to activation of SYK, which in turn activates CARD9-BCL-10-Malt1 (Fig 18A). Further downstream of the pathway triggers NFκB translocation (p65 as well as p50), which ultimately results in release of cytokines (Robinson *et al.*, 2009; Bi *et al.*, 2010). Dependent on the organism different cytokines are being released. In mice and murine models IL-6, IL-23, TNF-α, as well as the anti-inflammatory IL-10 and IL-2. This is thought to promote a T_H17 response, in turn important for anti-fungal immunity (Yonekawa *et al.*, 2014; Teunis B. H. Geijtenbeek and Gringhuis, 2016). While in humans the p50 dependent release of IL-23p19 and IL-1β is confirmed, reports of dectin-2 mediated release of TNF-α and IL-1β exist, although it is not clear whether dectin-2 was responsible for these cytokines by itself (Bi *et al.*, 2010; Yonekawa *et al.*, 2014).

Soon after its discovery multiple similar receptors were discovered in relation to dectin-2, all of which are located on the chromosome 12 in humans. Among them are blood dendritic cell antigen 2 (BDCA-2), dendritic cell immunoreceptor (DCIR), as well as the more prominent mincle and MCL (Kerscher, Willment and Brown, 2013). Both dectin-2 and mincle are thought to also have a functional connection or synergy with MCL, but its exact nature is yet to be unravelled (Zhu et al., 2013; Ostrop et al., 2015). Summing up the dectin-2 family is an interesting group of receptors and their precise role and function are still under investigation.

Mincle

Macrophage inducible C-type lectin (mincle) was first described in (Matsumoto *et al.*, 1999) and was named after its inducible expression in macrophages *via* inflammatory ligands such as LPS, TNF-α, and IL-6. Evolutionary, MCL and dectin-2 are thought to have been gene duplications of mincle (Yonekawa *et al.*, 2014). It is therefore not surprising that mincle and dectin-2 share the same signal transduction pathway via FcRγ as described below in the section of dectin-2. Mincle just like dectin-2 associate with FcRγ with a conserved arginine residue in its transmembrane domain (Sato *et al.*, 2006; Yamasaki *et al.*, 2008). Interestingly while mincle is a classic CLR with a EPN motive and know to recognize mannose structures,(Yamasaki *et al.*, 2009) it mainly recognizes a group of ligands that consists of carbohydrates as well as lipophilic ligands. Mincle recognizes ligands such as trehalose dimycolate (TDM) as well as synthetic analogues such as TDB (Fig 4) and so the lectin functions as a PRR. TDM is present in the cell wall of mycobacterium tuberculosis and so is an active component of freund's adjuvant. Therefore it is not surprising that the interest in mincle stems from its ability to recognize adjuvants (Decout *et al.*, 2017). After association with FcRγ the mincle pathway runs along via SYK, CARD9-MALT1-Bcl10 which in turn activates NFκB ultimately resulting in the expression of various cytokines such as TNF-a, IL-10, IL-6, and G-CSF (Yamasaki *et al.*, 2008; Werninghaus *et al.*, 2009). While mincle serves clearly as PRR, it also is a receptor for cell damage and cell-death. In that function it senses SAP130, which is released after cellular integrity is lost, as well as aggregates of cholesterol and other sterols (Yamasaki *et al.*, 2008). Another noteworthy feature of mincle is its inducible expression. It was clearly shown in that endogenous mincle express is induced by inflammatory stimuli such as LPS or Zymosan. Additionally, the expression of MCL does enhance mincle levels, which is facilitated by formation of a heterocomplex between the two lectins. While it is currently know that MCL binds mincle for this purpose with its hydrophobic stalk, the exact molecular mechanism and effect on physiology is still being investigated (Miyake, Oh-hora and Yamasaki, 2015).

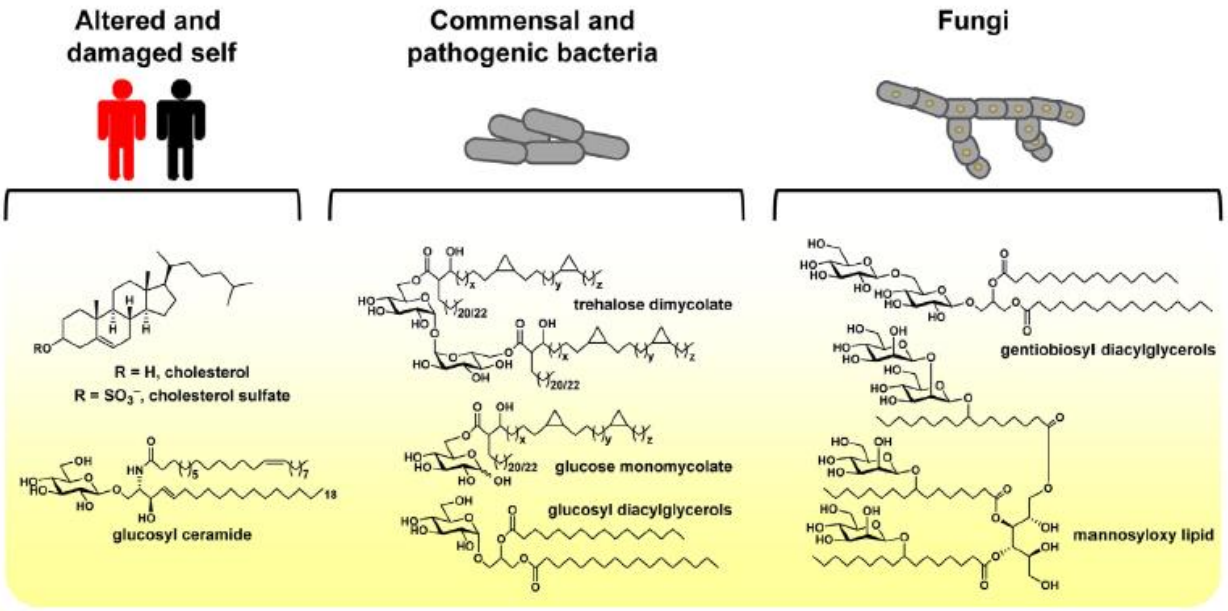

Figure 4: Origins of mincle ligands can be either from damaged self or non-self pathogens/commensals. Prominent examples are cholesterol aggregates as DAMP and TDM (Trehalose-6,6-dimycolate; cord factor) from *M. tuberculosis* as PAMP. Adapted from Williams, 2017.

MCL

Macrophage C-type lectin (MCL) also referred to as dectin-3 was first discovered in (Balch *et al.*, 1998). While MCL does fall into the same cluster as dectin-2 (Fig 5) and was shown to signal via SYK, it is neither specifically expressed on macrophages nor does it have a CLRs CRD (Graham *et al.*, 2012). While MCL is closely connected to mincle as well as dectin-2 function, it is currently not known whether MCL has ligands and function by itself. Unlike dectin-2 or mincle, MCL does not have the conserved arginine residue to associate with FcRγ; it is however thought to have various hydrophobic amino acids that facilitate the association with FcRγ, which was shown in mice and guinea pigs (Miyake *et al.*, 2013; Toyonaga, Miyake and Yamasaki, 2014). It was clearly shown that expression of MCL enhances mincle expression by interactions in the stalk region (Miyake, Oh-hora and Yamasaki, 2015). There is also evidence for various other modes in which MCL and mincle cooperate by hetero dimerization upon ligand binding. The exact mechanism of that interaction is yet to be uncovered (Ostrop and Lang, 2017). In addition, synergy and association between dectin-2 and MCL have been described in mice (Zhu *et al.*, 2013). MCL is therefore seen in a supporting role for signalling and recognition of other CLRs rather than acting on its own (Richardson and Williams, 2014).

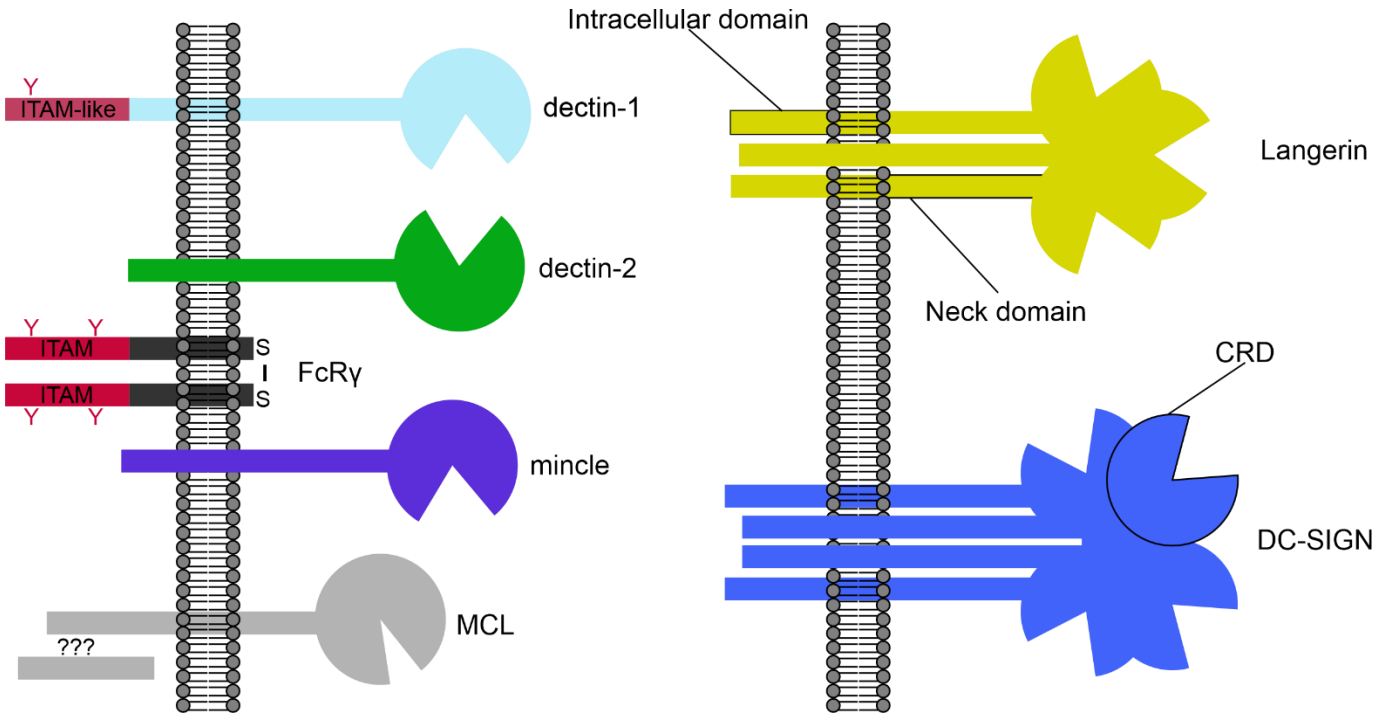

Figure 5: Schematic depiction of various CLRs, while all bear a CRD, neck, and intracellular domain, the function of these lectins differ. DC-SIGN and Langerin are thought to be uptake receptors with less or no involvement in signal transduction pathways. Dectin-2, mincle and MCL are closely related, mincle and dectin-2 are triggering important immunological pathways. MCL so far has no known ligands or signalling pathway by itself. Dectin-1 is signalling via an ITAM like domain.

3.3.3 Dectin-1 exemplifies the concept of cluster signalling

Dendritic Cell-associated C-type Lectin 1 (dectin-1) was first described in (Ariizumi, Shen, Shikano, Xu, *et al.*, 2000), but is now known to be expressed in various myeloid cells such as monocytes, macrophages, and neutrophils (Taylor *et al.*, 2002). Dectin-1 is a Ca^{2+} independent fungal PRR, which recognizes β-glucans. The lectin is known to activate multiple phosphoproteins such as ERK, SYK, and STAT-1 (Eberle and Dalpke, 2012; Bode *et al.*, 2019; Negi *et al.*, 2019). Interestingly, while many immunological signalling receptors such as FcRγ and CD3 use a ITAM, dectin-1 has a ITAM-like motif, which does not adhere to the usual YxxL ITAM consensus sequence (Underhill and Goodridge, 2007). It is further well established that one of the tyrosines in dectin-1's ITAM-like domain is not involved in signalling (Herre, 2004; Rogers *et al.*, 2005). Dectin-1 signalling and activation was very well described by (Goodridge *et*

al., 2011) and is thought to work by clustering: Upon ligand recognition, dectin-1 receptors associate to form an immunological (also phagocytic) synapse around a recognized ligand. This high receptor association then excludes the usually present phosphatases, shifting their equilibrium with kinases and initializes the signal transduction pathway (Fig 6). This concept of clustering and signal propagation can also be seen in the signalling of other lectins. The process of clustering and synapse formation is found in various immunological processes such as T-cell and antigen presenting cell synapse (Dustin, 2014). It was recently shown that dectin-1 is not exclusively a PRR, but also involved in self-recognition and clearance of apoptotic cells (Bode *et al.*, 2019).

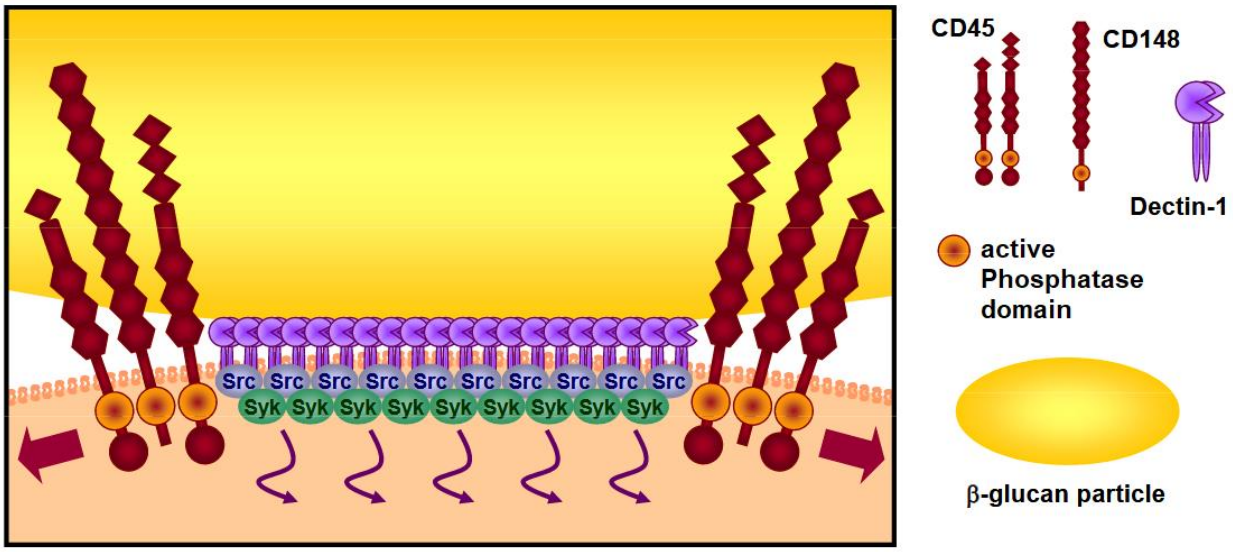

Figure 6: β-glucan particles organize dectin-1 and its associated kinases as phagocytic synapse. β-glucan particles are being recognized by dectin-1 which clusters around the ligand. The phosphatase domains of CD45 and CD148 are then excluded from the synapse by simple mechanics. Due to the lack of phosphatases the SYK is being phosphorylated and giving way for signal transduction. Scheme adapted from Goodridge et al., 2011.

3.3.4 Lectins bearing ITIMs and CD33

The study of ITIM-related signalling is inherently difficult since first the signal or pathway that those lectins inhibit has to be found and resolved. It is therefore not surprising that less is known about ITIM bearing CLRs. For human DCIR (CLEC4A) for example, a lectin expressed on dendritic cells, macrophages, and monocytes, no specific ligand is known yet, although the receptor is known to bind mannose and fucose glycans (Bates *et al.*, 1999). Additionally, no clear murine equivalent has been identified which further complicates studying the receptor (Sancho and Reis e Sousa, 2012). Among human lectins a very prominent class of lectins the Siglecs (sialic acid binding Ig-like lectins) exist, these are of exceptional interest since sialic acid is a monosaccharide which is usually not found in plants, bacteria, and invertebrates; thus seem to be a correlated with the "higher" forms of life (Varki, Schnaar and Schauer, 2015). Siglecs are the binder of sialic acids and are the best described group within the I-type lectins, these are named for their characteristic Ig-like fold. Most commonly Siglecs are bearing ITAIM domains as signalling motifs. CD22 (Siglec-2) for example the marker for B-cells is mainly known to be a negative regulator of the BCR (B-cell receptor), although other functions of this receptor are known (Clark and Giltiay, 2018).

Another example is CD33 or Siglec-3 myeloid lectin receptor that is strongly linked to Alzheimer's disease. While it is known to preferably bind α2-6 linked sialic acid and to be responsible for phagocytosis in macrophages, dendritic cells, and microglial cells, the lectins precise function is currently unknown (Zhao, 2019). Multiple genome wide association studies (GWAS) have so far shown CD33 loci connected with Alzheimer's disease some protective, most risk associated (Lambert *et al.*, 2013; Reitz, 2014; dos Santos *et al.*, 2017). Due to its restricted expression, siglec-3 could also be used for the treatment of acute myeloid leukaemia with Gemtuzumab an antibody-toxin conjugate which is taken up by the cancerous cells via CD33 mediated endocytosis (Godwin, Gale and Walter, 2017). The phagocytosis of human and murine CD33 were recently shown to function differently, due to a number of divergent features in the proteins (Bhattacherjee *et al.*, 2019). This emphasizes the importance of research dedicated towards siglec-3 and its function.

3.3.5 C-type lectins receptors without ITIM or ITAM

DC-SIGN

DC-SIGN (Dendritic Cell - Specific ICAM3 Grabbing Non-integrin) was first identified in the early 1990s(Curtis, Scharnowske and Watson, 1992). However it took almost a decade to unravel its function and role (Geijtenbeek *et al.*, 2000). DC-SIGN is also a Ca^{2+} dependent CLR with an EPN motif, albeit organized as a tetramer on the cellular surface. The lectin recognizes fucosylated glycans such as Le^X, Le^Y as well as high mannose structures. Interestingly, DC-SIGN can subsequently trigger two distinct pathways: one for the fucose based ligands and one for mannose (Garcia-Vallejo and van Kooyk, 2013; Teunis B H Geijtenbeek and Gringhuis, 2016). This example also demonstrates that very early differences in the recognition process of a lectin can determine the outcome of the whole signalling pathway. Due to these relatively broad recognition capacities, it can not only recognize endogenous glycans like ICAM2 and ICAM3, but also pathogens such as HIV, *C. albicans, H. pylori* and SARS-Cov2 (Geijtenbeek and Gringhuis, 2009; Gringhuis and Geijtenbeek, 2010; Gringhuis *et al.*, 2014; Thépaut *et al.*, 2020). Since DC-SIGN was found to be a uptake receptor able to facilitate MHC II, and MHC I cross presentation, (Tacken *et al.*, 2012) it is viewed as an intriguing target for vaccine development (Cruz *et al.*, 2017). However, while many fascinating phenomena were uncovered for DC-SIGN in vitro, the translational bottleneck is the absence of a murine equivalent. Eight different protein candidates have been found, yet none of them can be named *murine* DC-SIGN (Garcia-Vallejo and van Kooyk, 2013). Therefore, investigations in DC-SIGNs in vivo functions are greatly hampered.

Langerin

Langerin was named after the Langerhans cells on which it was discovered by (Valladeau *et al.*, 2000). It is a trimeric classic CLR and just like DC-SIGN known to be an uptake receptor which can facilitate cross presentation via MHC I and MHC II presentation (Clausen and Stoitzner, 2015). Langerin binds mannose, fucose, and *N*-acetyl glucosamine (GlcNAc) (Feinberg *et al.*, 2011). Thus it is not surprising that it was identified as a receptor for the following pathogens: *M. tuberculosis*, HIV, *Candida spp* , HSV 2, and *S. aureus* (de Witte *et al.*, 2007; de Jong *et al.*, 2010; van Dalen *et al.*, 2019). The interaction of *S. aureus* and Langerin was shown to be affected by common SNPs (single nucleotide polymorphisms), N288D and K313I which enhances langerin membrane-expression, yet also compromised *S. aureus* recognition (van Dalen *et al.*, 2020). Furthermore while Langerin has many assigned functions and roles in immunity, it

seems to be redundant, since the mutation W264R was identified which completely abrogates Langerin functions, without negative consequences for its carriers (Kissenpfennig *et al.*, 2005; Ward *et al.*, 2006). Unlike DC-SIGN, Langerin uptake does restrict HIV transmission in dendritic cells and can also be thought of a sole uptake receptor, since to date no signalling has been reported for it (Geijtenbeek and Gringhuis, 2009).

MGL

Macrophage galactose binding lectin (MGL) was first described by (Kawasaki *et al.*, 1986). The lectins binds galactose residues like the cancer associated Tn antigen on human mucin 1 protein (Muc1) (Napoletano *et al.*, 2007). MGL forms a homo-trimer and is expressed on dendritic cells and macrophages. Despite some reports showing activation of signal transduction pathways such as NFκB, MGL is thought like Langerin to be mainly responsible for endocytosis; this in turn makes it an similarly interesting target (Higashi *et al.*, 2002; Napoletano *et al.*, 2012).

3.4 Information encoded within bacterial glycans

Bacteria just like eukaryotes and archaea are using glycans as post translational modifications for their proteins. For vertebrates it is currently known that at least 50% of all proteins are being glycosylated (An, Froehlich and Lebrilla, 2009). In bacteria no quantitative data about this rate is known yet. Although since it was only noticed recently that bacterial proteins are regularly glycosylated, one can estimate that the percentage of glycosylated proteins is much lower (Szymanski *et al.*, 1999; Schäffer and Messner, 2016). A number of differences exists between the functions of glycans in bacteria and Eukarya.

First of all, the chemical diversity of monosaccharides used by bacteria is much higher. This is not surprising, since also the genetic diversity within the bacterial domain is higher than the one within eukaryotes, so the use of diverse monosaccharides might simply be a result of that. Secondly, bacteria are preferring O-glycans over N-glycans, even though the evolutionary origin of N-glycosylation seems to be proto-bacterial (Schwarz and Aebi, 2011; Lombard, 2016). The preference towards O-glycans seems to be a result of the less compartmentalized cells of bacteria. With the simple lack of an ER or Golgi for N-glycan generation the possibility for N-glycan generation is limited and process usually takes place in

the periplasm. Also given the high importance of N-glycans in cell-cell communication and therefore multicellular organization, the unicellular bacteria have less need for them.

As a consequence, glycans in bacteria themselves work more as a structural feature for stabilization of proteins, rather than carrying information. It is apparent that bacterial virulence is closely associated with protein glycosylation (Ribet and Cossart, 2010; Lu, Li and Shao, 2015). But since it is not known what percentage of bacterial proteins are being glycosylated. In host pathogen-interactions glycans are often of high importance, since the clearly non self-glycans serve as pathogen associated pattern for the immune system. A most prominent example would be LPS where not only the lipid A part, but of course also the core O-oligosaccharide are being recognized by TLRs and lectins like langerin, respectively (Raetz and Whitfield, 2002; Hanske *et al.*, 2016). Changes in glycosylation are therefore often significant advantages of certain strains and bacteria to escape immune surveillance. One of the most interesting strategies is by molecular mimicry, where bacterial pathogen display glycans that are closely related or identical to self-glycans of the host. *Neisseria meningitidis* as well as group A and B *streptococcus* are known to employ this mechanism (Poole *et al.*, 2018). In some cases, the molecular mimicry can even lead to the induction of autoimmune diseases. Guillain-Barré syndrome has been linked to the ganglioside mimicry of *C. jejuni* infection (Moran, 1996; Yuki and Koga, 2006). It should therefore be clear that while bacteria do not seem to encode much information themselves into glycans, the correct decoding or recognition of bacterial glycans is of key interest to the host. Subsequently the tug of war between bacterial recognition and evasion from host immune system is an interface at which a lot of change in glycan presentation occurs.

3.5 Use of Information theory in biology

Information theory goes back to the 1940s when Claude Shannon quantified the information of communication channels. Shannon derived key measures to achieve this, first the 'Shannon measure of information' and the 'channel capacity' (Shannon, 1948). His view of an information channel was later also applied to biological problems as was suggested in (Mian and Rose, 2011; Rhee, Cheong and Levchenko, 2012).

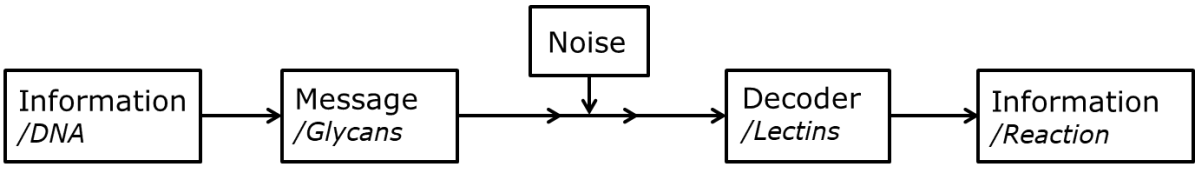

Figure 7: Transfer process of an information channel. In the general scheme information flows as a message under the influence of noise. A decoder translates the message back into information. In a lectin channel most information originally stems from the DNA. It is being transmitted via glycans and decoded into a biochemical reaction by lectins. Noise is omnipresent in any information channel including lectins and interferes with information transmission.

In this thesis biological receptors and their connected signal transduction pathway are viewed as information channels (Fig 7) which decipher the information contained within a ligands dose curve (input) into cellular reactions (output). The relationship between the input and output is then quantified with the use of the 'mutual information' and the maximal mutual information, which is known as 'channel capacity'. Mutual information itself and channel capacity are a quantification of how well the information of an input corresponds to an output.

3.5.1 Key measures in the mathematical theory of communication

The key metric Shannon used in his work is known as Shannon entropy or Shannon measure of information (SMI), which is symbolized by *H*. The metric uses various events and their probability of occurrence, these could be for example the events and probabilities of rolling a certain number with a six-sided die, the probability of hitting a certain area on a dart disc, or the frequency of letters in the alphabet it can generally be written as:

$$H(x) = -\sum_{i}^{n} p_i \, log \, p_i$$

H then quantified the information content of this probability distribution in *bit,* with *p* being the probability of the i^{th} event and *log* the logarithm to base 2. Bit is an abbreviation from binary digits and also the reason why the logarithm to the base of 2 is used by Shannon. In theory other logarithms could be used, but since any electronic information technology at the time and also most of it today is based on relay switches which are either set *off* or *on*, 0 or 1, thus bit was used (Shannon, 1948). This measure also however is not suited to quantify channels which transmit information (Fig 11). In order to do so one needs to employ the mutual information which consist of two probability distributions, one of the input and one of the output message as well as the joint entropy of the two. The input SMI can be written as:

$$H(input) = -\sum_{i}^{n} p_i \log p_i \qquad\qquad H(output) = -\sum_{j}^{m} p_j \, log \, p_j$$

where p_i is the probability of i^{th} input. p_j is the probability of the j^{th} index of output.

$$H(output) = -\sum_{j}^{m}\sum_{i}^{n} p(i,j) \, log \, \sum_{i}^{n} p(i,j),$$

where $p(i,j)$ is the joint probability of i^{h} (input) and j^{th} (output) index. Finally, from the joint entropy

$$H(input, output) = -\sum_{j}^{m}\sum_{i}^{n} p(i,j) \, log \, p(i,j),$$

mutual information is calculated as follows:

$$I(input; output) = -\sum_{i}^{n} p_i \log p_i - \sum_{j}^{m}\sum_{i}^{n} p(i,j) \log \sum_{i}^{n} p(i,j) + \sum_{j}^{m}\sum_{i}^{n} p(i,j) \log p(i,j).$$

The maximum of this mutual information I then give then maximum possible information the channel can transmit.

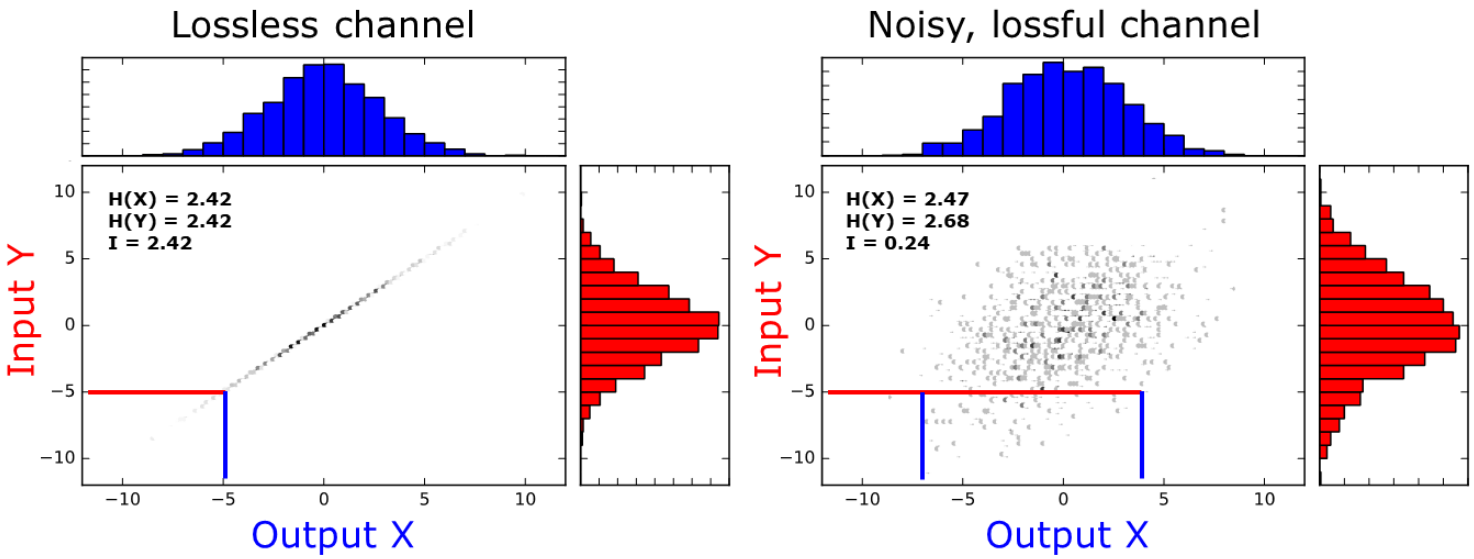

Figure 8: Theoretical example of the mutual information between input and an output. The left panel shows an ideal channel where input and output perfectly correlate without an influence of noise. On the right a noisy and lossful channel where the majority of information is lost. Biological channels are usually found somewhere in between those two extremes. Example kindly provided by Dr. Dongyoon Kim.

It does by itself not matter what these input and output distributions are, but in a biological setting the input (Y) is usually a ligand, which triggers a receptor mediated cellular reaction as output (X) (Fig 8). How well the output then corresponds to the input is quantified by the mutual information (I) or the channel capacity (maximal mutual information (I)). Figure 8 gives an example of how two information channels, one being a flawless channel with no loss of information due to noise, the other being noisy and lossful channel. The probability distributions of all input and outputs are roughly the same at about 2.5 bits. The difference between the two channels is then due to the correlation of the two distributions. Whereas the lossless channel perfectly correlates the input to the output (*e.g:* input of -5 is received as -5 output) the lossful channel has an output for anything from -7 to 4 for its input.

3.5.2 Application of information theory in biological studies

The Levchenko group was the first to apply the mathematical framework of information theory to biological problems (Cheong *et al.*, 2011). They used immunofluorescence microscopy and quantified the information transmitted by the well-characterized TNF-α pathway to the transcription factor NFκB. From their calculation, they derived that a maximum of 0.92 bit of information is transduced by the TNF-a pathway to NFκB itself. Later on, they use reporter cell system, here GFP expression is controlled by a NFκB response element, so upon NFκB activation the cells express GFP. Therefore, information is integrated over time since the expressed protein does only degrade slowly (Corish and Tyler-Smith, 1999). Their calculations derived from this give 1.64±0.36 bit of information as channel capacity for the TNF-α pathway. At the time it was astounding that a biological system could not transmit much more information than 1 bit, which effectively only can encode for a single yes or no decision (Thomas, 2011). It however soon became clear that about 1 bit of information transferred by a biochemical information channel is the rule rather than the exception. This became apparent in the study of (Suderman *et al.*, 2017) where multiple studies that had calculated channel capacities were compared. This also implies that when the maximum of most channels is 1 bit under normal conditions, one can often expect less information to be transmitted and at a population level therefore not all cells will react to a stimulus. This also implies that one cannot simply view signal transduction pathways as simple on-off switches, but rather the individual receptors as being tuning points, causing a certain number of cells to react. Therefore, as oppose to these deterministic switches cellular signalling should be viewed in a stochastic way, which calls for single cell resolved data. With such a framework the information flow of cellular receptors can be quantified in a view that takes the spread and variation of a whole ligand titration into account.

3.6 Noise in biological communication

Like in all communication processes noise also accompanies biological communications. The most commonly used metric for biological noise in gene expression is the squared relative standard deviation, but the metric can be applied to any biological data (Colman-Lerner *et al.*, 2005; Guinn *et al.*, 2020).

$$Noise = CV^2 = \left(\frac{sdev}{mean}\right)^2$$

While it was already noted by Claude Shannon that any signal transmission is inevitably accompanied by noise, it is now known that noise especially in biology is not always a nuisance, but can be beneficial (Shannon, 1949; Raj and van Oudenaarden, 2008). In a fibroblast NFκB model system for example it was shown that under fluctuating ligand concentrations high noise did help with synchronizing the cells response (Kellogg and Tay, 2015). Furthermore, it was shown that when observing information transmission in cellular populations over time, the disrupting effect of cell-to-cell variation was much less important (Selimkhanov *et al.*, 2014). Cell-to-cell variation or cellular microheterogeneity can also be an important driver of survival, in unicellular organisms for example heterogenous phenotypes secure adaptability in response to a sudden environmental changes (Raj and van Oudenaarden, 2008; Magdanova and Golyasnaya, 2013). Altogether while noise within (cellular) communication is an inherent problem, it can in certain cases also have beneficial effects.

3.6.1 Two distinct categories of biological noise

Stochastic or noisy processes in biology such as gene expression distinguish two kinds of noises depending on origin: (Hilfinger and Paulsson, 2011; Singh and Soltani, 2013)

- Intrinsic noise is being generated by inherent stochastic processes such as transcription and translation, these are dependent on chance such as thermodynamic fluctuation of the mRNA translation for example.
- Extrinsic noise is a result of cell-to-cell variation. For example, the amount of nutrients available to a cell or the mitotic phase the different cells are in at a given moment.

The decomposition of these two sources of noises in gene expression for example, is facilitated with the use of dual equivalent gene expression systems. In such a system two genes, usually fluorescent proteins (FPs) for easy quantification, are dependent on the same promoter. The expression of the two will of course correlate. Yet since the intrinsic noise affects expression of the two proteins independently the resulting variation can be seen perpendicular to the correlation. Extrinsic noise will then be the variation with the correlation itself (Fig 9A). To exemplify: Cells with a higher capacity to produce proteins due to stored nutrients, size, or similar things will produce both proteins better, than cells with a low capacity for protein production. This is classified as extrinsic noise. But if a cell just by chance has 50% more mRNA for one of the FPs and expresses more of that FP, then the resulting variation has to be due to intrinsic noise (Elowitz, 2002).

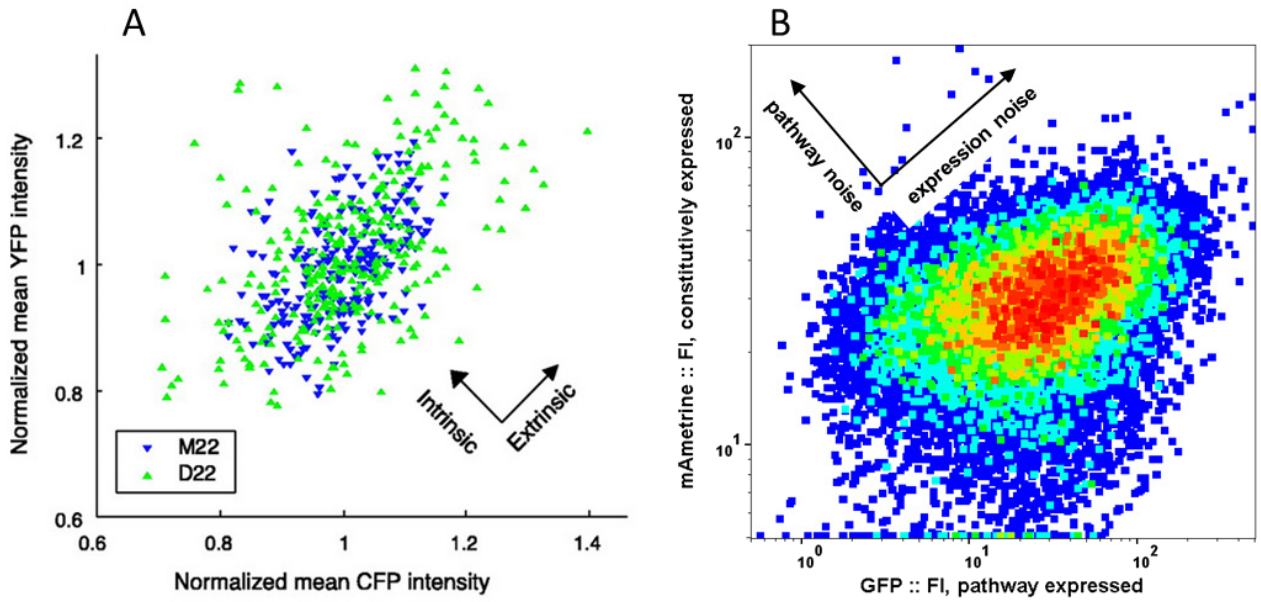

Figure 9: Examples of dual reporter noise analysis. A) Expression of fluorescent proteins in two bacterial strains M22 and D22. Each point represents the mean fluorescence intensities of single cell. Spread of points perpendicular to the correlation of CFP and YFP intensities are equal corresponds to intrinsic noise, whereas spread along the correlation is caused by extrinsic noise. Figure taken from Elowitz et al., 2002. B) Expression of fluorescent proteins in U937 cells. GFP is expressed dependent on an signaling pathway and mAmetrine is expressed constitutively. In this case spread of points perpendicular to the correlation of GFP and mAmetrine is due to pathway specific noise, whereas spread along the correlation is due to general protein expression noise between cells.

Using the same principles and multiple fluorescent proteins one can also distinguish noise originating from gene expression or biological pathways (Colman-Lerner *et al.*, 2005). Here a non-equivalent reporter system is used, where one FP is constitutively expressed and another FP at the end of the pathway of choice. These two fluorescent proteins can be plotted against one another as seen in Figure 9B. The expression of these two fluorescent proteins correlate, since some cells have a higher capacity to produce protein than others and these cells then express both proteins (GFP and mAmetrine) well. Therefore, noise along the correlation line can be called expression noise, dependent on both intrinsic and extrinsic noise of the expression. Whereas the noise perpendicular to the correlation is a result of effects that influence the two proteins disproportionately. Since mAmetrine and GFP are almost identical in sequence and structure (Shcherbakova *et al.*, 2012) such disproportionate influences are connected to their different expressions. The different expressions being constitutive expression with no "pathway" attached and in case of GFP a signalling pathway dependent expression. Thus, a non-equivalent fluorescent protein expression system can be very useful for determination of noise origin.

3.7 Model cell lines

Almost 70 years have passed since the establishment of the first human cell line in 1951. These cell lines have become basic tools for research in the field of life science as well as hosts for biopharmaceutical production. In their role as models, cell lines are very cost effective and can yield exciting results in a reproducible and repeatable manner. The adequate use and interpretation of these models should be ensured. The cellular identity should be ensured, since misidentified or contaminated cells can hurt studies integrity (Alston-Roberts *et al.*, 2010). Additionally, cells should be well maintained at low passage if possible and contamination with mycoplasma needs to be evaluated regularly. The data derived from model cell lines are of course *in vitro* and one should take car to not over-interpret the gained results. For exploration of basic concept and ideas, where cells are continuously manipulated and expanded, cell lines are feasible and often the only option, due to high sensitivity and low abundance of equivalent primary cells. The chosen cell line should reflect the context of research so for researching myeloid CLRs one should pick a myeloid immunological cell line (Kerscher, Willment and Brown, 2013). For research in monocyte like cells the most commonly used cell lines are HL-60, U937, or THP-1 cells (Riddy *et al.*, 2018).

3.8 Reprogramming of lectin expressing cells

Targeted delivery is an approach where molecules can be delivered specifically to a certain set or subset of cells. This can be facilitated by the use of a specific receptor expressed on a cell. Subsequently with the delivery of nucleic acids cells can be manipulated in various ways. siRNA for example can be delivered to interfere with protein expression, the CRISPR cas9 system can be used for genetic manipulation, or mRNA itself can be delivered for protein synthesis (Sahin, Karikó and Türeci, 2014; Xu *et al.*, 2019; Wadhwa *et al.*, 2020). The latter example is famously used for the first time as an approach for vaccination against a SARS-CoV2. Upon administration the mRNA is encapsulated in lipid nanoparticles and translated within immune cells into antigens and presented to T and B cells (Wu, 2020).

As with any endocytic receptor, targeted delivery to lectins can be achieved using either antibodies or specific ligands of the lectin. A promising candidate for such an approach was recently developed for targeted delivery to Langerin expressing cells (Wamhoff *et al.*, 2019).

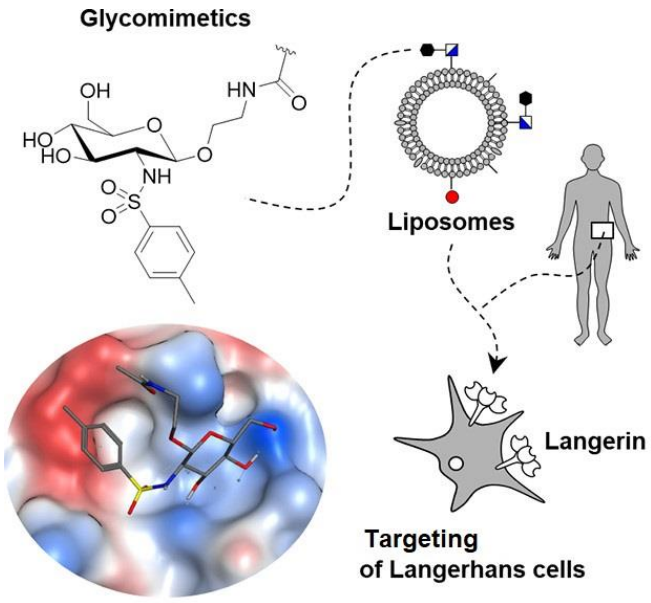

Figure 10: Principles of the Langerin targeted delivery system (TDS). A specific glycomimetic ligand was designed first. This human langerin ligand is the used to decorate liposomes, which are then specifically targeted towards langerin expressing cells. The targeted liposomes are then taken up via langerin mediated endocytosis on Langerhans cells. Such a system can be used to deliver the content of liposomes to skin resident Langerhans cells. Figure taken from Wamhoff et al., 2019.

In the Langerin targeted delivery system (TDS) the nucleic acid is formulated into a lipid nanoparticle (LNP), which due to the targeting Ligand is bound and taken up via Langerin receptor mediated endocytosis (Schulze *et al.*, 2019). Afterwards in the endosomal compartments Langerin will detach its cargo due to the loss of its Ca^{2+} cofactor, which is mediated by the endosomal change in pH. These LNPs contain an ionizable lipid DLin-MC3-DMA, which will then trigger endosomal escape of the cargo/mRNA, this cytosolic mRNA can then be translated into protein.

With the use of such a delivery system, cells expressing langerin can be specifically reprogrammed and manipulated, this in turn has tremendous potential for biotechnological applications.

4. Aim and purpose of this thesis

Glycan-lectin interactions remain an enigmatic, yet essential part of life. A systematic approach could help better understand how information is being encoded and decoded by glycans and lectins and how this information is transmitted into biological signals. With this thesis I aimed to quantify the information transmission in glycan-lectin interactions. To achieve this, I have generated a vast array of immunological cell line models expressing lectins, but also other receptors such as TNFAR, TLR1 and TLR2. This array of receptors includes, but is not limited to DC-SIGN, Langerin, dectin-2, dectin-1, MCL, mincle, TNFAR, TLR1&2, and CD33; and these can also be expressed in any combination of up to four receptors on a cell line. With the use of single cell resolved assays I then compared the signalling of the information transmitting channels/signal transduction pathways that the receptors can trigger. The methods employed for this were a NFκB reporter cell assay, specific quantification of phospho-proteins (phosflow), as well as binding of fluorophore tagged molecules in flow cytometry. I then analysed the data generated in these cell line models using information theory. Thus, I could quantify the transmitted information of the channels with the channel capacity as a metric. This put the signalling pattern of all observed receptors in context to one another and to channel capacities noted in other studies. Specifically, for the lectin receptors dectin-2 could demonstrate its inefficient signalling relative to other receptors, which is rooted in a noisy signalling behaviour of the cellular population. Additionally, using two lectins, dectin-1 and dectin-2 the question of signal integration was approached. Here I could demonstrate that cells compromise between the two channels, relying on both of them rather than one over the other. Finally, we (in collaboration) could also show that endocytic lectin receptors such as Langerin can be used to reprogram immune cells specifically with the use of targeted delivery.

5. Material and Methods

All reagents were bought from Sigma-Aldrich, if not stated otherwise.

5.1 Cell lines used in this thesis

All suspension cell lines were routinely cultured in RPMI 1640 (Gibco) with 10% fetal bovine serum (Sigma-Aldrich), 1% Penicillin-Streptomycin (Gibco), and 1% Glutamax (Gibco). Adherent cells were cultured in DMEM with the same additions. All cells were cultured at 37°C with 5% CO_2 and tested for mycoplasma infection every six months (Minerva Biolabs kit).

U-937 (ATCC® CRL-1593.2™) suspension cells

The monocytic cell line U937 was first generated in the Nilsseln Lab in 1974 from a 37 year old male Caucasian suffering from histiocytic lymphoma (Sundström and Nilsson, 1976). The cells show regular formation of blebs and a characteristically high doubling rate (about 20-24h) under ideal conditions. Just like THP-1 cells it is possible to differentiate U937 cells into macrophage like cells using PMA (phorbol 12-myristate 13-acetate) (Daigneault *et al.*, 2010).

THP-1 (ATCC® TIB-202™) suspension cells

THP-1 cells were generated it 1980 isolated from the blood of a 1 year old boy suffering from acute monocytic leukaemia (Tsuchiya *et al.*, 1980). The possibility to differentiate those cells with phorbol diesters was noted soon afterwards (Tsuchiya *et al.*, 1982).

RAJI (ATCC® CCL-86™) suspension cell

RAJI cells were generated in 1963 by Pulvertaft from Burkitt's lymphoma of a 11-year-old male. This work was then published by (Epstein and Barr, 1965) who discovered the Epstein-Barr virus within the same tissue (Epstein, Achong and Barr, 1964).

293T (ATCC® CRL-3216™) adherent epithelial cells

Originally derived from human embryonic kidney (HEK) cells the 293 cells were established by the transformation with sheared adenoviral DNA in the 1970s (Russell *et al.*, 1977). The further addition of the SV40 large T antigen enhanced the cells ability to produce protein on plasmid vectors with a SV40 ori

and established the cells as a robust go-to cell line in recombinant protein production (Thomas and Smart, 2005).

5.2 Cloning, establishment of cell lines and associated assays

Since the model cell lines of choice are notoriously, and did in practice prove to be, very hard to transfect, all lectin and receptor expressing cells were generated using a third-generation lentiviral system. Lentivirus vectors are based on the HIV-1 and were established as an alternative to retroviruses for viral transduction, with the advantage that the lentivirions can infect dividing and non-dividing cells (Zufferey *et al.*, 1998). Due to safety concerns the proteins making up the virus are divided onto multiple plasmids in the lentiviral system as Figure 11 demonstrates: The system consists of sometimes multiple packaging plasmids, a transfer and an envelope plasmid. In this work two different lentiviral vector systems were used: the BIC-PGK-Zeo-T2a-mAmetrine:EF1a as reported in (Wamhoff *et al.*, 2019), and the Trono labs system as reported in (Dull *et al.*, 1998). The BIC-PGK-Zeo-T2a-mAmetrine:**EF1a** (name of the transfer plasmid) uses an envelope plasmid pMDG and a packaging plasmid pCMVR8.91. The Trono lab system uses two packaging plasmids pRSV-Rev (Addgene# 12253) and pMDLg/pRRE (Addgene# 12251), with pMD.2G (Addgene# 12259) as envelope plasmid. The transfer plasmid in this case is the pLV-**EF1a**-IRES plasmid with one of three resistances (Neomycin, Hygromycin, and Blasticidin) rather than only one. Therefore, even though two different system were used in the end all genes of interest are under the same strong constitutive EF1a promoter. In any lentiviral system the different plasmids are transfected into 293 cells and will then produce the lentivirions. These can then be used to transduce the DNA of interest into the chosen cell line.

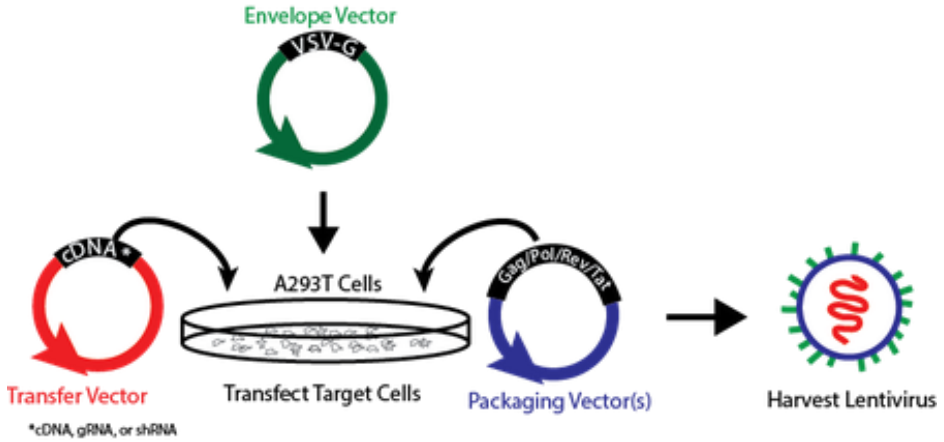

Figure 11: Schematic depiction detailing the generation of lentivirions. Multiple vectors are being transfected into a production cell line. Only when all three are present lentivirions are being made. Scheme from Addgene: Lentiviral Guide, 2016

The cDNA of MINCLE, dectin-2, MCL, human Langerin. and DC-SIGN were cloned into vector BIC-PGK-Zeo-T2a-mAmetrine:EF1a. This bicistronic vector expresses mAmetrine as a fluorescent marker under the PGK promoter. To combine multiple GOI the lentiviral vector pLV-EF1a-Hygro/Neo/Blast a gift from Tobias Meyer (Addgene plasmid # 85134) was used to transduce DC-SIGN, dectin-2, MCL, FcRγ, dectin-1, and MGL. 293T or 293F cells were transfected using Mirus LT1 (Mirus Bio, USA) with vectors coding for the lentivirus and gene of interest (GOI). The ratio of vectors was 1:1:2 of packaging:envelope:transfer vector with a total amount of 0.5 µg plasmid per 1 mL of 293 cells. Lentivirions were generated for 72h and the supernatant frozen to kill any remaining 293 cells. This supernatant was used to transduce the GOI into U937 cells *via* spin transduction at 900g and 33°C in the presence of 0.8µg/mL polybrene. After 48h rest, the cells were selected with appropriate antibiotics.

5.3 Reporter cell generation and reporter cell assay

U937, and THP-1 cells (a kind gift from Dr. Nina van Sorge, UMC Utrecht, the Netherlands) were seeded at $2x10^5$ and $3 x10^5$ cells/mL, respectively in a 48 well plate in full RPMI media (RPMI with 10% FBS, 1% Glutamax, 1% Pen/Strep, (Gibco)). Subsequently, NFκB-GFP Cignal lentivirus (Qiagen) at a ratio of 15 lentivirions/cell was added in presence of 0.8 µg/mL polybrene (Sigma-Aldrich). This solution of cells and lentivirions was then spun down at 800g for 90 min at 33°C in the 48 well plate. The cells were then diluted 1:2 with fresh media and rested for 2 days at 37°C and 5% CO_2. Subsequently, cells were put under puromycin (Gibco) antibiotic pressure at 2 µg/mL for 1 week. For monoclonal expansion, single cells were seeded and then grown over the course of about 4 weeks at 37°C, 5% CO_2 in full RPMI media. 8 monoclonal U937 cells were generated in this way and evaluated by their ability to produce GFP upon TNF-a stimulation, clone #5 was chosen for its great signal to noise ratio and used in all experiments, unless stated otherwise. For THP-1 only two clones were viable and clone #1 was used. A single monoclonal cell line of THP-1 or U937 was used for all experiments of this thesis.

Reporter cell assay

One day before the experiment, U937 cells were suspended at $1.5\text{-}2x10^5$ cells/mL to reach log phase on the day of experiment. THP-1 cells were suspended at $2x10^5$ and cultivated for 48 to reach log phase. For the experiment ligands were distributed in 96 well flat bottom tissue culture plate at various concentrations in 5-20 µL per well in PBS. Then log phase reporter cells (then at $3\text{-}4x10^5$ cells/µL) were resuspended in fresh full media (RPMI with 10% FBS, 1% Glutamax, 1% Pen/Strep) and added to the 96

well plate to total volume of 100 µL per well. The challenged cells were then incubated for 16h, the exception being when TNF-α was used as ligand, here the optimal incubation time was found to be at 13h. After incubation, cells were re-suspended once in PBS in a 96 well u-bottom plate and measured via flow cytometry. About 16000 cells were measured from every well to gain robust results.

Mincle ligands

Since mincle ligands are hard to dissolve and often do not stimulate when administered in solution to mincle, all mincle ligands were first dissolved in iso-Propanol + 5% Chloroform. This solution was then further diluted in propanol. 5-20 µL of each dilution step were added to an empty 96 well flat bottom tissue culture plate (Greiner Biolabs) and the propanol solvent was evaporated in a biosafety workbench. Ultimately, the cells were added in medium to the crystalline ligands in the well plate and incubated for 16h with measurements as in the standard reporter cell assay, see description above.

Cell culturing and passage

U937, RAJI, and THP-1 cells were kept between $1x10^5$ and $1.5x10^5$ cells/mL in full media (RPMI with 10% FBS, 1% Glutamax, 1% Pen/Strep, (Gibco)) with passage 2-4 times a week. 293 cells were adherently cultured in DMEM with 10% FBS, 1% Glutamax, 1% Pen/Strep, (Gibco) and split 2-3 times per week. All cells were tested for mycoplasma contamination using Minerva biolabs Venor®GeM Classic.

5.4 Antibody stains and quantification

For surface stains cells were incubated in with the respective antibodies and isotype controls for 30 minutes at 4°C, then washed once in DPBS +0.5% BSA and measured via flow cytometry. For perforated stains cells were first fixed in 4% PFA (Carl Roth) at 4°C for 20 minutes, then perforated in perforation solution (DPBS + 0.5% BSA + 0.1% Saponin) for 20 min at 4°C. The cells were then re-suspended in perforation solution containing the respective antibodies, incubated for 20 minutes at 4°C, and measured via flow cytometry after being washed once.

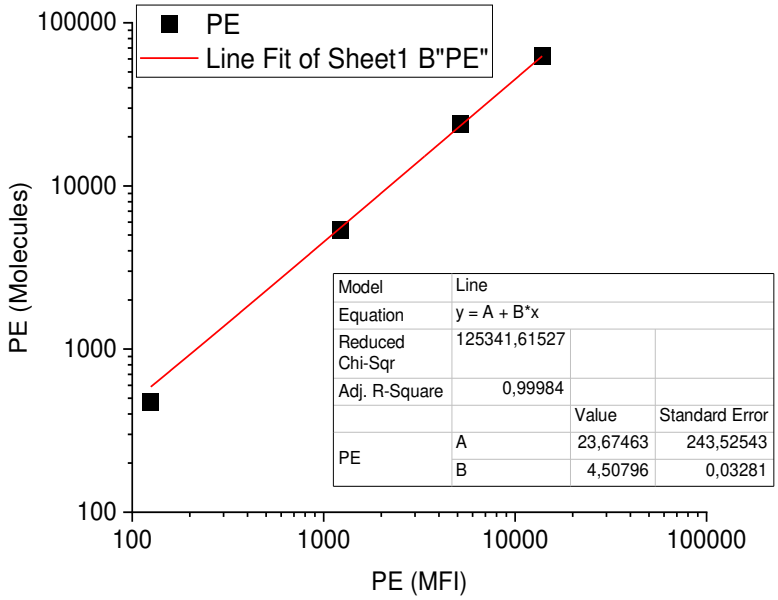

Figure 12: Calibration line connecting the MFI values obtained from the beads in the BD kit with the number of molecules on those beads. The equation derived from this was used to calculate FI values into number of PE molecules.

To quantify the fluorescent intensities a BD PE quantitation kit was used (Fig 12). Briefly the four bead populations were measured via flow cytometry at the same PE laser voltage as the cells stained with antibodies (320 V on Attune NxT). Since the number of PE molecules on each bead population is known, this allows to derive a calibration curve as seen in Figure 12 and subsequently transform the FI of an antibody stain to the corresponding number of PE molecules. See list of used antibodies for providers.

5.5 Labelling of Proteins

Proteins were labelled with Atto647N-NHS dye (AttoTech) according to the manufacturer's protocol. In short, Invertase (Sigma-Aldrich) 10 mg/mL was heat inactivated in PBS buffer (Phosphate-Buffered Saline, pH 7.4, 8 g NaCl, 0.2 g KCl, 1.44 g $Na_2HPO_4 \cdot 2\ H_2O$, and 0.24 g KH_2PO_4, per 1 litre distilled water) for 40 min at 80° In short, the protein solution was set to pH 8.3 with a solution of 0.2 M sodium bicarbonate of pH 9.0. Next Atto647N-NHS dissolved at 10 mg/mL in amine free DMSO (Sigma-Aldrich) was added in a twofold molar excess of dye. The labelled protein was purified using Sephadex 20 column and aliquots were frozen at -80°C. Since it was found that the labelled Invertase contains less

impurities (Fig 13) Atto647 labelled Invertase was used for all experiments. Human TNF-α (PeproTech) was labelled with the same procedure, yet without heat inactivation. The degree of labelling was found to be about 1 in all batches, as measured by extinction coefficient using a nanodrop (Implen™ NanoPhotometer™ NP80).

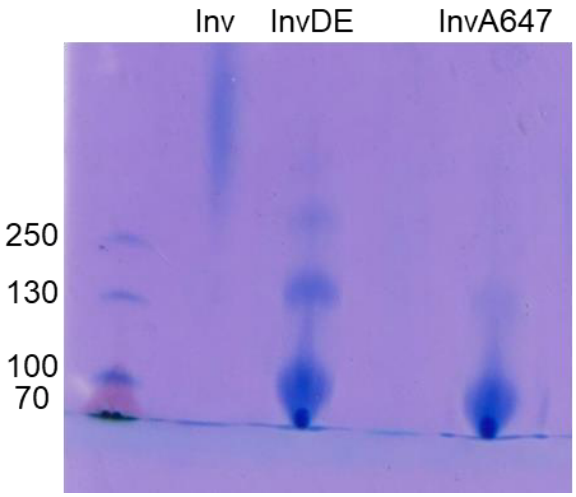

Figure 13: High MW SDS-gel showing native Invertase (Inv), denatured Invertase (InvDE) and denatured Atto647N labelled Invertase (InvA647).

5.6 Detection of phosphoproteins with flow cytometry

The staining buffer for this method is made of DPBS + 0.5 % BSA + 1:100 phosphatase inhibitor cocktail (Merck, Germany).

U937 cells were resuspended in fresh full media at $5x10^5$ cells/mL and rested for 1h at 37°C in a u-bottom cell 96 well plate at 100µL per well. After the rest, 1µL of phosphatase inhibitor cocktail (Merck, Germany) was added to each well of the 96 well plate. 5-10 µL of ligand solution were then added to the rested cells for a stimulation of 1-60 min at 37°C. Afterwards, all cells were fixed simultaneously by adding 10% PFA fixing solution (Carl Roth, Germany) to the cell suspension to a final concentration of 3% PFA and incubated on ice for 20 min. The cells were then washed once with staining buffer and re-suspended in ice-cold methanol containing Perm Buffer III (BD biosciences, USA) for 20-30 min. Afterwards, the cells were washed once in staining buffer and resuspended in 50 µL staining buffer per

well with FcBlocking reagent (1:10, Miltenyi Biotec, Germany) and pSYK, pERK, pSTAT antibodies (1:5, BD biosciences, USA). The suspension was incubated for 30 min at RT, subsequently 100µL of staining buffer per well were added and the plate was spun down at 500g for 5 min. Finally, cells were resuspended in 100µL DPBS and measured in flow cytometry.

5.7 Channel capacity calculation

Calculations of channel capacity were based on (Cheong *et al.*, 2011) with the only major difference being, that logarithmic binning for output was employed rather than linear, since the output response (GFP) is logarithmic with respect to the inputs doses. The adaptation of channel capacity calculations to flow cytometry data were undertaken by Dr. Dongyoon Kim and Felix Fuchsberger. The scripts used in this calculation can be found at https://github.com/FFuchsbe/GlycanComm.

To calculate the channel capacity from discrete, finite input and output data set, the data set should be projected onto two-dimensional, finite rectangular grid plane where the marginal and joint probability can be calculated by counting the number of data points in the individual rectangles. In the dose response of cells, the doses are predetermined and thereby the marginal probability of inputs (*e.g.* doses) is written as

$$p_{input}(i) = \sum_{j}^{M} p(i, j, w_i) = w_i p_i,$$

where p_i is the marginal probability of i^{th} input, j is the index of output, w_i is the weighting value of the i^{th} input and M is the number of output binning. Therefore, the input entropy can be written as follows:

$$H(input) = -\sum_{i}^{N} w_i p_i \, log \, w_i p_i,$$

where N is the number of input binning. Likewise, the marginal probability of output and corresponding entropy are as follow, respectively:

$$p_{output}(j) = \sum_{i}^{N} p(i, j, w_i) = \sum_{i}^{N} w_i p(i, j)$$

and

$$H(output) = -\sum_{j}^{M}\sum_{i}^{N} w_i p(i,j)\, log \sum_{i}^{N} w_i p(i,j),$$

where $p(i,j)$ is the joint probability of i^{th} (input) and j^{th} (output) index. Finally, from the joint entropy

$$H(input, output) = -\sum_{j}^{M}\sum_{i}^{N} w_i p(i,j)\, log\, w_i p(i,j),$$

mutual information is calculated as follows:

$$I(inpt; out) = -\sum_{i}^{N} w_i p_i\, log\, w_i p_i - \sum_{j}^{M}\sum_{i}^{N} w_i p(i,j)\, log \sum_{i}^{N} w_i p(i,j) + \sum_{j}^{M}\sum_{i}^{N} w_i p(i,j)\, log\, w_i p(i,j).$$

Now the mutual information for the given input and output is the function of w_i, and the channel capacity is the maximum value of the function. With the normalization condition$\sum_i^N p_i w_i = 1$, as the constraint, several maximization algorithms can find the input distribution w_i that maximize the mutual information. We used scipy.optimize.minimize from Python for the maximization. Prior to the channel capacity calculation, the 2% of front-end and 2% tail-end of output data sets were excluded. 20 bins and logarithmic binning was used for all calculations in this thesis. To validate the used sample size of 15000 cells per well, recorded data sets were subsampled (Fig 14). The calculated channel capacity values for both dectin-2 and TNF- α were constant down to about 20% showing that enough cells were measured.

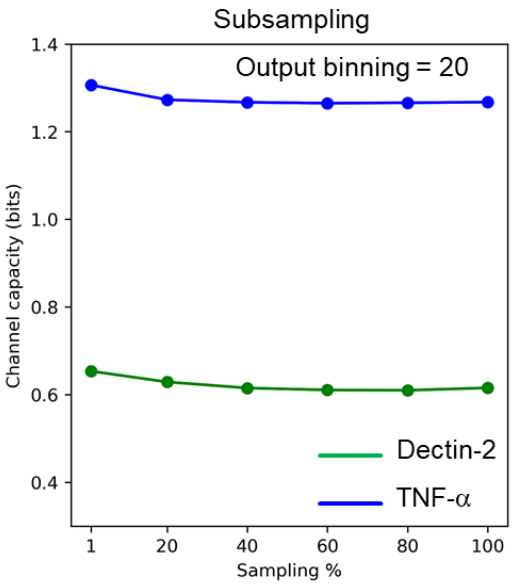

Figure 14: Effect of subsampling on channel capacity. Datasets on dectin-2 and TNFaR were subsampled at random, even when using 20% of the 15000 events per point in the dose-response curve the calculated channel capacity is stable and at a similar level.

5.8 Noise decomposition of GFP reporter cells

Since the BIC-PGK-Zeo-T2a-mAmetrine:EF1a vector is mainly used for lectin expression, the transduced cells are also expressing fluorescent mAmetrine constitutively as marker for the vector. This mAmetrine expression can then be used to correct the cellular pathway noise of NFκB dependent GFP expression for general protein expression noise (Fig 15). See section 3.6.1 for details on noise decomposition. To calculate and correct GFP for mAmetrine expression noise, datasets at maximal stimulation were used. Before being used for this procedure, the flow cytometry data was compensated since mAmetrine and GFP are close in their emission spectra. Only the data points corresponding to single U937 cells were used for this calculation. Figure 15B shows the raw dataset which consists of about 15000 events, each representing a cell with a fluorescent intensity (FI) value for GFP and mAmetrine. The data points were then fitted in python with sklearn.linear_model and a linear regression function, to gain the intercept d and coefficient k.

$$y = k * x + d$$

Using the arctangent of the coefficient to this correlation line, the angle α between the correlation line and the x-axis can be determined (Fig 15B). Subsequently all raw datapoints were transformed into polar coordinates and turned by that angle α. The resulting data points then show the noise of GFP corrected for mAmetrine correlation in x-axis direction. The datapoints are then transformed back into Cartesian coordinates and from their x values a mean and standard deviation can be calculated. With this mean and standard deviation the noise is calculated:

$$Noise = CV^2 = (\frac{sdev}{mean})^2$$

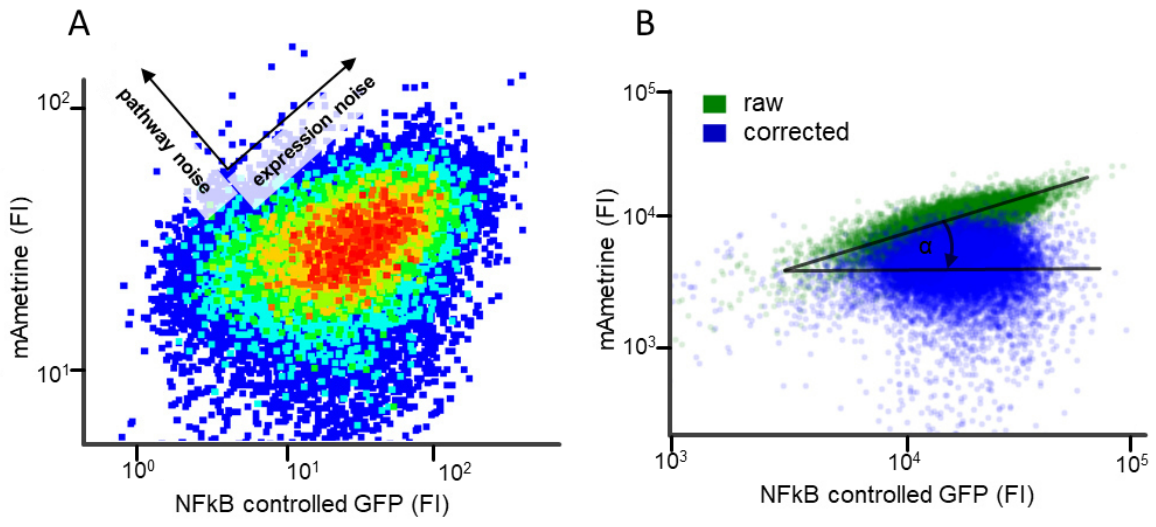

Figure 15: Example and demonstration of noise decomposition. A) Expression of fluorescent proteins in U937 cells. GFP is expressed dependent on an signaling pathway and mAmetrine is expressed constitutively. In this case spread of points perpendicular to the correlation of GFP and mAmetrine is due to pathway specific noise, whereas spread along the correlation is due to general protein expression noise between cells. B) Plot showing NFκB expressed GFP data before and after correction for mAmetrine expression. Each data point represents a single cell. Correction for mAmetrine was always done with samples at a ligand concentration of maximal stimulation. Black lines represent correlation and are drawn schematically for demonstration.

The scripts used in this calculation can be found at https://github.com/FFuchsbe/GlycanComm.

5.9 Liposomal formulations

To distinguish these specific PEGylated FDA approved lipid nanoparticles from other (lipid) nanoparticles the term liposomes is used in this thesis (Feng, 2006). Liposomes are not to be confused with lipid nanoparticles (LNPs) which are of another formulation as described below.

The liposomes were prepared as described in (Wamhoff *et al.*, 2019) and did consist of (in mol %) 57% DSPC (1,2-distearoyl-snglycero-3-phosphocholine, 18:0, Avanti Polar Lipids), 38% cholesterol (Sigma-Aldrich), 4.5% of the human Langerin targeting ligand coupled to PEG-DSPE (Wamhoff *et al.*, 2019) and 0.5% Alexa Fluor 647-PEG-DSPE. In short DSPC and PEG-DSPE coupled lipids were dissolved in DMSO stocks at 10 mg/mL. Appropriate amounts were taken from the stocks into a glass vial and freeze-dried to remove DMSO. Afterwards DSPC and cholesterol were added to the dried glass vials dissolved in chloroform. Subsequently the chloroform was gently removed by evaporation to generate a thin film of dried solids in the glass vial. This solid film was then thoroughly dried in a desiccator for 12h. The solid lipids were then dissolved with gentle sonication in DPBS. Using a mini-extruder (Avanti Polar Lipids) and nucleopore polycarbonate membranes with a pore size of 0.2 and 0.1 µm (Whatman, USA), a uniform solution of liposomes was generated. Dynamic light scattering (DLS) was used to confirm Liposome integrity and uniform size of about 110 nm, all spectra were recorded on a Zetasizer Nano ZS (Malvern).

5.9.1 Lipid nano particles (LNPs)

The composition of these LNPs was based on the liposomes already described before, the major difference was that LNPs contain the ionizable lipid Dlin (DLin-MC3-DMA, Biorbyt) and well as their mode of preparation.

The prepared LNPs did consist of (in mol%) 49% Dlin, 39% Cholesterol, 6% human Langerin targeting ligand coupled to PEG-DSPE, 5.75% DSPC, and 0.25% Alexa Fluor 647-PEG-DSPE. Appropriate amounts of Dlin were weighted (usually 2.5 µg per batch) into a glass vial. Appropriate amounts of the other components were added from ethanol stocks with the following concentrations: Cholesterol 12 mg/mL, human Langerin targeting ligand coupled to PEG-DSPE 6 mg/mL, DSPC 10 mg/mL, and Alexa Fluor 647-PEG-DSPE 20 mg/mL. The resulting lipid solution was used undiluted for formulation, which resulted in a total lipid concentration of 22 mM. LNPs were then formulated using Precision NanoSystems spark nanoassemblr according to the manufacturer's instructions (Precision NanoSystems, Canada). In short,

the system consists of a pump and a microfluidic system, in the microfluidic system the lipid solution (ethanol) is mixed with an aqueous buffer solution in laminar flow. This buffer solution contains the nucleic acid (mRNA, DNA), which needed to be delivered with the LNP. Since those LNPs are self-assembling particles, they then spontaneously formed around their cargo, encapsulating it. After the encapsulation, the loaded LNPs were diluted 1:3 to and dialyzed against buffer to dilute the remaining ethanol and free nucleic acids. DLS was used to confirm LNP integrity and unformal size of 200±50 nm, all spectra were recorded on a Zetasizer Nano ZS (Malvern).

5.10 Flow cytometry, data, and statistics

The majority of cells and experiments were measured with an Attune NxT Flow cytometer (Thermo Fisher, USA). Cells were never higher concentrated than $1x10^6$ cells/mL and measured at speeds of 100-500 µL/min. Recorded events were gated for single events and for their corresponding scatter pattern (Fig 16). Of the resulting events, 16000 were recorded for samples stimulated via the NFκB reporter system, and 10000 events for other experiments.

Only experiments of Figure 35-37 were measured with a MACSquant MQ16 (Miltenyi Biotech, Germany) at medium speed and cell concentrations of $2\text{-}8x10^5$ cells/mL.

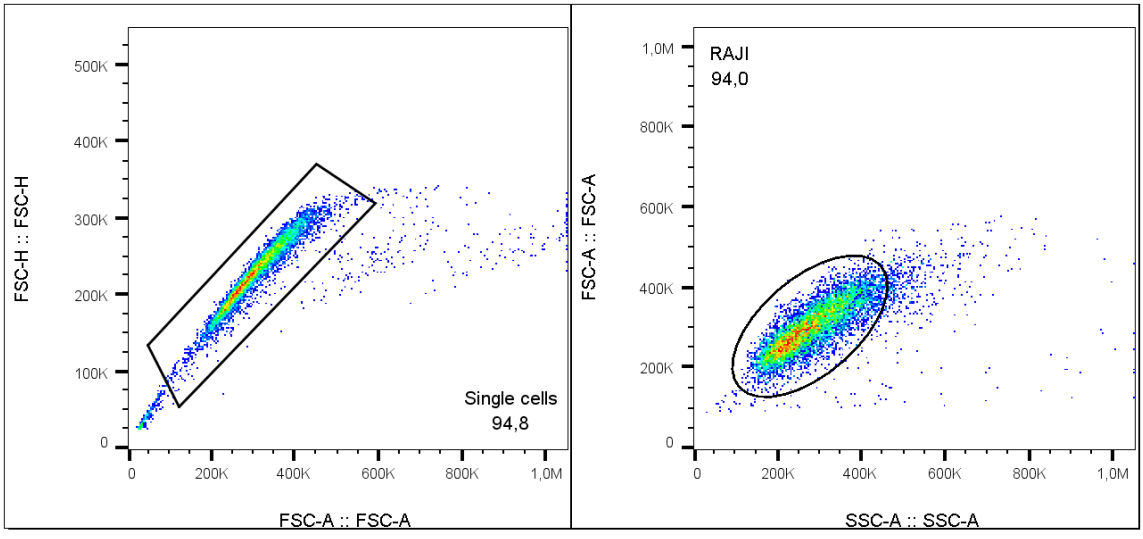

Figure 16: Gating strategy for all cell lines, example shown for RAJI cells. Left panel shows doublet discrimination gate, subsequently the subpopulation is gated with its characteristic scatter pattern as seen on the right.

5.11 Statistics and data

Data are shown as mean ± standard deviation unless stated otherwise. Statistical significance determined with an unpaired t-test; with symbols in graphs representing ns for p-value > 0.05, * for p-value ≤ 0.05, ** for p-value ≤ 0.01, *** for P ≤ 0.001. EC_{50}s were calculated with graph pad prism 9 four parametric dose vs. response. Here x is the concentration or dose of ligand, y the cellular response, d the bottom plateau of the curve and e the top plateau both in the unit of the cellular response, EC_{50} is the concentration of the half maximal effect, and h the unitless hill or slope factor (Motulsky, 2019).

$$y = d + \frac{(x^h) * (e - d)}{(x^h + EC50^h)}$$

When necessary statistical differences between EC_{50}s were compared using an extra-sum-of-squares F test. FlowJo v.10 was used for analysis and export of flow cytometry data.

5.12 Methods used by collaboration partners

5.12.1 *S. aureus* bacterial cultivation

As described in (van Dalen *et al.*, 2019): *S. aureus* strains were grown overnight at 37°C with agitation in 5 ml Todd-Hewitt broth (THB; Oxoid). For S. aureus strains that were plasmid complemented, THB was supplemented with 10 µg/mL chloramphenicol (Sigma-Aldrich). Overnight cultures were subcultured the next day in fresh THB and grown to an optical density at 600 nm (OD_{600}) of 0.6 to 0.7, which correspond to mid-exponential growth phases.

5.12.2 Bacterial binding

As described in (van Dalen *et al.*, 2019): To test binding of bacteria to cells, THP1-EV or THP1-langerin cells were incubated with GFP-expressing S. aureus Newman or GFP-expressing S. aureus Newman cells at indicated bacterium-to-cell ratios from in TSM buffer (2.4 g/liter Tris [Roche], 8.77 g/liter NaCl [Sigma-Aldrich], 294 mg/L CaCl2·2H2O [Merck], 294 mg/liter MgCl2·6H2O [Merck] at pH 7.4) with 0.1% bovine serum albumin (BSA; Merck) for 30 min at 4°C. Binding was blocked by 15 min of preincubation with 10 µg/ml mannan (Sigma-Aldrich), 50 mM GlcNAc (Serva), or 20 µg/mL anti-langerin blocking antibody

(clone 10E2; Sony Biotechnology). Cells were washed once with TSM–1% BSA, fixed in 1% formaldehyde (Brunschwig Chemie) in PBS, and measured by flow cytometry.

5.12.3 Generation of muLCs

As described in (van Dalen *et al.*, 2019): MUTZ-3 cells (ACC-295; DSMZ) were cultured in 12-well tissue culture plates (Corning) at a density of 0.5×10^6 to 1.0×10^6 cells/ml in minimal essential medium alpha (MEM-alpha) (Gibco) with 20% fetal bovine serum (FBS; HyClone, GE Healthcare), 1% Glutamax (Gibco), 10% conditioned supernatant from renal carcinoma cell line 5637 (ACC-35; DSMZ), 100 U/ml penicillin, and 100 µg/ml streptomycin (Gibco) at 37°C with 5% CO2. MUTZ-3-derived Langerhans cells (muLCs) were obtained by differentiation of MUTZ-3 cells for 10 days in 100 ng/ml granulocyte-macrophage colony-stimulating factor (GM-CSF; GenWay Biotech), 10 ng/ml transforming growth factor β (TGF-β; R&D Systems), and 2.5 ng/ml TNF-α (R&D Systems).

5.12.4 muLCs cytokines assays

As described in (van Dalen *et al.*, 2019): 5×10^4 muLCs were stimulated with gamma-irradiated S. aureus strains at indicated bacterium-to-cell ratios in IMDM with 10% FBS. After 24 h, supernatants were collected by centrifugation (300 × g, 10 min, 4°C) and stored at −150°C until further analysis, and cells were washed once in PBS–0.1% BSA. Concentrations of IL-6, IL-8, and TNF-α cytokines were determined by Luminex xMAP assay (Luminex Corporation), performed by the Multiplex Core Facility, UMC Utrecht, Utrecht, The Netherlands.

5.12.4 Soluble beta glucan ligands for dectin-1

Soluble beta glucan (SBG) were kindly provided by Prof. Dr. Bjørn Christensen and fractioned by Size Exclusion Chromatography (SEC) as described in (Qin, Aachmann and Christensen, 2012). In short SBG extracted from cell walls of S. cerevisiae bought from Biotec Pharmacon ASA (Tromsø, Norway), either as 2% aqueous solutions, or as freeze-dried materials. The degree of polymerization (DPn) ranged from 70 to 250. The supplier reported a purity of 98%. No protein or mannoprotein could be detected. Batch 221-7 (DPn = 117) was used as starting material and then further degraded using acid hydrolysis (0.1–100 mM H2SO4, 100 °C, 0–1 h, N_2 atmosphere), followed by neutralisation, dialysis and freeze-drying.

5.13 Recombinant langerin expression and labelling

The extracellular domains (ECDs) of truncated langerin were recombinantly expressed from codon-optimized constructs in pUC19 and pET30a (EMD Millipore) expression vectors as described in (Hanske *et al.*, 2016). In short, recombinant langerin was insolubly expressed in *E. coli*, refolded, and purified via mannan-coupled Sepharose beads (Sigma-Aldrich). Bound protein was eluted with Tris-buffered saline solution (pH 7.5) containing 5 mM EDTA. The proteins were fluorescently labelled by slowly adding 100 µL of 1 mg/ml fluorescein isothiocyanate (FITC; Thermo Fisher) in DMSO to 2 ml of a 2 mg/mL protein solution in HEPES-buffered saline (pH 7.2) containing 20 mM d-mannose (Sigma-Aldrich) and 5 mM $CaCl_2$.

5.14 List of antibodies and primers

List of antibodies

Antigen	Supplier	Product Number	Dilution used
dectin-2	biotechene	FAB3114P	1:100
MINCLE	Sho Yamasaki	N/A	1:50
DC-SIGN	BioLegend	330105	1:200
MCL	Miltenyi Biotec	60522010	1:50
TNFAR	Miltenyi Biotec	130-120-149	1:50
TLR1	Thermo Fisher	12-9011-80	1:50
TLR2	Miltenyi Biotec	130-099-017	1:50
dectin-1	BioLegend	355403	1:100
MGL	Miltenyi Biotec	130-109-641	1:50
Anti-FcεRI Antibody, γ subunit	Millipore Sigma	FCABS400F	1:50
Mouse anti-Syk (pY348)	BD biosciences	560081	1:5
Mouse Anti-ERK1/2 (pT202/pY204)	BD biosciences	612593	1:5
Mouse Anti-Stat1 (pY701)	BD biosciences	612564	1:5

List of primers

GOI		Sequence 5'-3'
	pLV-EF1a-IRES	
DC-SIGN	PFw pLV DC-SIGN	gtcgtgaggatccACCACCatgagtgactccaag
	PRv pLV DC-SIGN	cctcgaggaattctcactacgcaggaggggggt
FcRγ	FcRγ fw	gtcgtgaggatccACCACCatgattccagcagt
	FcRγ rv	cctcgagGAATTCctactgtggtggtttc
MCL	Pfw MCL	gtcgtgaggatccACCACCatggggctagaaaaa
	Prv MCL	cctcgagGAATTCctagttcaatgttgttcca
dectin-1	Pfw d-1	gtcgtgaggatccACCACCatggaatatcatcctgatttag
	Prv d-1	cctcgagGAATTCttacattgaaaacttcttctcac
	RP172	
mincle	MINCLE Fw	GAGCTAGCAGTATTAATTAACCACCatgaattcatctaaatcatc
	MINCLE Rv	GTACCGGTTAGGATGCATGCTCAttaaagagattttcctttg
dectin-2	dectin-2 Fw	GAGCTAGCAGTATTAATTAACCACCatgatgcaagagcagcaac
	dectin-2 Rv	GTACCGGTTAGGATGCATGCTCAataggtaaatcttattcatc

6. Results and Discussion

6.1 Adequate models for lectin signal transduction

To gain insights into the signalling of CLRs at a single cell level, adequate cells which are easy to genetically engineer, manipulate, and grow needed to be found. Additionally, a CLR with a well researched signal transduction pathway and an observable cellular response was needed. THP-1 cells due to their immunological origin as monocytic cells (Tsuchiya *et al.*, 1980) were initially chosen with DC-SIGN overexpressed as model lectin. While the signalling pathway of DC-SIGN is well characterized, the lectin did prove to have no feasible readout for signalling in THP-1 cells. This is because DC-SIGN mainly modulates other signalling pathways such as TLR4 (Teunis B. H. Geijtenbeek and Gringhuis, 2016). THP-1 cells were also found to be hard to transfect and additionally their slow growth rate made them tedious to work with. Subsequently U937 cells, also of monocytic origin, were chosen as model system (Sundström and Nilsson, 1976).

In U937 cells a NFκB responsive GFP reporter system was introduced and found to be feasible, as it provided an easily observable readout at single cell resolution (Fig 17A). These reporter cells produced GFP upon translocation of the immunological transcription factor NFκB. U937 dectin-2 expressing cells did show specific GFP production upon stimulation with the high mannose carbohydrate mannan (Fig 17A).

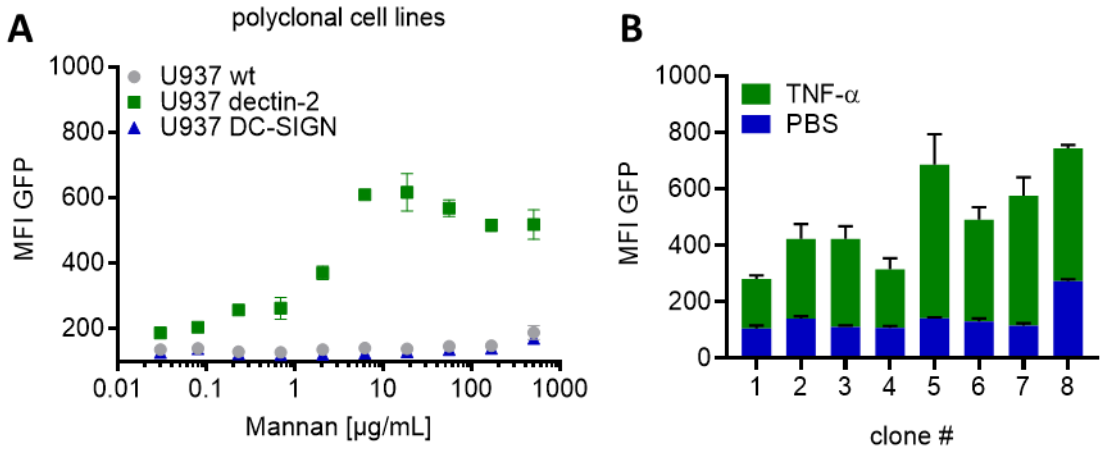

Figure 17: Polyclonal reporter cell lines stimulated with mannan and evaluation of monoclonal cells. A) U937 polyclonal reporter cells expressing dectin-2, DC-SIGN, or wt were stimulated with mannan for 16h, shown is mean ± standard deviation (SD) of n=3 experiments. B) Monoclonal cultures of U937 reporter cells were stimulated for 24h using 5 ng/mL TNF-α, shown is mean ± standard deviation (SD) of n=3 experiments.

Yet as dectin-2 was transduced into the cells before the reporter cell system, genetic diversity could potentially greatly influence comparison to other CLRs. This is because the lentiviral system used for transduction works at a low virion to cell ratio, where approximately 0.1-2% of cells are initially infected at random with the lentivirus. Therefore, the given polyclonal U937 population transduced with two lentiviral constructs in parallel can show big genetic diversity which in turn can affect the subsequent results of signal reporter assays. To avoid this issue polyclonal U937 cells were first transduced with the NFκB responsive GFP reporter system and subsequently expanded from a single cell. In total eight of these monoclonal cultures were generated and clone #5 was picked and used for all following experiments (Fig 17B).

6.1.1 Dectin-2 reporter cell lines behave in line with previous reports

In the established monoclonal U937 reporter cell lines dectin-2, dectin-1, and mincle were expressed (Fig 18). Also, in the monoclonal cells signal transduction of the lectins can be monitored by GFP expression. Three ligands were found to stimulate dectin-2 specifically: Mannan and Invertase, both extracts from *S. cerevisiae*, and FurFurMan a yeast extract from *M. furfur* (Fig 18). The latter had already been described by (Ishikawa *et al.*, 2013) and its additional ability to stimulate dectin-1 was noted by its commercial supplier (InvivoGen, 2018). Invertase is a protein expressed in yeast and glycosylated with high-mannose structures such as Man8GlcNAc2, Man9GlcNAc2, Man9GlcNAc2, and higher (Zeng and Biemann, 1999; Stambach and Taylor, 2003). Hence, its ability to stimulate the mannose binding dectin-2 is not surprising. Mannose as a monosaccharide could not stimulate dectin-2 but is able to inhibit the stimulation of dectin-2 (Fig 18B-C). To sum up, reporter cell lines were generated and their stimulation of human dectin-2 was in line with previous reports on its murine homolog. Murine dectin-2 can be triggered by Man-α1-2 Man moieties presented on scaffolds such as proteins, glycans, or polystyrene beads (Sato *et al.*, 2006; Zhou *et al.*, 2018).

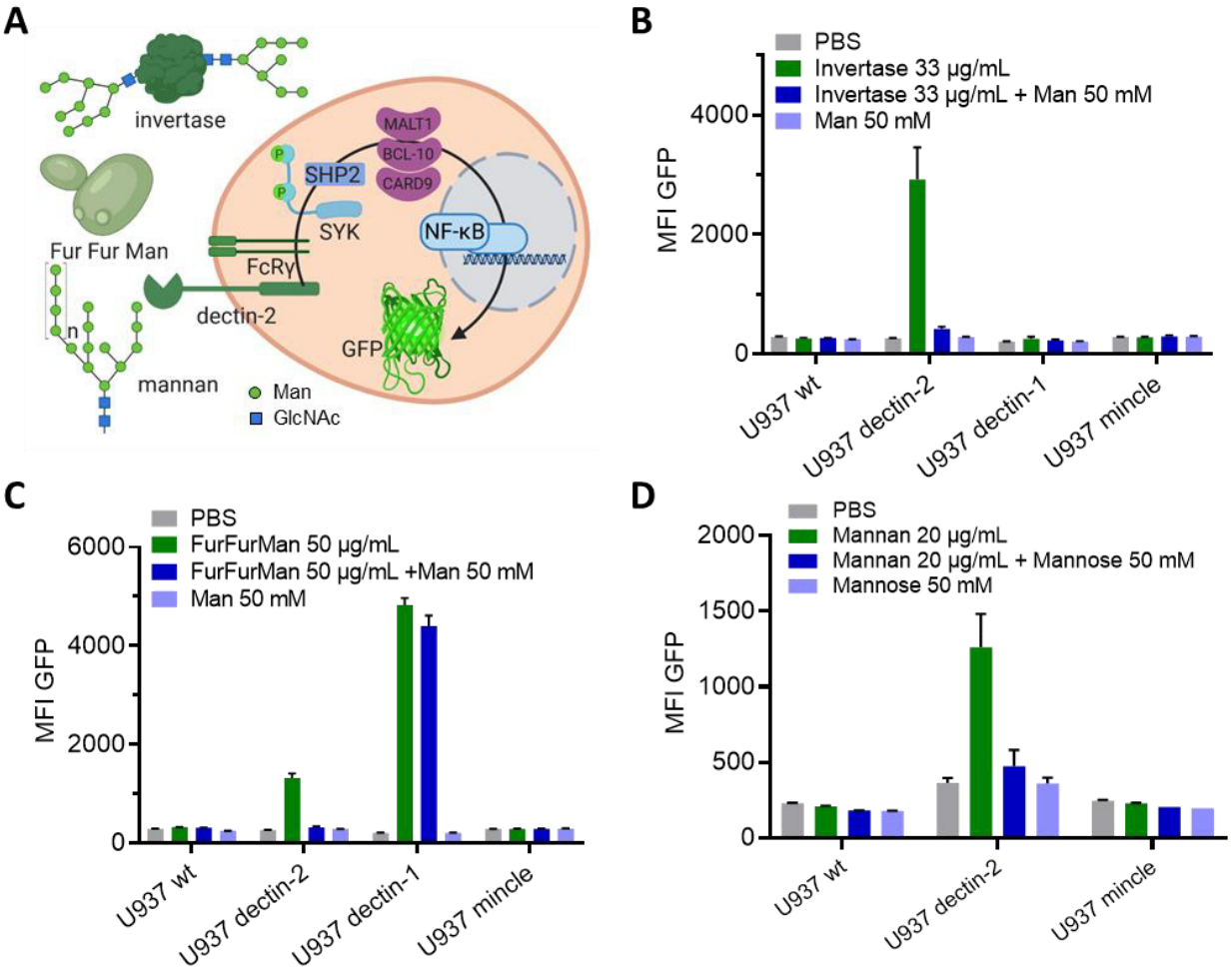

Figure 18: A) Schematic representation of dectin-2 signalling pathway with GFP under control of NFκB, on the left three ligands for dectin-2 (invertase and mannan from *Saccharomyces cerevisiae*, and FurFurMan from *Malassezia furfur*). Scheme created with BioRender.com. B) U937 Monoclonal reporter cells expressing dectin-1, mincle, dectin-2, or wild type were stimulated with invertase for 16h or C) FurFurMan, or D) Mannan, shown is mean ± standard deviation (SD) of n=3 experiments.

6.1.2 Dectin-2 reporter cells show broad population distribution

Next a dose response curve of FurFurMan and dectin-2 expressing reporter cells was recorded. A surprisingly broad distribution of the NFκB dependent GFP expression was noticed (Fig 19A). This dose response can be viewed in two ways: (Fig 19B) On one hand as geometric mean, where the average between multiple experiments is shown ± standard deviation. This is a classic view of flow cytometry data where one might think the data points such as 333.3 µg/mL and 12.5 µg/mL for example are significantly different. On the other hand, when one views the same data as Boxplot it becomes clear that all steps in the titration curve show an overlap with one another. This demonstrated that the spread of cellular population should be taken into account when analysing such data. Additionally, since even the unstimulated population did show an overlap with maximally stimulated cells, it became apparent that dectin-2 does not show a clear two state behaviour with distinct on- and off-states (Fig 19B). Therefore the calculations of (Cheong *et al.*, 2011) were adapted to fit flow cytometry data (see details in Material and Methods). In short, for the cellular output the script is binning the data logarithmically and subsequently assigns each bin to a probability derived from the cellular population distribution. *E.g.:* At the second concentration step, 20% of the cellular population is in bin 3, which translates to a 20% probability of bin 3 at this ligand concentration (Fig 19C). The cellular input are already given as distinct events with a probability, in this case 8 concentrations of FurFurMan with a probability of 1/8 each. The bins are then adjusted to maximize the mutual information between the ligand concentration and the FI (fluorescence intensity) of GFP thus calculating the channel capacity. This channel capacity is a metric to quantify the maximal mutual information, which can be transmitted by the dectin-2 channel by FurFurMan as ligand. The information channel is in this case dectin-2 and its signal transduction pathway to NFκB (Fig 18A). In sum a script was developed to calculate the channel capacity of the NFκB reporter cells.

Despite dealing with monoclonal reporter cells, it was questioned whether the broad cellular distribution in the dectin-2 response had a genetic component. Therefore, stimulated dectin-2 cells were sorted in two discrete population: one low and one high GFP when reacting to mannan. Those two populations where then stimulated again two weeks afterwards and did show an equal cellular response and distribution. This demonstrated that the monoclonal cellular population was indeed homogeneous in its signalling behaviour (Fig 19D).

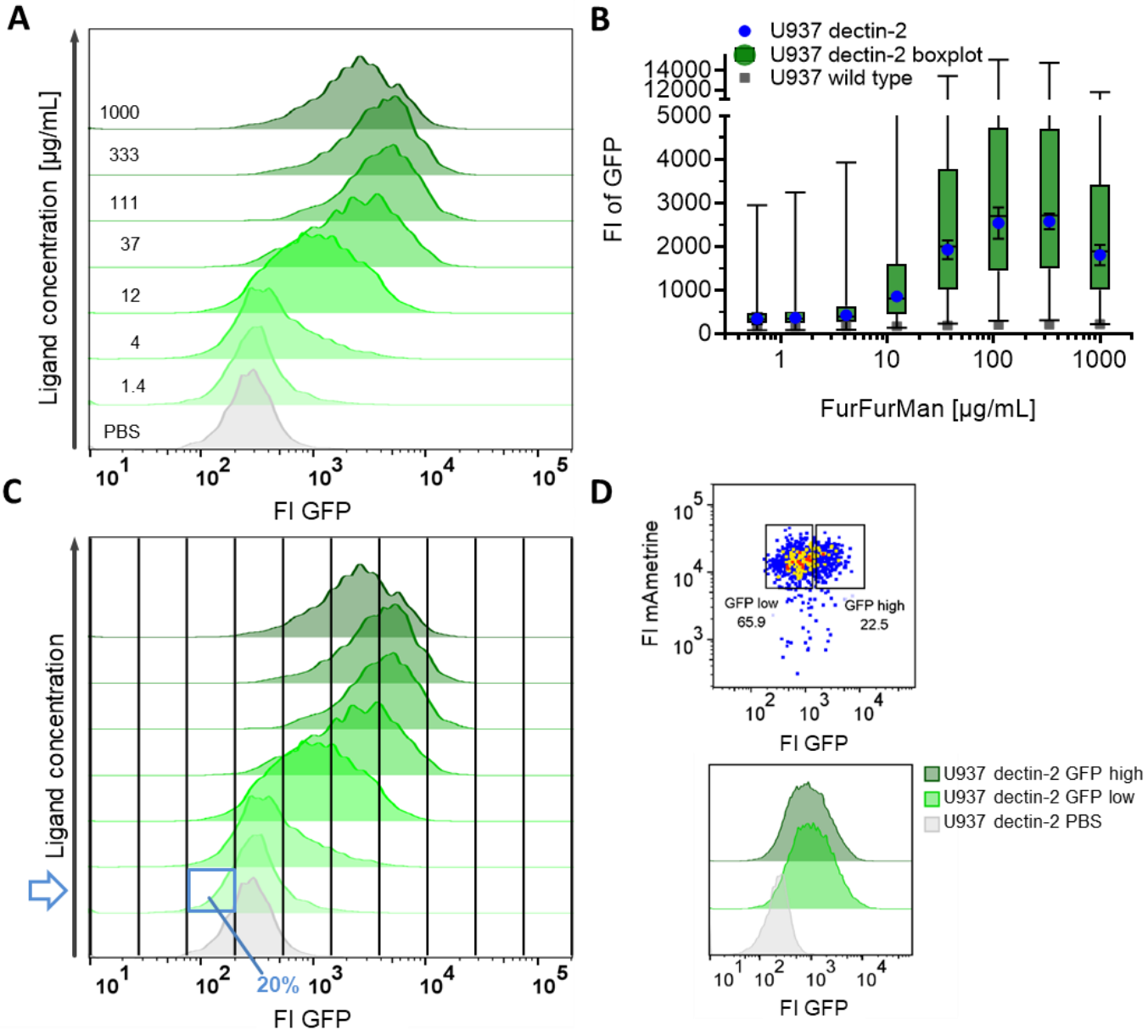

Figure 19: A) Dose response of U937 dectin-2 reporter cells reacting to FurFurMan stimulation (16 h) as representative histograms of the same titration curve as seen in B) Dose response of dectin-2 reporter cells is shown both as mean with standard deviation and Boxplot with the whiskers representing the 1 percentile of the cellular population (n=6). C) Again, dose response of dectin-2 reporter cells as histograms, exemplifying the calculation of channel capacity. D) Top: U937 dectin-2 reporter cells were stimulation for 16 h with 300 µg/mL Mannan and sorted in a GFP high and low population. Bottom: The sorted reporter cells were then re-stimulated two weeks later with 500 µg/mL Mannan.

6.1.3 Logarithmic binning of flow cytometry data is apt for channel capacity calculation

The work of Cheong et al., 2011 is based on microscopy data and uses linear binning of the output (cellular response). Flow cytometry data however is distributed and plotted logarithmically (Fig 19C); therefore, logarithmic binning was used (Fig 20). Additionally, the binning number used in the calculation needed to be evaluated, as it could potentially influence the calculated channel capacity. Therefore, U937 reporter cells expressing dectin-2 were either stimulated with Invertase or TNF-α to gain data on the associated channels. Figure 20 shows the calculated channel capacity from TNF-α (blue) and dectin-2 (green) channels under the logarithmic and linear output binning method. In the case of logarithmic binning, the channel capacity reaches its plateau from around 2^3 to 2^9 bins, therefore 20 bins were used for all calculations.

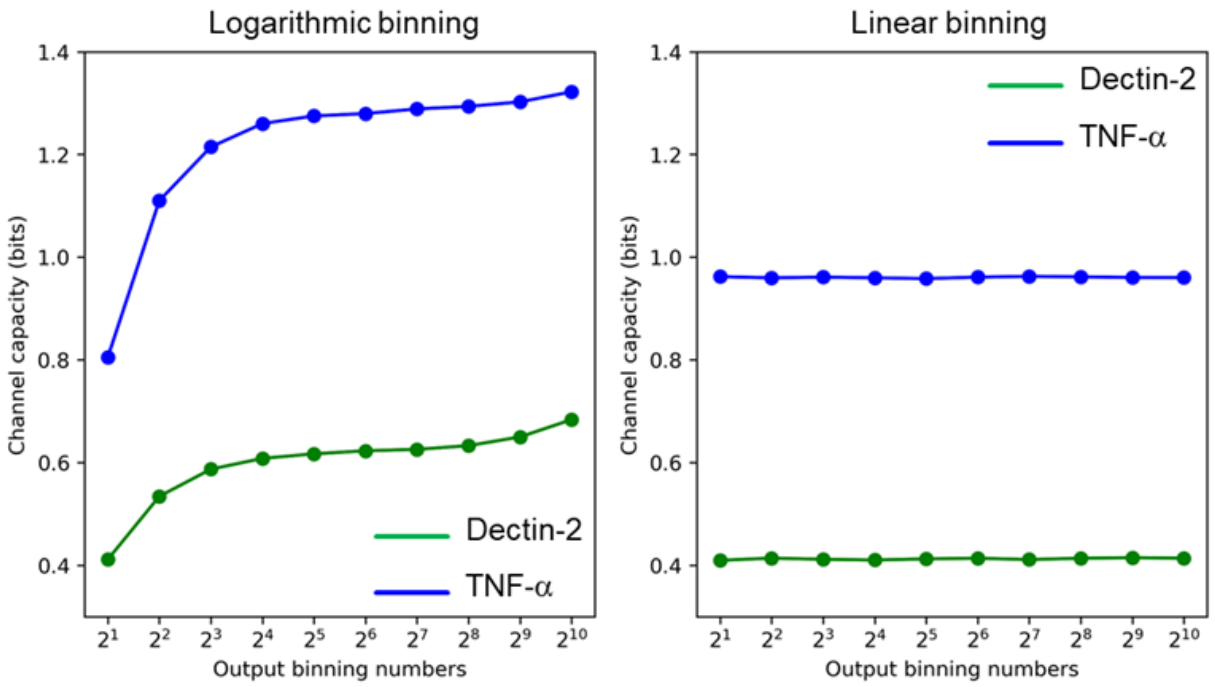

Figure 20: Influence of binning number and mode on channel capacity. Calculated channel capacities with logarithmic binning (left) and linear binning (right). In channel calculations shown in this thesis logarithmic binning was used, due to the logarithmic nature of the data.

6.1.4 Receptor quantifications points out dectin-2 inefficiency

To see whether other related lectins would show a similar or different signalling pattern as dectin-2, dectin-1 and mincle expressing reporter cells were made. Dectin-1 could specifically be stimulated with depleted zymosan (DZ) and mincle with the ligands Trehalose-6,6-dibehenate (TDB) and Trehalose-6,6-dimycolate (TDM). Additionally, U937 cells endogenously express the TNFAR and TLR1&2, which could be stimulated with TNF-α and PAM3CSK4 respectively. A total of five channels (each consisting of receptor + connected signal transduction pathway) could be stimulated and the channel capacity for various ligands calculated (Fig 21A, B). The TNFAR channel was found to have the highest capacity of 1.35±0.05 bit, which was not influenced by the introduction of additional lectins (*e.g.* mincle, dectin-2, and DC-SIGN, see Fig 21C). Dectin-1 came second at 1.22±0.06 bit, while both mincle and TLR1&2 had a channel capacity of 1.00±0.01 bit. In contrast, dectin-2 stimulation resulted in a channel capacity of 0.74±0.14 bit using FurFurMan. Stimulation using heat inactivated Invertase or mannan gave 0.77±0.10 and 0.44±0.09 bit, respectively. MGL, MCL and DC-SIGN could not be stimulated using known adequate ligands such as Tn-Muc1, TDB and Invertase, and mannan and Invertase, respectively (Fig 34, Fig 30, Fig 25). Although mannan was expected to be a strong stimulant for dectin-2 due to its many mannose residues, it did prove to be a rather poor ligand supposedly due to many other glycosidic linkages than Man α1-2 that is thought to be the minimal stimulating motif of dectin-2 (Zhou *et al.*, 2018). THP-1 cells were also transduced with the NFκB reporter construct, but showed much lower GFP expression than U937 cells. Also in these cells TNFAR stimulation did result in much higher GFP expression than dectin-2 stimulation (Fig 35).

Potentially the channel capacity could be limited by the number of receptors available, which might explain the relative inefficiency of dectin-2. Therefore, the number of receptors on the cells was quantified with antibody stains. No relationship was found between the number of proteins and the channel capacity of a given receptor (Fig 21D, E). In addition, the amount of protein did differ greatly between the receptors: DC-SIGN for example was around 200-fold more expressed than dectin-2, which is striking since they are being expressed in the same cell line with the same vector under the same promoter (Fig 21E). With the use of an in vitro model system and channel capacity as a quantitative metric, dectin-2 was found to be relatively ineffective when stimulated with three ligands, while the closely related mincle uses the same pathway effectively. Overall, this points towards the receptor molecule itself determining very early on its use of a signal transduction pathway.

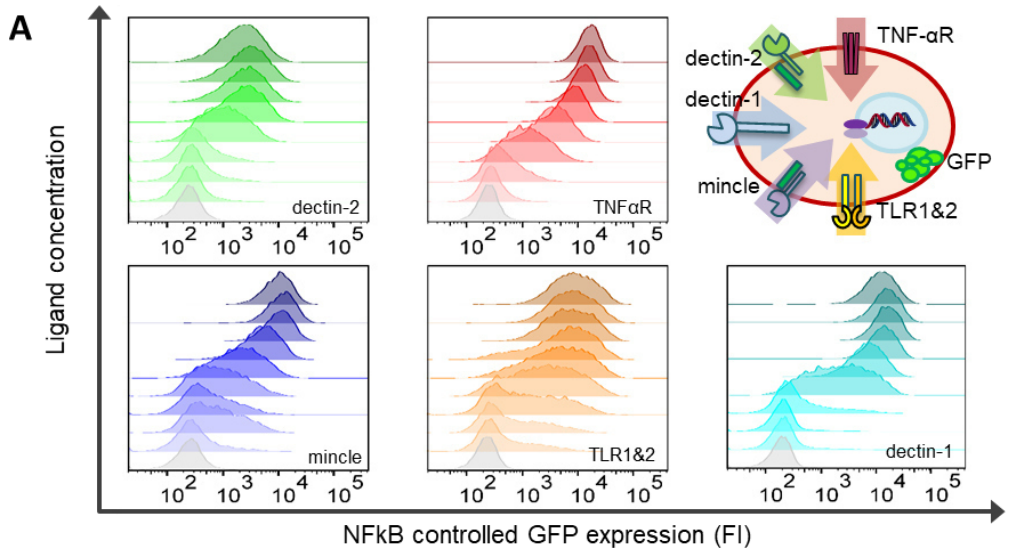

B

Receptor	Ligand	Max. I (bit)
TNFAR	TNF-α	1.35±0.05
dectin-2	FurFurMan	0.77±0.10
dectin-2	Mannan	0.44±0.09
dectin-2	Invertase	0.74±0.14
MINCLE	TDB	1.00±0.01
MINCLE	TDM	1.01±0.02
TLR1&2	PAM	1.00±0.01
dectin-1	DZ	1.22±0.06

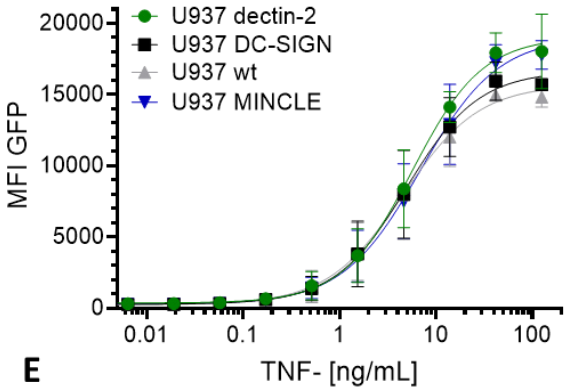

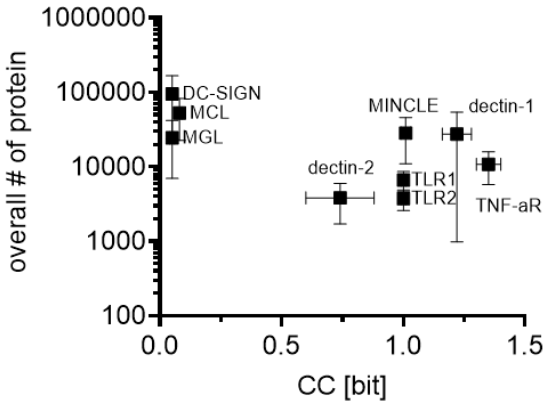

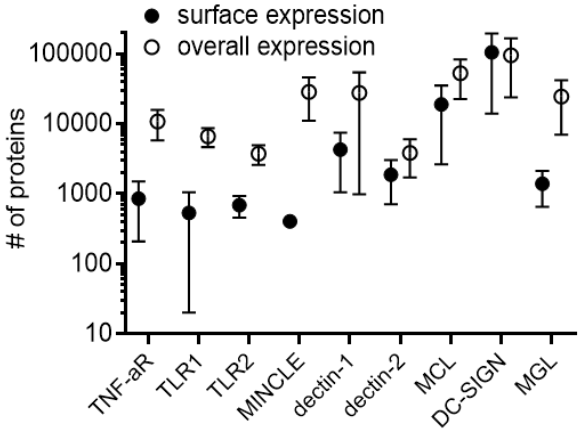

Figure 21: Quantification of immune receptor signalling and expression. A) Representative histograms of U937 reporter cells dose response, stimulated specifically with invertase for dectin-2, TNFα for the TNFαR, TDB for mincle, PAM3CSK4 for TLR1&2, and depleted zymosan for dectin-1. Top right panel shows a schematic representation of the five analyzed receptor channels. B) Table summarizing the receptors calculated channel capacities with the respective ligands showing mean ± SD of n≥3 of independent experiments. Channel capacity values given are an average of all experiments conducted. C) Reporter cell lines expressing various lectins stimulated with TNF-α, n=2. D) Correlation of the overall number of receptors expressed and the channel capacity E) Quantitation of surface and overall expression of receptors expressed in U937 reporter cells. Cells were stained either for their surface expression, or their overall protein expression. Graph shows geometric mean ± robust SD of the cellular population.

6.2 Signal integration compromises between lectin receptors when both are engaged.

Since FurFurMan is able to stimulate both dectin-1 and dectin-2, reporter cells expressing either of these lectins were generated. Additionally, a cell line expressing both dectin-1 and dectin-2 was generated. All three of these were then stimulated with FurFurMan, with the following results: Dectin-1 expressing cells gave a higher maximal signal and channel capacity than dectin-2 expressing cells, however the latter channel showed higher sensitivity (EC_{50}) to FurFurMan. We can also see that the double positive cells do compromise between the two channels displaying the lower EC_{50} of dectin-2 cells as well as the higher channel capacity of dectin-1 cells (Fig 22A, B). The results of the dectin-2 dectin-1 cells are particular interesting since at high levels of FurFurMan the dectin-2 channel inhibits dectin-1 function, resulting in a lower response that only dectin-1 expressing cells would (Fig 22A). When depleted zymosan (DZ) a dectin-1 specific ligand was used, dectin-2 expression did not significantly influence the cellular reaction. Dectin-2 specific signalling in turn was also not influenced by dectin-1 expression (Fig 22C-E). This shows that neither channel by itself does influence each other, unless activated. It was also found that the level of receptor expression for dectin-2 or -1 did not change upon expression of the other lectin (Fig 22F). Additionally, inhibition of dectin-2 with mannose turned U937 dectin-2 dectin-1 expressing cells to exhibit the dose response curve of dectin-1 expressing cells upon FurFurMan stimulation. (Fig 36)

These results demonstrate that when multiple lectins using a similar pathway are engaged simultaneously, the cells will integrate both channel by compromising between them rather that favour one over the other or using the most active channel available. This is an exciting discovery since there have not been any studies showing quantitatively how the signals of multiple lectin receptors are being integrated. From this, it can be imagined that during a fungal infection with multiple (carbohydrate) ligands, the precise arsenal of immune receptors and connected pathways a given immune cell expresses are integrating the information contained within the carbohydrate and non-carbohydrate ligands. This in turn leads to a compromise of all activated receptors and results in a specifically tailored biochemical response of the given immune cell.

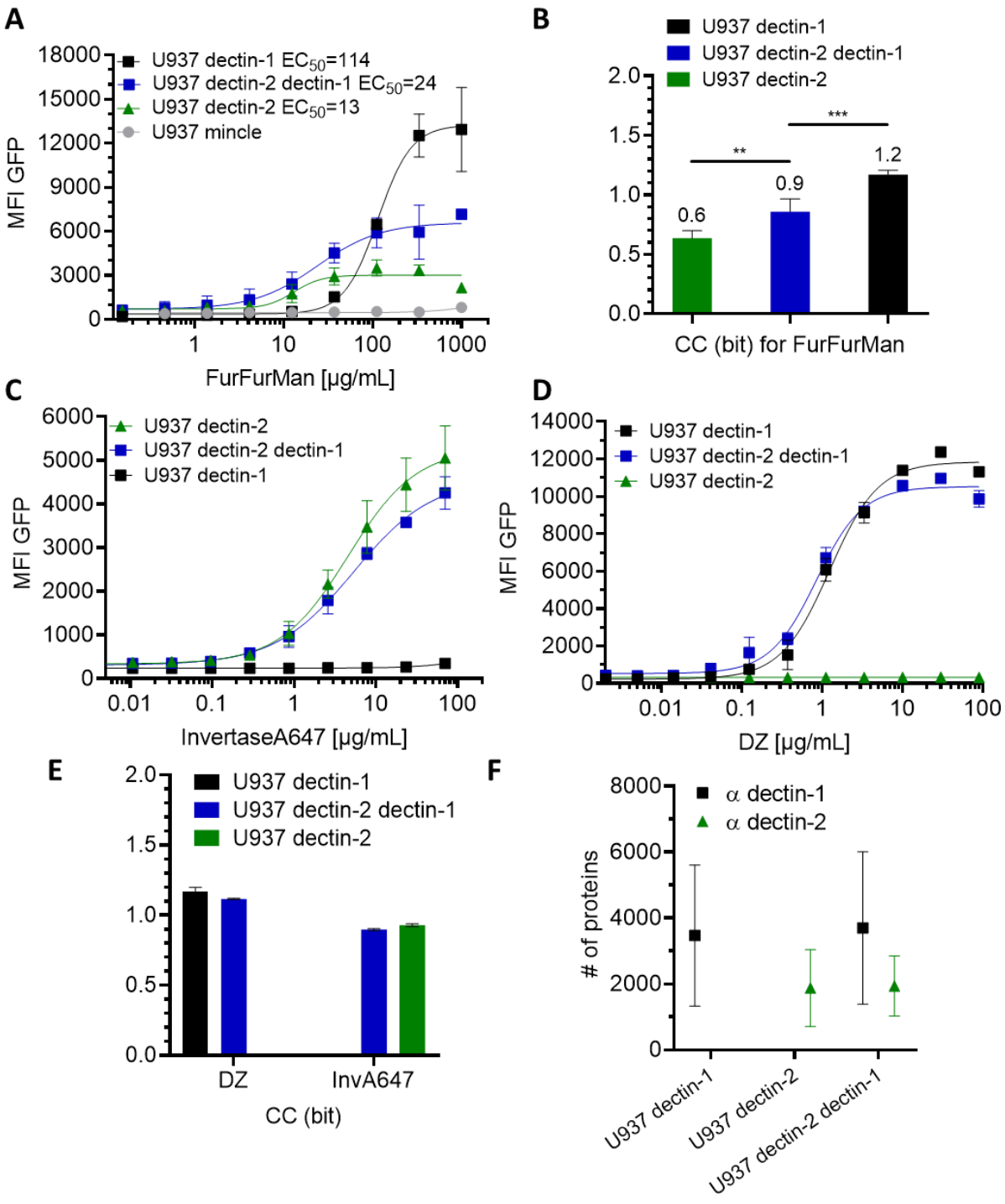

Figure 22: Signal integration between dectin-1 and dectin-2. A) Monoclonal reporter cells either expressing mincle, dectin-2, dectin-1, or both dectin-2 and dectin-1, (n≥3) were stimulated for 16h with various concentrations of FurFurMan. The 95%CI (profile likelihood) for the EC50 are as follows for dectin-1 99-132 µg/mL, for dectin-2 9-18 µg/mL, for dectin-2 dectin-1 16-42 µg/mL. B) Channel capacities of the data in A. C) and D) Monoclonal reporter cells either expressing dectin-2, dectin-1, or both dectin-2 and dectin-1, (n≥3) were stimulated for 16h with various concentrations of InvertaseA647, or depleted zymosan respectively. E) Channel capacities of the data in C and D. F) Quantitation of surface expression of U937 dectin-1, dectin-2, and dectin-1 dectin-2 U937 reporter cells. Graph shows geometric mean ± robust SD of the cellular population.

6.2.1 Dectin-1, but not dectin-2 signalling is phosphorylating proteins in multiple signal transduction pathways

To gain more insight into the mechanism of signal integration, three phosphoproteins were used as activation markers: pERK (pT202/pY204), pSTAT1 (pY701), and pSYK (pY348). These three were chosen due to their importance in innate immune signalling and each being present in different signal transduction pathways (Bi *et al.*, 2010; Zhong *et al.*, 2011; Khodarev, Roizman and Weichselbaum, 2012). pERK for example is found in the MAP kinase pathways, it can also be phosphorylated by SYK, and its signalling cascade is generally found in a plethora of processes (Wortzel and Seger, 2011). The three markers were investigated with antibody staining of their phospho-epitopes a techniques also known as phosflow. Albeit being a complex technique, phosflow has the advantage of having single cell resolution (Krutzik and Nolan, 2003). While dectin-1 activation by SBG could be observed with these three markers within 60 minutes, dectin-2 did not show a response for pERK, pSTAT, or pSYK (Fig 23). Therefore, SYK Y348 is not phosphorylated upon dectin-2 stimulation with FurFurMan, unlike dectin-1 stimulation with a soluble beta glucan (SBG). Section 6.5 of the results gives more information on the soluble beta glucan ligands. pERK and pSTAT1 are known to be activated by dectin-1 (Eberle and Dalpke, 2012; Negi *et al.*, 2019), as neither of the two responded to dectin-2 stimulation this could be an explanation of how dectin-1 can overall transmit more information to NFκB, by activating more pathways than dectin-2. pSYK on the other hand is known to be phosphorylated in dectin-1 and dectin-2 signalling on Y525/526 for subsequent NFκB activation (Bi *et al.*, 2010; Bode *et al.*, 2019). The additional phosphorylation on pSYK (Y348) could potentially be a mechanism by which dectin-2 and dectin-1 might differentially influence the pathway downstream of SYK.

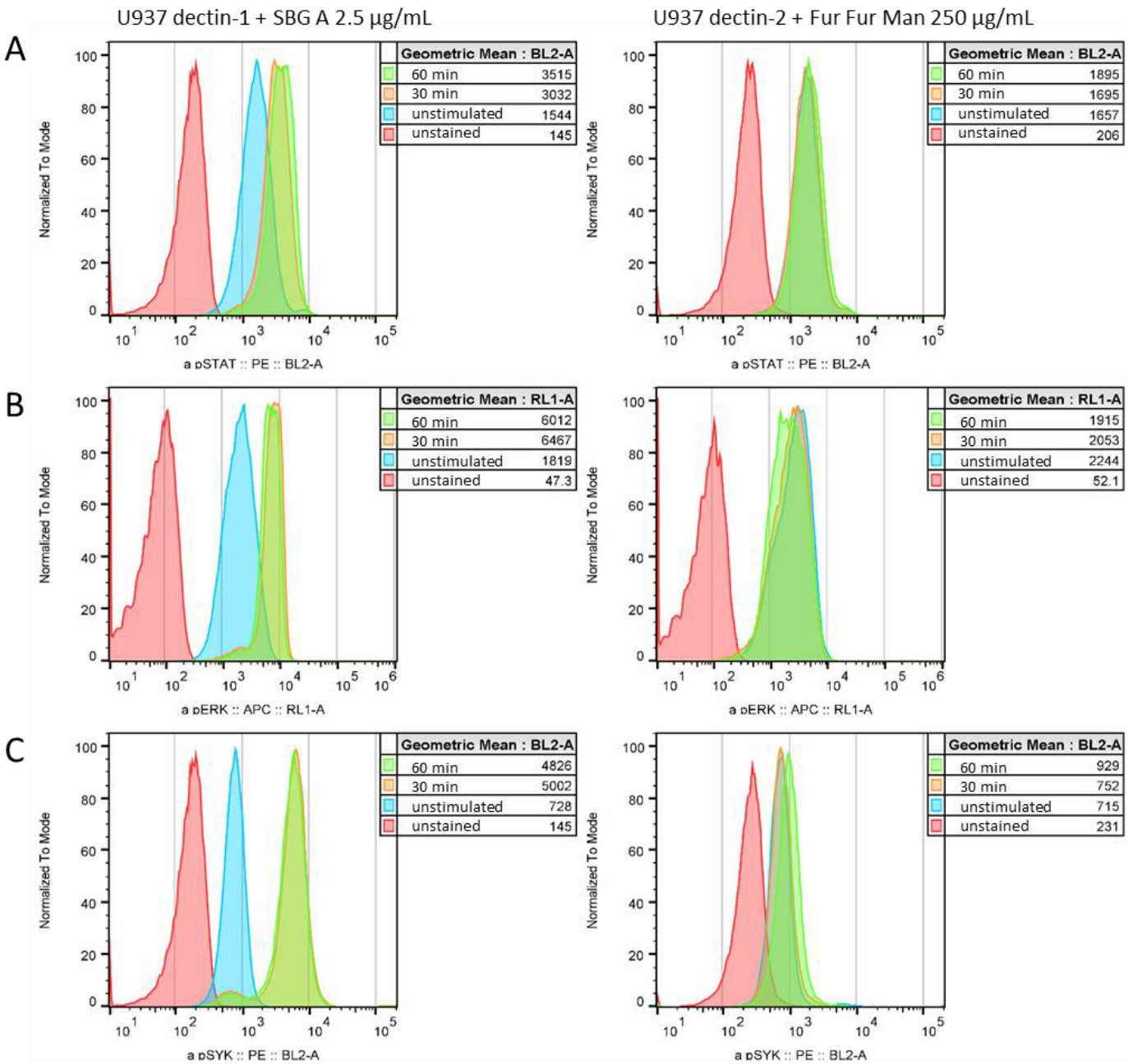

Figure 23: Staining of phospho-epitopes upon dectin-1 and dectin-2 stimulation. Histograms of U937 reporter cell either expressing dectin-1 or dectin-2 were stimulate using soluble beta glucan or FurFurMan for the indicated period. Cells were stained with specific antibodies for A) pSTAT1 (pY701), B) pERK (pT202/pY204), C) pSYK (pY348). Unstained cells were stimulated but not stained with the indicated antibody. Unstimulated cells were stained with the indicated antibody, but not stimulated with the indicated ligand.

6.3 Signal adapter molecule overexpression does not rescue dectin-2 channel capacity

The relatively low channel capacity of dectin-2 was still striking especially as mincle uses the very same signal transduction pathway to transmit more information. One possible reason might be the overexpression of FcRγ, since for effective mincle signalling this signalling protein had to be overexpressed in U937 cells. We hypothesized overexpression of the signalling protein FcRγ might increase the information transmitted via dectin-2. The overexpression of FcRγ resulted in at least twofold increase of this signalling adapter, as seen by antibody stain (Fig 24A). While the overexpression of FcRγ did increase the maximal MFI of dectin-2 cells a high basal activation of these cells can be seen. Interestingly the channels sensitivity for its ligand (EC_{50}) increased about 50-fold in the dectin-2 FcRγ cells as compared to the dectin-2 cells (Fig 24B). The channel capacity on the other hand decreased to 0.36±0.14 bit at the same time, due to this high basal level of activation (Fig 24C). From this example of dectin-2, it was concluded that the channel capacity of a glycan-based communication channel is not necessarily coupled to its sensitivity and that the capacity of a communication channel is not well described by its amplitude (*e.g.* MFI) either. Since dectin-2 can be inhibited by mannose, the U937 reporter cells were cultivated in the presence of either 25mM mannose (Man cult) or galactose (Gal cult) or under normal cell culture conditions (Norm cult). Only mannose was able to significantly reduce the basal level of the U937 dectin-2 FcRγ cells, which indicates that the activation is indeed dectin-2 mediated (Fig 24D).

By staining U937 cells with recombinant dectin-2, it was shown that dectin-2 recognizes moieties on U937 cells (Fig 24E). We suspected these moieties to be Man9GlcNAc2 structures since Man9GlcNAc2 possess three terminal Man α1-2 disaccharides. Therefore, U937 cells were treated with Kifunensine (KIF), an inhibitor of class I α-mannosidases, which effectively blocks the processing of N-glycans in the ER resulting in an overproduction of Man9GlcNAc2 moieties. We expected this to greatly increase the basal recognition of dectin-2 cells, however, the exact opposite took place and KIF treated dectin-2 cells were unable to react to Invertase while still able to signal via other receptors such as TNFAR (Fig 24F, Fig 37). A possible explanation for this is that Man9GlcNAc2 structures are bound by dectin-2 but do not trigger signalling. Since the Man9GlcNAc2 are spread out over the whole cellular surface no clustering of dectin-2 can take place and no signalling can be initiated.

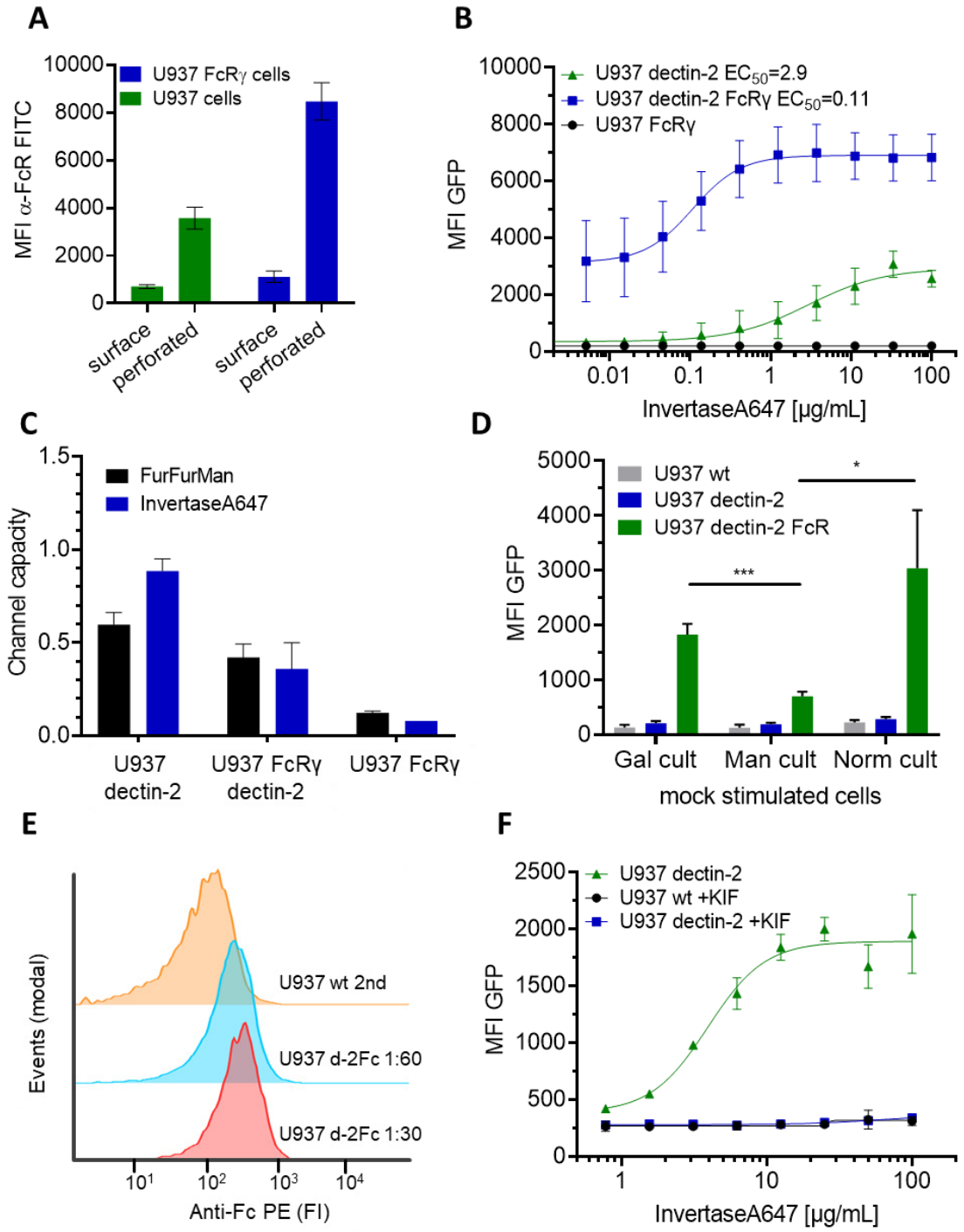

Figure 24: Signal adapter overexpression, and manipulation of U937 cells. A) Bar graph showing the mean fluorescent intensity of an anti-FcRγ stain, either U937 wt of U937 FcRγ cells, surface or total protein stain. n=2 B) Monoclonal reporter cells either expressing dectin-2 (n=3), FcRγ (n=2), or dectin-2 and FcRγ (n=5) were stimulated for 16h with various concentrations of invertase. The 95%CI for the EC50 are as follows for dectin-2 1.3-12.3 µg/mL, for dectin-2 FcRγ 0.03-0.22 µg/mL. C) Calculated channel capacities from invertase stimulation (n=3), data also seen in Figure C) and FurFurMan stimulation (n=2) of U937 reporter cells. D) Mock stimulated reporter cells 16h after cultivation with 25 mM mannose, or galactose, or under normal conditions for 48h (n=3). Statistical significance determined with an unpaired t-test. E) U937 cells were stained with recombinant dectin-2Fc and detected with a secondary anti-Fc antibody-PE. F) U937 cells cultivated with or without the inhibitor kifunensine (7.5 µM) for 48h, then stimulated with Invertase for 16h, shown is the mean ± SD of n=3.

Taken together, the relatively low amount of information transmitted by dectin-2 cannot be increased by overexpression of FcRγ, but its sensitivity (EC_{50}) can. Additionally, recombinant dectin-2 does bind moieties on U937 cells and the basal level of dectin-2 FcRγ can be inhibited by mannose.

6.3.1 Directly labelled ligands are consistent with unlabelled ligands

The channel capacity calculations shown so far are based on the different concentrations of a dose-response curve. However, in this case no information about ligand to cell binding is observed. This in turn could mean that essential data about information transmission from ligand to receptor is not taken into account in the mutual information calculations. Therefore, the protein ligands TNF-α and Invertase were labelled with the fluorescent dye Atto647N. Now it was possible to use continuous binding data rather than discrete concentration steps (Fig 25A). The channel capacity calculated from labelled ligand experiments was the same as from the unlabelled ligand experiments, validating the results of the unlabelled experiments. Also, channel capacities from a discrete concentration curve or a continuous labelled input did give the same channel capacities (Fig 25B). Additionally, from the binding response graphs it was possible to see, that the cellular reaction reaches saturation well before receptor binding does (Fig 25A). However, this conclusion is speculative, since it only takes about 6h for the reporter cells to reach full stimulation (Fig 25C) and in the remaining incubation time more ligand can potentially be taken up.

6.3.2 Synergistic lectins do not enhance dectin-2 channel capacity

Since neither overexpression of adapter molecules nor taking binding data into account would enhance dectin-2 channel capacity it was hypothesized that dectin-2 needs another lectin to synergistically increase its signalling capacity. Therefore DC-SIGN and MCL were expressed alone or in combination with dectin-2 on U937 reporter cells (Fig 26A). DC-SIGN was picked as it is a mannose binding lectin known to influence NFκB signal transduction and MCL because it has known interactions with dectin-2 and mincle (Zhu *et al.*, 2013; Ostrop *et al.*, 2015). Although DC-SIGN does not elicit signalling on its own in U937 cells, it is known to recognize high mannose structures present on Invertase (Gringhuis *et al.*, 2009).

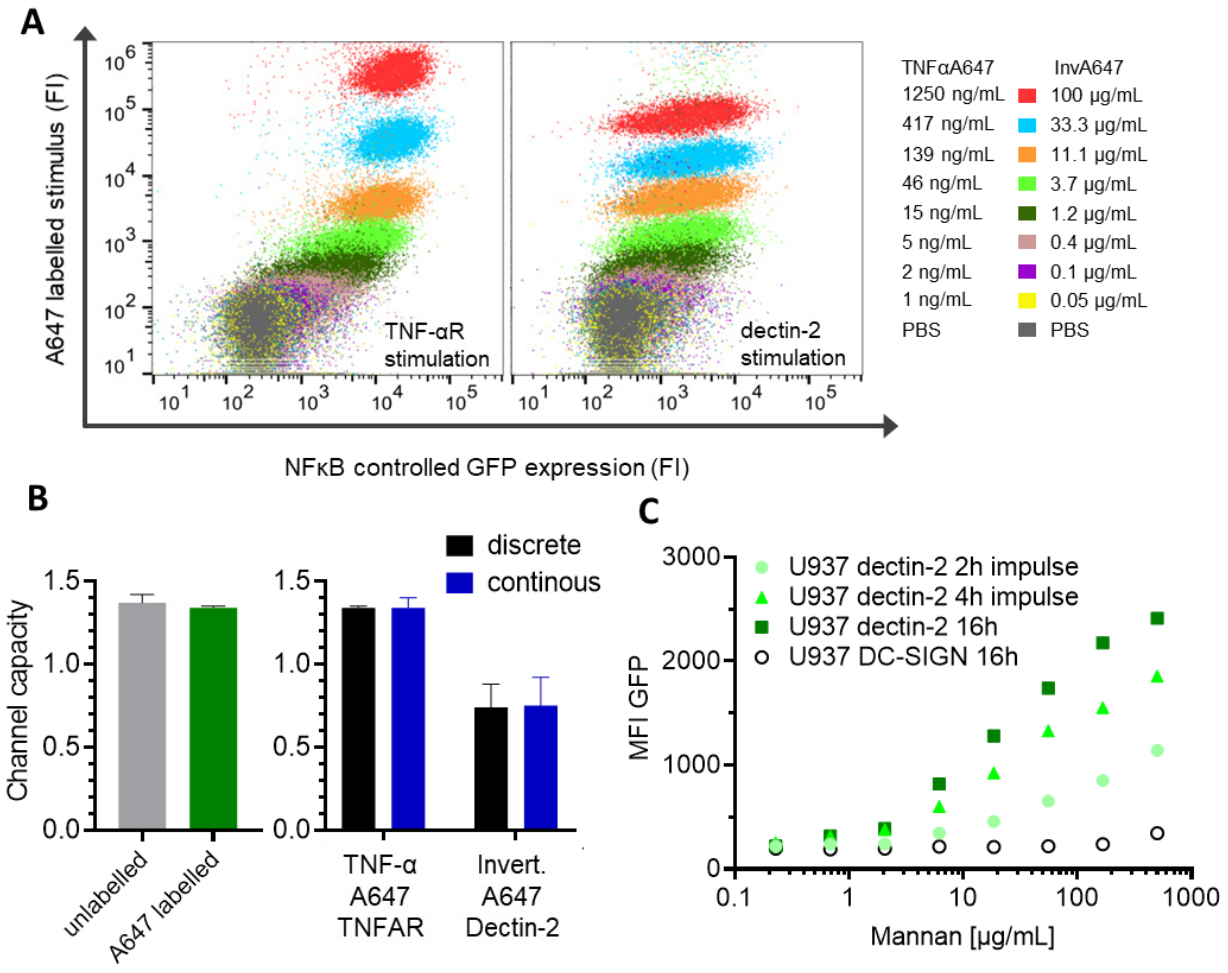

Figure 25: U937 reporter cell stimulation with labelled ligands A) 2D plots of single cells resolved dose responses of U937 dectin-2 reporter cells. Left: cells were stimulated with Atto647 labelled TNF-α. Right: cells were stimulated with Atto647 labelled invertase. Colors from red to grey represent titration of the ligands. B) Left: A647 labelled and unlabeled TNF-α result in the same channel capacity in U937 reporter cells. Right: Comparison of channel capacities for Atto647N labelled Invertase or TNF-α, calculated with discrete titrations of ligand or with using the discrete A647 FI instead. n≥5 bars represent mean ± SD C) Dose response of dectin-2 and DC-SIGN expressing reporter cells stimulated for 16h, or stimulated for 2 and 4 h, washed in fresh media and incubated to a total of 16h.

As expected, DC-SIGN expression significantly increased ligand binding of the U937 cells (Fig 26C). It was then speculated that this would either aid the recognition by pre-concentration of the ligand on the plasma membrane or serve as a decoy receptor decreasing stimulation of dectin-2. In fact, DC-SIGN mediated ligand binding did not alter the dectin-2 channel capacity for FurFurMan or Invertase stimulation (Fig 26B). Although dectin-2 DC-SIGN cells did show a lower EC_{50} and therefore higher sensitivity than sole dectin-2 cells (Fig 26A). MCL expressing cells did not respond or bind Invertase and no synergistic effect with dectin-2 was observed (Fig 26A-C).

It could be that the difference in channel capacity between dectin-2 and other receptors is simply a matter of affinity, since TNFAR for example has a nanomolar affinity for its ligand (Grell *et al.*, 1998). Therefore, an anti-dectin-2 antibody was used to stimulate dectin-2 cells. Even under these conditions, no increase in channel capacity compared to dectin-2 cells was seen (Fig 26D). In sum, dectin-2 channel capacity could not be increased by additional lectin expression (DC-SIGN, MCL), and the use of an antibody as ligand did not increase dectin-2 channel capacity.

6.4 High noise results in dectin-2 signalling inefficiency

A striking feature throughout this study that distinguished the high capacity TNFAR channel from dectin-2 in our reporter cells is its broad distribution of the cell population (Fig 27A). A commonly used measure for the variation of a cell population, or rather cellular noise, is the squared normalized standard deviation (CV^2) (Colman-Lerner *et al.*, 2005). Therefore, data obtained from the dose response measurements was used and the noise quantified. While TNFAR and mincle showed low noise at their point of maximal stimulation, dectin-2 noise increased and remained at elevated levels during titration of both FurFurMan and Invertase (Fig 27A, B). In addition, the high channel noise of TLR1&2 and the low noise of dectin-1 were able to reach a relative minimum at maximal stimulation (Fig 27B). The question raised then was whether the high noise associated with the dectin-2 channel could be a result of cellular characteristics in turn dependent on environmental factors. If for example bigger cells were able to signal via dectin-2 with less associated noise than smaller cells. Then cell size would show a correlation with expressed GFP and cellular volume would play a significant role in dectin-2 signalling. But neither forward scatter (a measure for cell size) nor sideward scatter (a measure for cellular granularity) did correlate with NFκB dependent GFP expression of the dectin-2, mincle, and TNF-αR channel (Fig 27C).

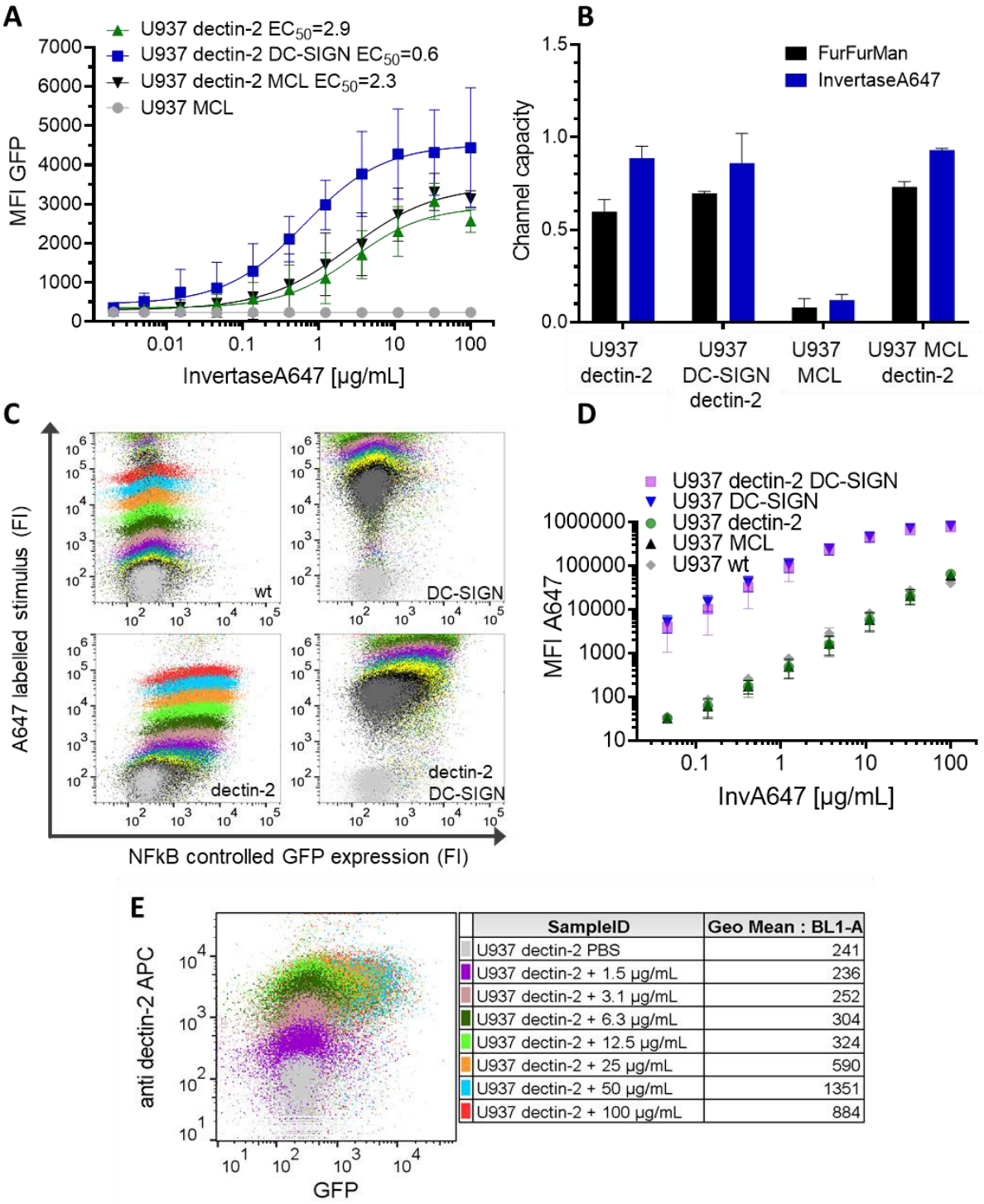

Figure 26: Potentially synergistic lectins expressed with dectin-2 in U937 reporter cells. A) Dose response of Atto647 labelled invertase stimulation of U937 cells expressing dectin-2 alone, in combination with DC-SIGN, or in combination with MCL n≥3. The 95%CI (profile likelihood) for the EC50 are as follows for dectin-2 1.3-12.3 µg/mL, for dectin-2 DC-SIGN 0.2-1.9 µg/mL, for dectin-2 MCL 1.0-16.8 µg/mL. The EC50 of dectin-2 DC-SIGN did significantly differ from dectin-2 (p=0.0415), but dectin-2 MCL did not. B) Channel capacities of dectin-2 in combination with DC-SIGN and MCL after stimulation with either FurFurMan or invertase n≥3. C) 2D dose response of U937 reporter cells expressing lectins as indicated, representative 2D plots of dose responses seen in A. D) InvertaseA647 binding to various lectin expressing cell lines, after 16h incubation. These are the binding data to B, n=3. E) 2D dose response of dectin-2 U937 reporter cells stimulated with anti dectin-2 for 16h.

The high noise of dectin-2 also was also not associated with a certain growth phase of the cell cycle (Fig 27D). In the U937 reporter cells two fluorescent proteins are expressed, the NFκB dependent GFP and the constitutively expressed mAmetrine, which originally served as a marker for vector presence in the cells. Additionally, such a non-equivalent protein expression can be used to distinguish factors that affect general protein expression and factors that are specific for pathway dependent protein expression. This is because a lot of the variation in protein expression is due to cell-to-cell differences: *e.g.* some cells are better equipped for protein expression due to extrinsic variation in cellular components or intrinsic variation (stochastic variation) (Colman-Lerner *et al.*, 2005). Therefore, pathway dependent GFP as well as constitutively expressed mAmetrine are correlated (Fig 27E). Factors disturbing this correlation therefore have to affect one factor more than the other. For example, if a mutation disturbing NFκB translocation was introduced, it would affect GFP but not mAmetrine expression. A mutation affecting protein expression or folding would affect both GFP and mAmetrine. In the same way the variation along the GFP-mAmetrine correlation is due to cell-to-cell differences in expression. But the variation normal to their correlation line is due to GFP specific expression, which in turn depends on the stimulated information channel or receptor (See Figure 9 and section 3.6.1 on page 33 for further information). Interestingly, the cellular response of TNFAR and mincle did correlate well with mAmetrine (R^2 of 0.68 and 0.67), in contrast to dectin-2 (R^2 of 0.31) (Fig 27E). The NFκB triggered GFP expression noise was corrected for the expression noise of the unrelated constitutively fluorescent protein mAmetrine, thus correcting for the general cell-to-cell noise in protein expression (See Material and Methods section on protein expression correlation). Nonetheless, the noise level of the dectin-2 channel stayed significantly higher than that of TNF-α and mincle (Fig 27F). Thus, dectin-2 NFκB signalling is accompanied by a high noise level, albeit not because of protein expression noise, cell morphology, or mitotic cell cycle. Therefore dectin-2 signalling seems to be inherently noisy and an inefficient transmitter of information relative to mincle and TNFAR.

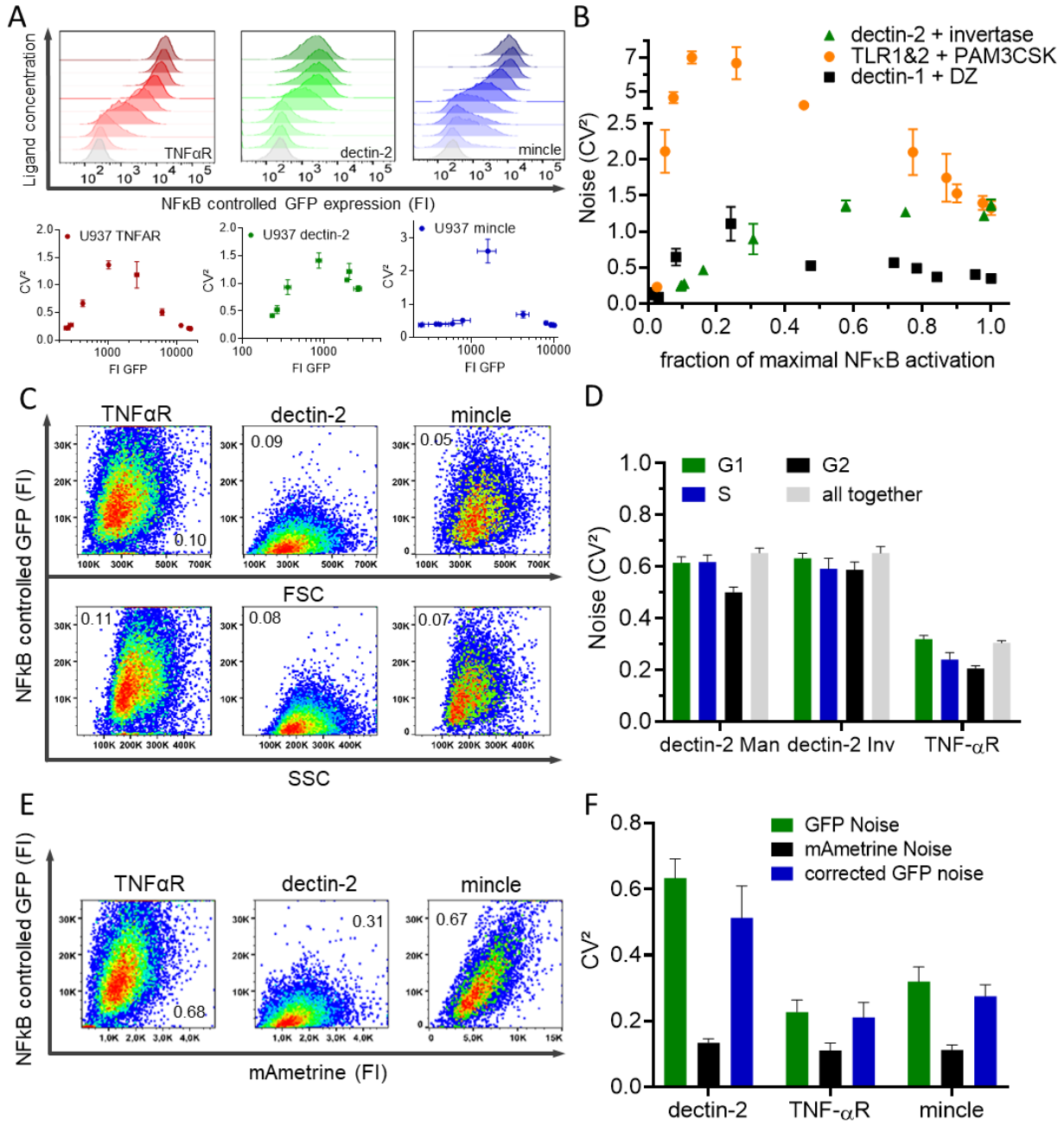

Figure 27: Population noise quantification of U937 reporter cells. A) Top row shows histograms seen in Fig 21A. Bottom row shows noise quantification of U937 reporter cells dose responses either by TNF-αR, dectin-2, or mincle stimulation. Y-axis shows CV^2 (Robust standard deviation/ geometric mean)^2 to quantify noise of the cellular population. The x-axis shows fluorescent intensity of the NFκB dependent GFP. The last three data points were compared using an unpaired t-test and for all three cases dectin-2 was significantly different from TNF-α and mincle p-value ≤ 0.01. B) Noise quantification of U937 reporter cells dose responses either by dectin-2 stimulation with Invertase, TLR1&2 stimulation with PAM3CSK4, dectin-1 stimulation with depleted zymosan (DZ) all n≥3, shown is mean ± SD C) Density plots of NFκB controlled GFP and either forward scatter (FSC) or mAmetrine. Number gives R^2 for a linear regression of each plot. D) U937 dectin-2 expressing reporter cells were stimulated with TNF-α or invertase and gated according to their DNA content and therefore mitotic state (shown is mean ± SD of n=3). E) Density plots of NFκB controlled GFP and mAmetrine. Number gives R^2 for a linear regression of each plot. F) Noise quantification of U937 reporter cells by TNF-αR, dectin-2, or mincle stimulation, quantified using the CV^2 of the cellular population either for GFP, mAmetrine, or GFP corrected for protein expression noise, shown is mean ± SD of n=3.

6.5 Soluble beta glucans are versatile ligands for dectin-1 stimulation

It has been noted before that dectin-1 is capable of distinguishing the size of its recognized particle (Goodridge *et al.*, 2011). Therefore, an investigation into the side chain dependency of beta-glucans on dectin-1 activation was started. In collaboration with the lab of Bjorn Christensen from NTNU in Norway dectin-1 reporter cells were used to evaluate a set of soluble beta glucans (SBG) extracted from *S. cerevisiae* cell walls. These cells wall extracts were degraded by acid hydrolysis in two steps, each yielding different ligand fractions. From the smaller low molecular weight fraction (LMV, less than 100 kDa) the Christensen group generated multiple fractions of various degrees of polymerization samples were named from A-F according to their degree of polymerization (Fig 28A, D). This degree of polymerization represents the number of glucose residues present on the side chains of the beta glucan. Interestingly, while all samples showed similar channel capacities, the sensitivity (EC_{50}) of the compounds was found to be vastly different: (Fig 28B-D) Sample A&B with the highest degree of polymerization were both able to stimulate dectin-1 expressing reporter cells at exceptionally low concentrations with an EC_{50} of a few ng/mL. Sample C was then found to be almost 1000-fold higher in EC_{50}. Lastly, another shift by about 100-fold was observed between samples D-F. These differences in EC_{50} clearly correlate with the degree of polymerization that the respective ligand has and in turn with the molecular weight. One can imagine that the dectin-1 receptors can cluster better with higher degree of polymerization since then the ligand density is higher(Goodridge *et al.*, 2011). It is also interesting to see such independence of channel capacity and sensitivity of a channel. This in turn is in line with the overexpression of FcRγ in dectin-2 cells (Fig 24B) where the channel capacity could not be increased, but the sensitivity could.

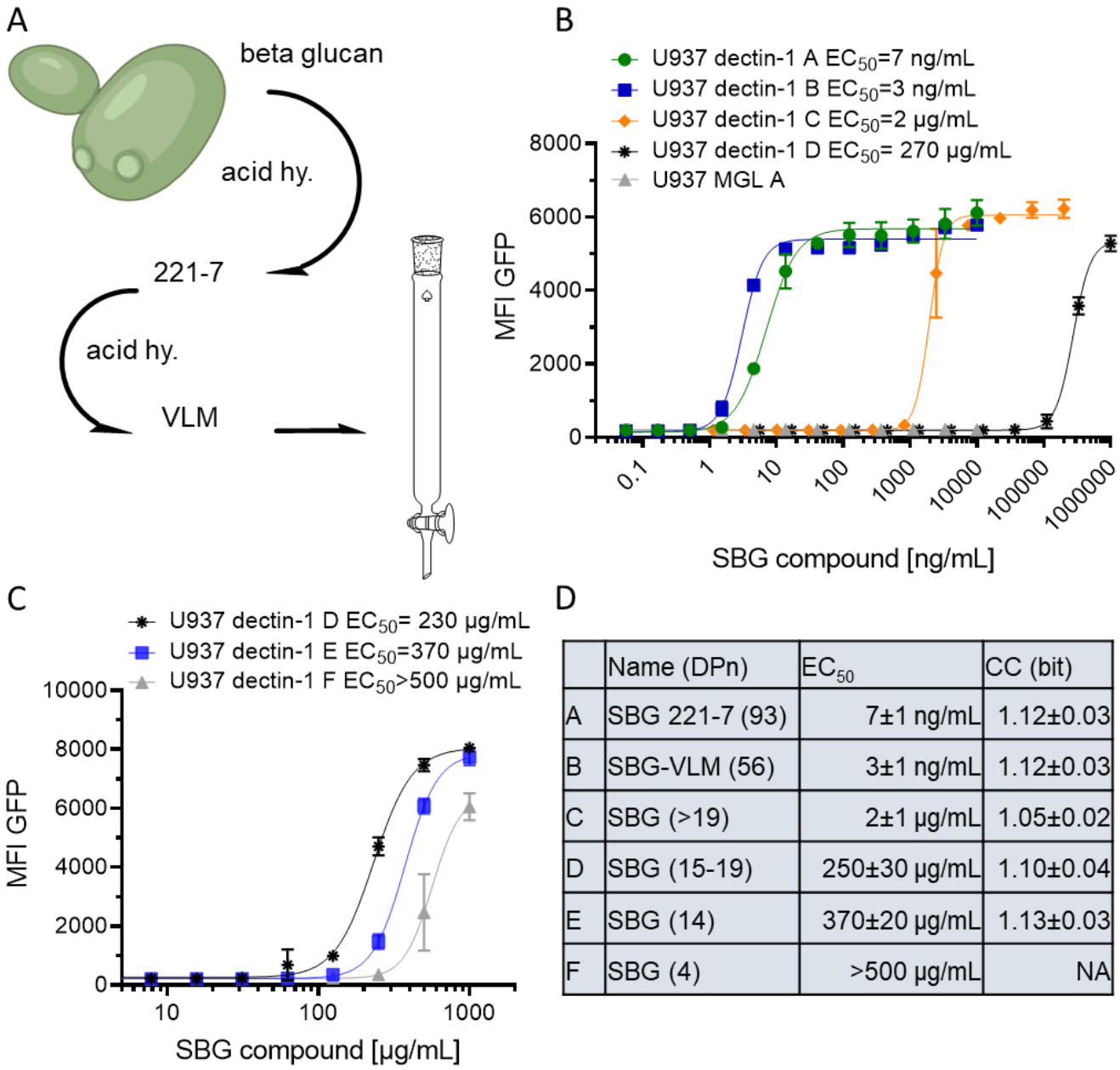

	Name (DPn)	EC_{50}	CC (bit)
A	SBG 221-7 (93)	7±1 ng/mL	1.12±0.03
B	SBG-VLM (56)	3±1 ng/mL	1.12±0.03
C	SBG (>19)	2±1 µg/mL	1.05±0.02
D	SBG (15-19)	250±30 µg/mL	1.10±0.04
E	SBG (14)	370±20 µg/mL	1.13±0.03
F	SBG (4)	>500 µg/mL	NA

Figure 28: Fractioned soluble beta glucan ligands for dectin-1. A) Scheme of the production process of the SBG ligands. SBGs are extracted from *S. cerevisiae* cell walls then degraded by acid hydrolysis to generate 221-7. Further degradation yields very low molecular (VLM) weight glucans, which are then separated by SEC. B) and C) U937 reporter cell lines expressing dectin-1 and or MGL as control lectin are being stimulated with various ligands (n=3) for dectin-1 cells (n=1) for MGL cells, shown is mean ± SD of n=3 D) summary table of the stimulation data for all SBG ligands. For SBG (15-19) the average between the dose response in subFigure C and D was used. Since the curve of SGB (4) does not go into saturation, the EC_{50} could only be estimated and no CC was calculated.

6.5.1 Signal cascade of dectin-1 demonstrates feasibility of reporter cell system

To further investigate the information transmission of dectin-1, the established assay for staining of phospho-epitopes was used. U937 reporter cells expressing dectin-1 were stimulated with SBG A. pSTAT1 (pY701), pERK (pT202/pY204), pSYK (pY348) were stained simultaneously (Fig 29A-C). In this case the concentration of ligand was constant at 2.5 µg/mL and stimulation of cells was stopped at different timepoints. Such a time-response can still be used to calculate the channel capacity, since only an unstimulated, a maximally stimulated and 1-2 samples in between the two extremes are necessary to calculate channel capacities of around 1 bit. Thus the channel capacities were read out at multiple points in the signal transduction pathway of dectin-1 (Fig 29D) (Negi *et al.*, 2019; Patin, Thompson and Orr, 2019). It is interesting to see that for all calculated phospho-epitopes the channel capacity is lower than 1 bit. This is not surprising, since phosphor-epitopes are transient and even at full stimulation some are expected to be unphosphorylated (Krutzik and Nolan, 2003). Thus, in the data used for channel capacity calculation the maximally stimulated cellular population will always have an overlap with the unstimulated population. Due to this overlap, there cannot possibly be more than 1 bit or two distinct states. Thus, the assay should only be compared to channel capacities of other assays with caution. The data is also taken at specific timepoints, whereas data from the NFκB reporter assay integrates the received signals over a longer period of time due to accumulation of GFP. Thus, for quantification of a pathway a maker further downstream is much better suited. It would however be interesting to see a full quantification of the different dectin-1 pathways, by staining of relevant phospho-epitopes for example. Such a full quantification is however extremely difficult to achieve. To sum up, multiple readouts within dectin-1 signal transduction demonstrate how the used NFκB dependent GFP expression is a better suited endpoint to quantify signal transduction.

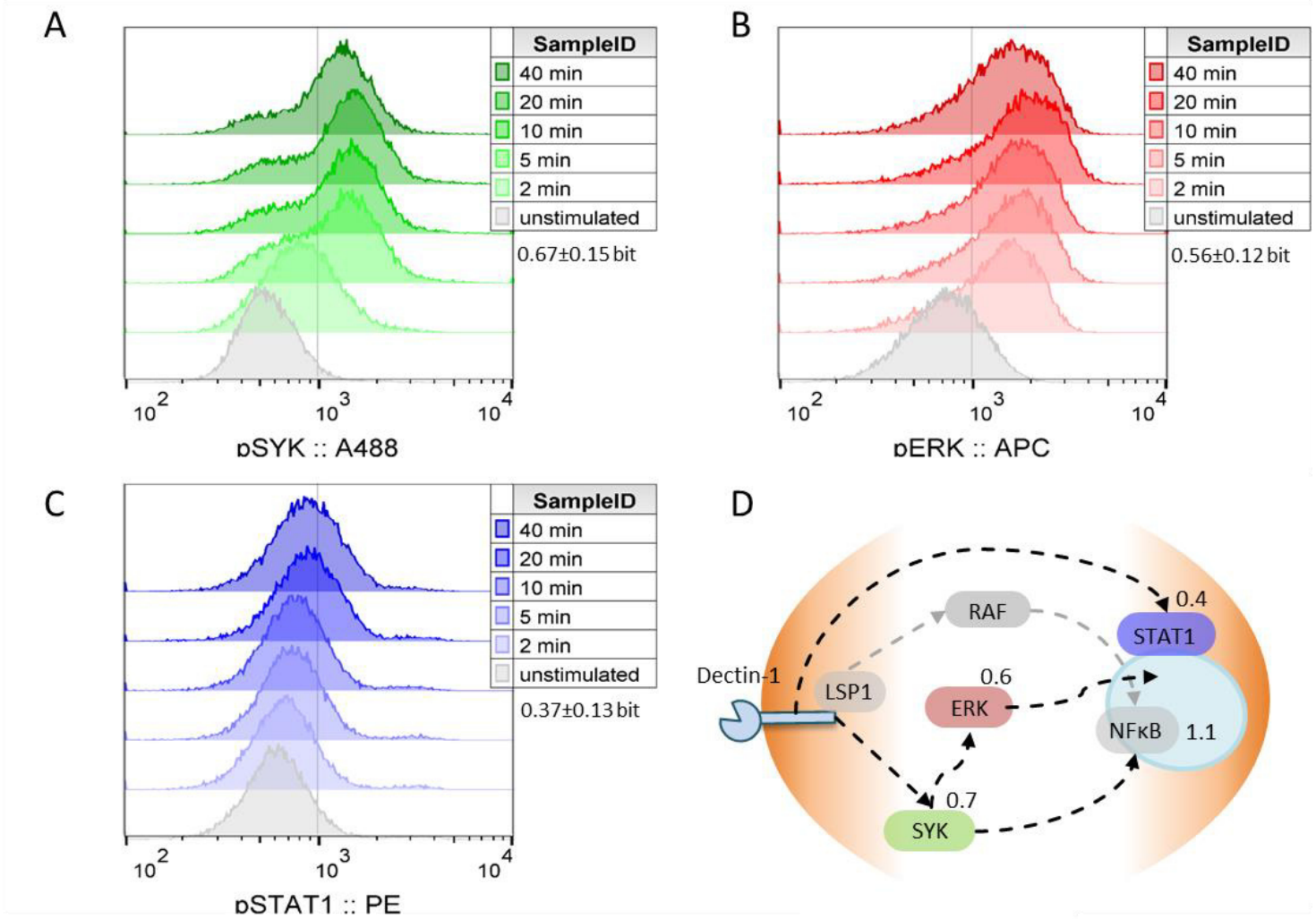

Figure 29: Staining of phospho-epitopes upon dectin-1 stimulation. A-C) Histograms of U937 reporter cell expressing dectin-1 were stimulate using SBG A for the indicated period. Cells were stained with specific antibodies for pSYK (pY348), pERK (pT202/pY204), and pSTAT1 (pY701), respectively. Grey histograms show unstimulated cells which were stained with the indicated antibody. The channel capacities of the individual markers are given, shown is mean ± SD of n=3, except for STAT1 n=2. D) Schematic depiction of the dectin-1 signal transduction pathway. Given are the channel capacity as measured with the connected readout and rounded to one decimal digit. Signal transduction pathway of dectin-1 is shown according to Patin, Thompson and Orr, 2019 as well as Negi et al., 2019.

6.6 Structurally diverse mincle ligands result in similar signalling

Since mincle and dectin-2 share a signalling pathway and many different mincle ligands are known (Williams, 2017), an investigation in mincle signalling was started. In collaboration with the group of Spencer Williams (The University of Melbourne) a diverse range of published ligands (van der Peet *et al.*, 2015) ranging from PAMPs like TDB or TDCM to DAMPs like the two cholesterol structures (Fig 30A). First it was found that mincle requires FcRγ overexpression for reliable and reproducible signalling, which was not surprising and in agreement with literature (Fig 30B) (Ishikawa *et al.*, 2009). Without FcRγ overexpression U937 mincle cells showed huge differences giving little to no signal at all (Fig 30B). Although the used range of ligands was quite diverse, little difference in their mode of mincle stimulation was found: All ligands were able to stimulate mincle with minute to insignificant differences in sensitivity (EC_{50}) between the ligands. The only exception was C22GlcC8, which failed to stimulate mincle reliably (Fig 24B-E). When calculating channel capacity, no difference between the various compounds was found, similar to the EC_{50s}. However, the cholesterol-like compounds (CholAcGlcC8 or C12) suggested that a small difference in chain length from C8 to C12 can make big difference in ligand sensitivity, the importance of chain length was also noted in literature (Fig 30C and E) (Decout *et al.*, 2017). To sum up, between the various mincle ligands there does not seem to be a high variation, which might be due to mincle recognizing aggregates of its ligands. Cholesterol for example by itself is not a mincle ligand, but when it forms aggregates, those can act as DAMPs,(Williams, 2017) thus the ligand density of those aggregates will always be very high. This in turn could be responsible for making differences between ligands less obvious.

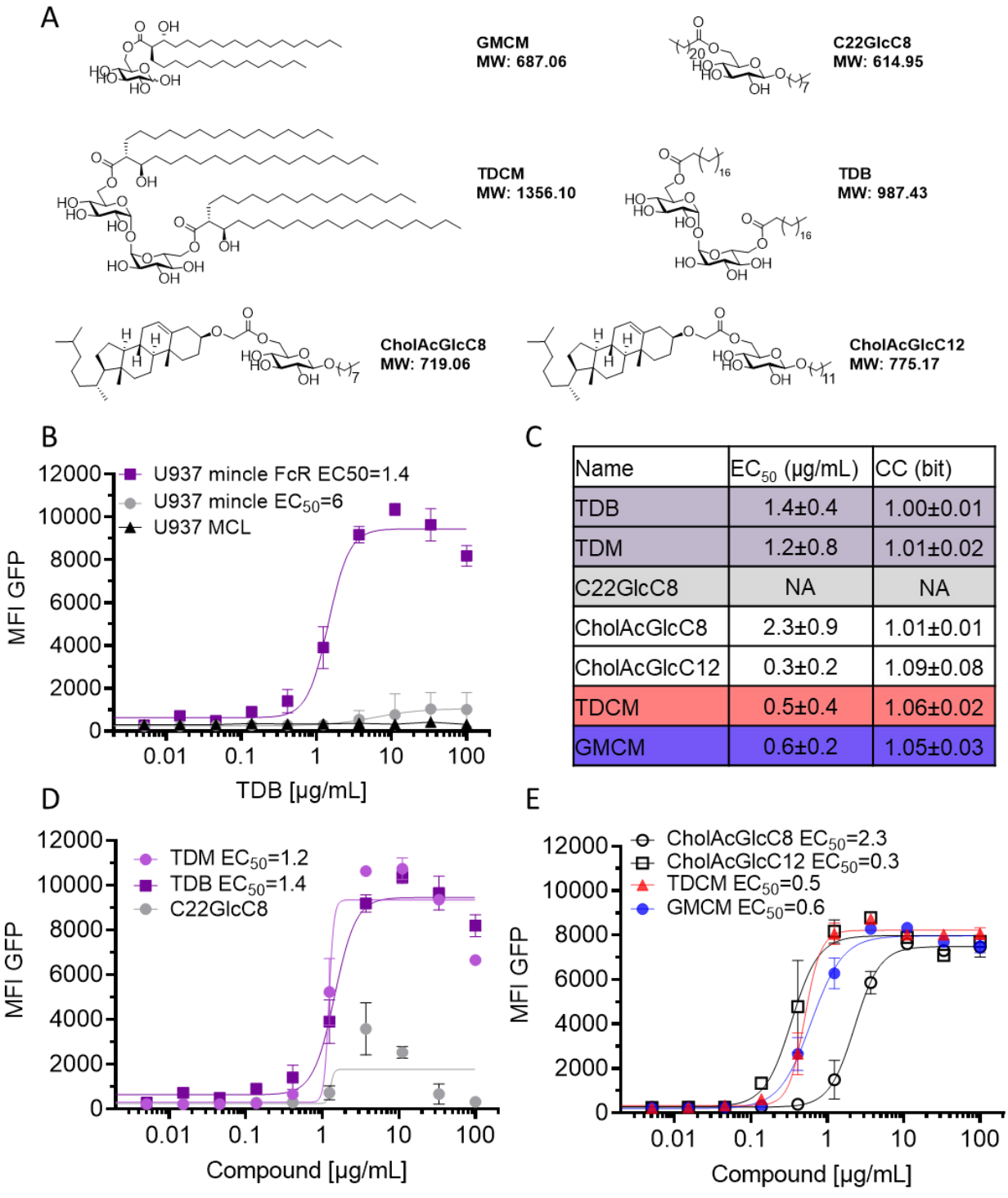

Name	EC_{50} (µg/mL)	CC (bit)
TDB	1.4±0.4	1.00±0.01
TDM	1.2±0.8	1.01±0.02
C22GlcC8	NA	NA
CholAcGlcC8	2.3±0.9	1.01±0.01
CholAcGlcC12	0.3±0.2	1.09±0.08
TDCM	0.5±0.4	1.06±0.02
GMCM	0.6±0.2	1.05±0.03

Figure 30: Stimulation of mincle expressing reporter cell lines with diverse mincle ligands. A) Structures of the used synthetic mincle ligands, name and MW given on the right of the structure. B) Dose response curves of U937 cells expressing mincle alone, or in combination with FcRγ, shown is mean ± SD of n≥3, except MCL where n=1. C) Table summarizing the results of the mincle ligand stimulation. D) and E) Dose response curves of U937 cells expressing mincle and FcRγ, shown is mean ± SD of n=2.

6.7 Cellular reprogramming of Langerin expressing cells

Recently a glycomimetic ligand for human langerin was developed (Wamhoff *et al.*, 2019). Langerin is an interesting target for drug development due to its expression on Langerhans cells a dendritic cell subset of the skin (Clausen and Stoitzner, 2015). The specificity of liposomes targeted via this ligand to Langerin expressing cells and Langerhans cells has been clearly shown (Fig 31A) (Wamhoff *et al.*, 2019). Specific administration of nucleic acids to Langerhans cells could then enable manipulation of the immune system such as induction of tolerance or priming against a specific antigen. However initial experiments did show that mRNA delivered specifically to langerin did not result in translation to protein (data not shown). To be translated the nucleic acids encapsulated in liposomes need to be able to reach the cytosol of the targeted cells. Therefore, it was tested whether the cargo of liposomes would end up in the cytosol *via* targeted delivery. Cytochrome C triggers apoptosis upon being delivered to the cytosol, which can be measured by PI staining (Fig 31B). Cytochrome C was encapsulated via liposomes did not reach the cytosol. Lipid nanoparticles (LNPs) however consisting of a different lipid composition were able to deliver Cytochrome C to the cytosol (Fig 31B). The main difference in composition between LNPs and liposomes is the use of an ionisable lipid known as DLin-MC3-DMA (Dlin). Dlin is commonly used to facilitate endosomal escape and this mechanism facilitates delivery of the LNPs cardo into the cytosol (Veiga *et al.*, 2018).

Since LNPs could facilitate endosomal escape, Cy5-tagged mRNA coding for GFP was encapsulated in them, one batch with (Dlin-T) and another one without the human Langerin targeting ligand (Dlin-N). As expected only Langerin expressing cells were able to specifically take up the targeted LNPs and also translate the mRNA into protein (Fig 31C). Additionally, a clear correlation between Cy5 and GFP was observed. This demonstrated that the more mRNA is taken up by the cells, the higher the amount of protein produced (Fig 31C). With the same LNPs plasmids encoding for GFP were delivered, albeit with much lower efficiency (Fig 31D). This is most likely due to the fact that DNA delivered into the cytosol still has to cross into the nucleus to be translated. In contrast, mRNA can be readily translated into protein right in the cytosol. Using microscopy, the time dependency of this mRNA translation was also looked into. Here the onset of GFP expression was found to be at around 7h, and the protein can clearly be observed 14h post mRNA delivery (Fig 31E). Those values are well in alignment with literature since the translation of GFP is known to be slow (Gubin *et al.*, 1999).

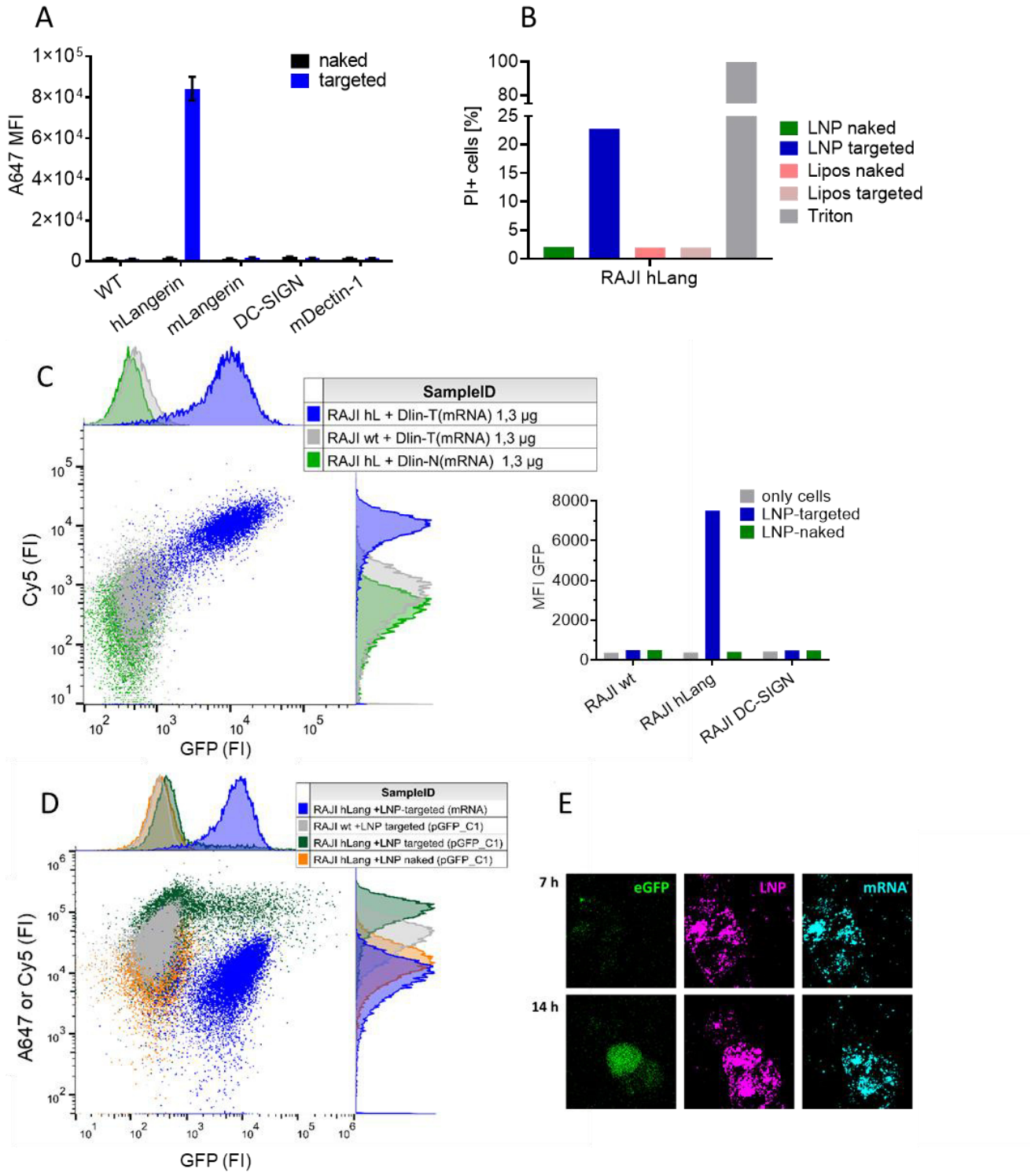

Figure 31: Cytosolic delivery of nucleic acids to langerin expressing cells. These experiments were a collaboration with Schultze, Rentzsch, Kim, and Rahhal. A) Liposomes decorated with the targeting ligand for human Langerin or naked Liposomes binding to RAJI cells expressing various receptors, shown is mean ± SD of n=3. B) LNP and Liposomes containing Cytochrome C incubated with human Langerin expressing cells. Only targeted nanoparticles were taken up by human Langerin+ cells n=3. C) LNPs containing GFP mRNA were incubated with RAJI cells either expressing human Langerin (CD207), DC-SIGN (CD209), or wt cells as control. Quantification of GFP expression on the right. D) Alexa647 dyed targeted LNPs containing pEGFP_C1 were used to transfect RAJI cells, again as a comparison Cy5 tagged mRNA was used. E) Alexa555 dyed targeted LNPs containing Cy5-mRNA (GFP) incubated with human Langerin expressing 293T cells.

To sum up it was shown that liposomes can be very well targeted towards Langerin, but a different lipid composition including and ionizable lipid is necessary for the successful delivery of nucleic acids into the cytosol. Furthermore, such LNP formulations were then successful in specifically transferring nucleic acids such a mRNA and DNA. These nucleic acids in turn were able to be translated into protein.

6.7.1 Investigation of bacterial glycosylation pattern with langerin

As DC-SIGN and Langerin are pattern recognition receptors of the innate immune system their biding of pathogenic bacteria was investigated. Langerin and DC-SIGN expressing cells such as THP-1, RAJI, and U937 were made. Although no feasible readout for signalling was found, in the course of investigation an exciting binding pattern was uncovered. First of all it was shown that langerin binds *S. aureus* via GlcNAc residues on its wall teichoic acid (WTA) (Fig 32A)(van Dalen *et al.*, 2019). By testing various strains of *S. aureus* it was also shown that a higher density of GlcNAc residues on the surface of the bacteria leads to higher langerin binding (van Dalen *et al.*, 2019). Using recombinant langerin and a series of specific knockouts it was also demonstrated, that β-GlcNAc rather than α-GlcNAc was recognized by langerin. These two sugar modifications are synthesized by the bacterial TarS and TarM genes, respectively (Fig 32B). These two are usually active in decorating WTA, loss of TarS is in this case thought to be compensated by TarM resulting in an overdecoration of α-GlcNAc. These α-GlcNAc residues are then resulting is lower langerin binding (Fig 32B). This data was further corroborated by a sophisticated Langerhans cell model, the muLCs. These muLCs are generated by differentiating the human monocytic MUTZ-3 cells with various cytokines, (van Dalen *et al.*, 2019). With the model in hand, it was shown that cytokine expression of the muLCs did increase with knockout of TarM, and therefore did also increase with the amount of β-GlcNAc.

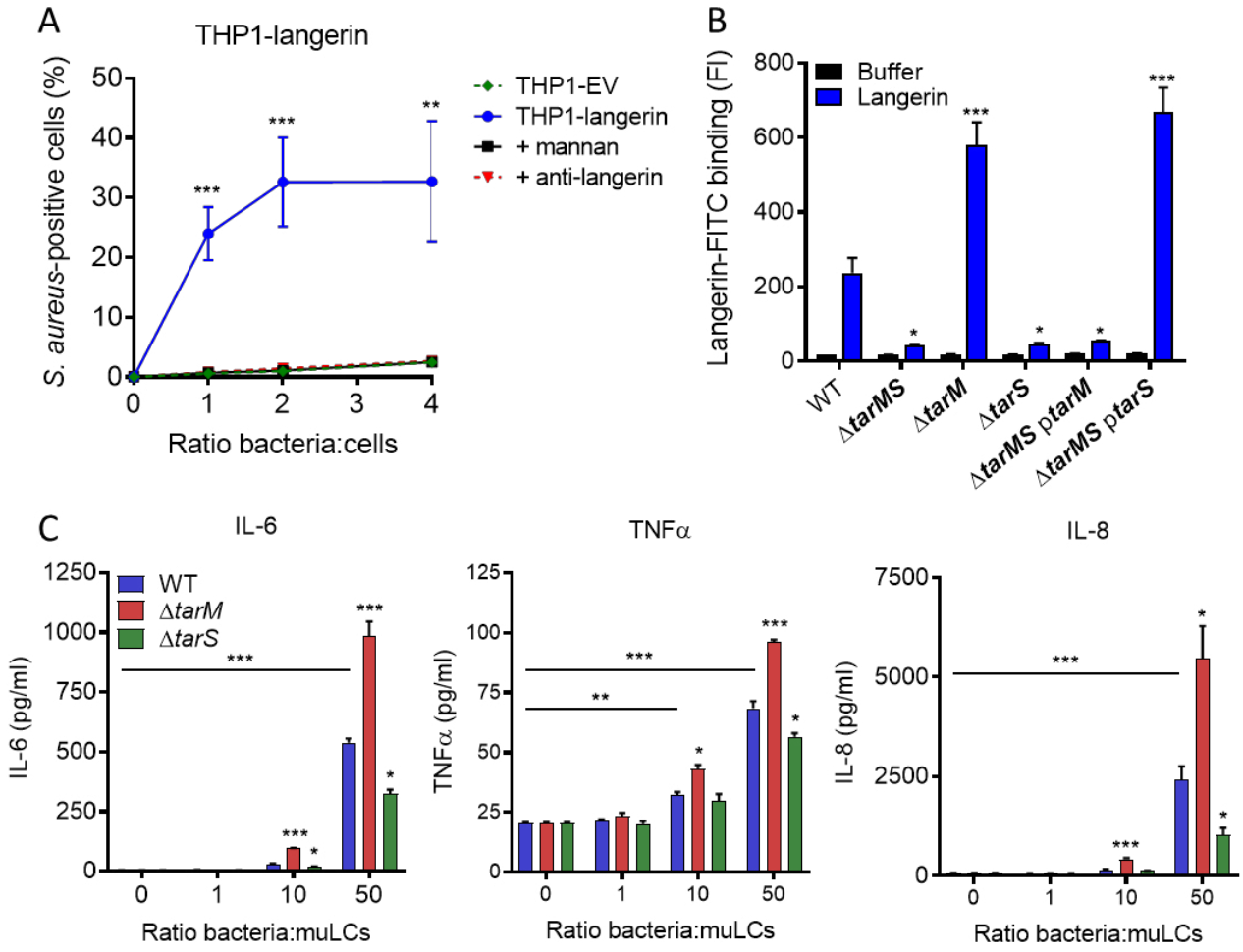

Figure 32: Langerin preferentially binds α-GlcNAc residues on *S. aureus*. A) Binding of *S. aureus* to THP1-langerin cells. THP-1 cells either langerin expressing or empty vector control incubated with GFP+- *S. aureus* bacteria (strain Newman). B) Recombinant human langerin FITC labelled binding to various knockouts and reconstitutions of *S. aureus* bacteria (strain USA 300). C) Quantification of cytokines TNF-α, IL-6, and IL-8 secreted by muLCs upon incubation with gamma-irradiated *S. aureus* (Strain USA300), either wild type or tarM/S knockout. Figures taken from van Dalen et al., 2019.

7. Conclusion and Outlook

7.1 Quantification of signal transduction pathways using information theory

The information transfer upon glycan-lectin-communication in single cell resolution was investigated by generating and analysing a human cell line model. First the stimulation of dectin-2 expressing U937 cell lines was observed with three ligands one of which was previously published in (Ishikawa *et al.*, 2013) (Fig 18). Here high variation in the dose response of dectin-2 expressing cells was observed on a cell population level could be observed. This led to an investigation into the stochastic nature of signal transduction (Fig 19). The gained results exemplify that signalling pathways and especially the dectin-2 signalling pathway should not be viewed as deterministic on/off-switches in a cellular population, but rather as stochastic differences in the probability of cells to be active at a certain ligand dose. This is in line with previous reports strengthening a quantitative view of cellular signalling and taking the spread of cellular population into account (Levchenko and Nemenman, 2014; Zhang *et al.*, 2017).

The calculations of (Cheong *et al.*, 2011) were adapted to determine channel capacities from flow cytometry data. A total of seven lectins (dectin-1, dectin-2, mincle, DC-SIGN, MGL, MCL, and Langerin) specifically expressed on U937 reporter cells was stimulated, three of which had an adequate and measurable response to allow calculation of channel capacities (dectin-1, dectin-2, and mincle). These three were then compared to two endogenously expressed receptors on U937 cells (TLR1&2 and TNFαR). All receptors did have a capacity of at least 1 bit, with the exception of dectin-2 (Fig 21A, B). This was a striking result since comparable systems using fluorescent reporter proteins as experimental readout did show at least 1 bit of channel capacity (Suderman *et al.*, 2017). In particular the comparison of dectin-2 and mincle was striking since both are using the same pathway, however mincle showed a higher channel capacity than dectin-2. Then it was found that the number of receptor proteins expressed did not determine the channel capacity of a receptors channel (Fig 21D, E). These findings imply that the receptor molecule itself determines very early on the use of its signal transduction pathway.

The receptor expression data of Figure 21E is also intriguing by itself since all lectin constructs were expressed under the same promoter and vector system, therefore their expression was expected to be at a similar level. However, there was a huge difference observed between dectin-2 at around 4000 receptor proteins and DC-SIGN at 200000. Since the expression of various biological replicates of DC-

SIGN was consistent at around 200000 copies, (Fig 33) one can assume that the number of receptors is regulated at protein or possibly mRNA level, due to structure or sequence.

7.1.1 Dectin-2 is less efficient than other receptors

The inefficiency of dectin-2 relative to other receptors in particular mincle seems counterintuitive for a pattern recognition receptor with a role of high importance such as pathogen recognition. But since dectin-2 binds mannose structure with a Manα1-2Man motif of eukaryotic origin such as Man9GlcNAc2, (McGreal *et al.*, 2006) a too sensitive reaction might lead to permanent self-recognition and hence aberrant autoimmune reactions. This hypothesis is supported by the dectin-2-dependent high basal activity of dectin-2 FcRγ cells, which in turn is responsible for a lower channel capacity in dectin-2 FcRγ cells (Fig 24B, C). Therefore, dectin-2 could have evolved to use the CARD9-BCL-10-Malt1 pathway to NFκB less effective whereas mincle did not. This hypothesis is however not directly supported by the kifunensine experiments (Fig 24D, E), unless the overabundance of Man9 structures does stop dectin-2 clustering.

To directly take ligand-receptor data in dectin-2 signalling into account, Invertase and TNF-α were labelled with Atto647N. Both ligand and cellular reaction were then observed on a single cell level via flow cytometry (Fig 25). Interestingly, dectin-2 did not seem to bind much ligand but did elicit the immunological reaction; in contrast to DC-SIGN (Fig 25C). It was then thought that a combination of multiple lectins might synergistically enhance dectin-2s signalling capacity. While DC-SIGN greatly enhanced ligand binding to the cells, it did not significantly increase in channel capacity. In fact, it increased the channels sensitivity (EC_{50}) (Fig 26A-D). It was also found that in contrast to murine dectin-2, the closely related lectin MCL (Dectin-3) did not have a significant synergistic effect on human dectin-2 signalling (Fig 26A-D). Based on those results for dectin-2 it was hypothesized that the channel capacity of a lectin is predetermined by the receptor itself. It was further speculated that the receptors channel sensitivity (EC_{50}) can be enhanced by synergistic receptors or signalling molecules, but its maximally transduced information cannot. The stimulation of dectin-1 with SBG is in agreement with this hypothesis, since it was shown how the sensitivity towards a ligand increases with density, but transmitted information does not. However, not every receptor would show the high basal activation as dectin-2 FcRγ cells do, so in other cases the maximally transduced information might increase by overexpression of signalling molecules.

The low channel capacity of dectin-2 (relative to other receptors) was connected to the high noise associated with its signalling. This high noise might have evolved as a mechanism to avoid self-recognition of endogenous high mannose structures, since then dectin-2 can be viewed as tuned to be only activated when the pathogen associated high mannose structures of yeast are encountered (Fig 3). Under physiological conditions the inefficient dectin-2 signalling might then be beneficial since it keeps the basal activation due to self-recognition of dectin-2 from triggering auto immune defects. However, as most of the data presented her were generated in model cell lines, experiments under physiological conditions could differ.

Since channel capacity calculations are applicable regardless of the nature of signal and medium, (Levchenko and Nemenman, 2014) one could use it to objectively quantify cellular responses in similar assays in the future. Along these lines time dependent activation of phospho-proteins in the dectin-1 signalling pathway was observed. It is possible to compare the calculated channel capacities of phosflow (Fig 29) to the one of the NFκB reporter assay. However, the transient nature of phospho-proteins (Krutzik and Nolan, 2003) fixes the calculated channel capacity at below 1 bit. It would be very exciting to see a quantitative characterization of receptor channels such as dectin-1 or dectin-2 in primary cells, for it could reveal how combination and integration of various channel leads to distinct cellular responses in the immune system. This could be achieved with the use of phosflow and help to better characterize communication channels especially in such a complex and enigmatic field of study as glycan lectin interactions.

7.2 Signal integration of dectin-1 and dectin-2

The established model cell line also enabled approaching the complicated topic of signal integration between multiple receptors. The signalling effects of dectin-2 and dectin-1 were combined, as the lectins both recognize moieties on FurFurMan. First, the effects were not additive, but a compromise between the two receptors, showing the low EC_{50} of dectin-2 but with a higher channel capacity derived from dectin-1. Second, the channel capacity of dectin-1 dectin-2 cells was a neat average of the individual channel capacities (Fig 22A, B). While such a compromise instinctively makes sense, this means that at high concentrations of FurFurMan the dectin-2 channel is actively influencing the one of dectin-1, resulting in a lower cellular NFκB activation. Since dectin-1 and dectin-2 are both signalling via SYK where phosphorylation of Y525/526 is required for NFκB signalling (Bode *et al.*, 2019), potentially the lectins are competing over the precise SYK phosphorylation pattern. For dectin-1 it was shown that

β-glucan ligands are able to fully phosphorylate SYK (Y525/526, Y348, and Y352) leading to NFκB activation. But dectin-1 dependent SYK activation with annexin ligands is only phosphorylating Y348 resulting in at least two different pathways for dectin-1 (Blanco-Menéndez *et al.*, 2015; Bode *et al.*, 2019). This phosphorylation was also observed by staining of phospho-epitopes. It was interesting to see that dectin-1 is able to activate multiple phosphoproteins which are used in many signal transduction pathways while dectin-2 is not (Fig 23, Fig 29). This could be the reason why dectin-1 overall had a higher channel capacity to NFκB, which lies at the endpoints of many signal transduction pathways. In sum, differential SYK phosphorylation and de-phosphorylation between dectin-1 and dectin-2 might integrate the signals received via the two lectins.

In further experiments, it was shown that dectin-1 and -2 themselves are not influencing one another when stimulated with specific ligands (Fig 22C-E). This exemplifies that when multiple lectins using a similar pathway are engaged simultaneously, the cells will integrate both channel by compromising between them rather that favour one over the other or using the most active channel available. This is an exciting discovery since there have not been any studies showing quantitative how the signals of multiple lectin receptors are being integrated. From this, it can be imagined that during a fungal infection with multiple (carbohydrate) ligands, the precise arsenal of immune receptors and connected pathways a given immune cell expresses are integrating the information contained within the carbohydrate and non-carbohydrate ligands. This in turn leads to a compromise of all activated receptors and results in a specifically tailored biochemical response of the given immune cell.

7.3 Soluble beta glucan and its application in biotechnology

The results of the soluble beta-glucans demonstrate very well how the ligand density can influence the sensitivity of a receptor, since by variation of the side chain length (degree of polymerization) the EC_{50} was modulated by about five orders of magnitude. At the same time, the information transferred by the SBG compounds was at around 1.1 bit, with little to no difference between the ligands. It is very interesting to see how ligand density can change the sensitivity of dectin-1 ligands. These SBGs were used in a number of applications ranging from fish feed to enhance salmon immunity, adjuvant for vaccination, and as wound healing agent (ArcticZymes Technologies, Norway (Paulsen *et al.*, 2003)). The presented results demonstrate that ligands with optimal density or degree of polymerization should be more effective at lower concentrations. Therefore, much less material is needed for the aforementioned applications if ligand density is at a high level.

7.4 Chemically diverse mincle ligands give similar signalling

Whereas dectin-1 SBG ligands showed a highly variable EC_{50} due to ligand density, mincle ligands showed only little variation. This might simply be due to the form in which mincle ligands are being recognized, since in all experiments mincle-expressing cells were added to crystalline ligands, which formed after solvent evaporation. Thus, in all of these ligands the density of ligands should be relatively similar. It is also interesting that DAMP ligands such as Cholesterol derivatives had a similar EC_{50} and CC as PAMP ligands such as TDB and TDM.

7.5 Reprogramming Langerhans cells with nucleic acids

Langerhans cells are interesting targets for manipulation of the immune system due to their ability to facilitate MHC I cross presentation and MHC II presentation (Clausen and Stoitzner, 2015). As those two presentation modes are then triggering T cell responses against a given antigen. Recently a glycomimetic ligand that strongly binds human Langerin was developed (Wamhoff *et al.*, 2019). With the use of this ligand liposomes as well as LNPs could be targeted specifically to langerin expressing cells. The cargo of nucleic acid in these LNPs was then clearly delivered into the cytosol and translated. Especially interesting here is the strong correlation of delivered mRNA and translated GFP per cell. Since this not only gives numbers of the mRNA to GFP conversion, but also demonstrates that the maximum of the cellular protein translation machinery was not reached yet (Fig 31). It should however be noted that the experiments in this case were done with cell lines, which are mere models of primary cells and experiments *in vivo* are needed to confirm what was found so far.

This reprogramming of immune cells opens up many opportunities in therapeutic or prophylactic immunomodulation (*e.g.* targeted delivery of nucleic acid to Langerhans cells, before subsequent antigen expression or even manipulation using the CRISPR system). The application of such targeted delivery bear enormous potential be it for vaccination or gene therapy. One can therefore envision the targeted delivery of CRISPR systems to correct virtually any defect in the DNA of a certain subset of cells. Here it was only possible to target only Langerin expressing cells, yet also other groups are designing ligands and systems for targeted delivery (Tacken and Figdor, 2011; Kranz *et al.*, 2016; Veiga *et al.*, 2018). So with the right set of ligands virtually any subset could be targeted. BioNtech in collaboration with Tel Aviv University for example are currently exploring the idea of using antibodies to target the

specific cellular subsets (Kotler and Steimle, 2018). Clinical mRNA technology is currently on the rise due to various companies using mRNA-based vaccines to combat the COVID 19 pandemic.

7.5.1 Langerin and bacterial glycosylation demonstrate host-pathogen adaption

It was show how Langerin binds *S. aureus* via β-GlcNAc residues rather than α-GlcNAc on its WTA. This GlcNAc decoration on WTA also distinguishes S. aureus from other staphylococci (van Dalen *et al.*, 2019). This is an excellent example of bacterial adaptability towards immune evasion, since it was shown that WTA glycosylation in *S. aureus* does change with the bacterial environment (Gerlach *et al.*, 2018; Mistretta *et al.*, 2019). It is also known that about 20-30% of humans show nasal colonization of the opportunistic *S. aureus*, which is a risk factor for invasive infection (van Dalen, Peschel and van Sorge, 2020). Interestingly, a number of SNPs exist both in the CRD as well as in the enhancer region of the langerin encoding gene (CD207). The ones located in the enhancer region were already linked to atopic dermatitis, which in turn is associated with *S. aureus* colonization (Paternoster *et al.*, 2015; Totté *et al.*, 2016). For the SNPs in the coding region it was shown that they do change glycan specificity of langerin, and they also had an effect on langerin mediated *S. aureus* uptake (Feinberg *et al.*, 2013; van Dalen *et al.*, 2020). This whole interface of langerin, the Langerhans cell; GlcNAc-WTA, *S. aureus* can therefore be seen as an exciting example of the molecular arms race taking place between host and pathogen. In the context of glycan lectin interaction, the recognition of β-GlcNAc-WTA of langerin can be a message decoding process. The pathogenic *S. aureus* on the other hand is interested in disturbing this decoding and might do so by specifically adapting its own glycosylation.

8. Appendix

8.1 Supplementary Figures

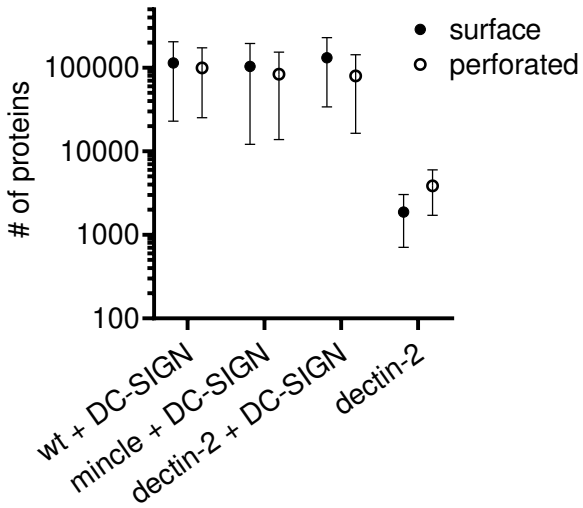

Figure 33: Quantitation of surface and overall expression of receptors expressed in U937 reporter cells. Cells were stained either for their surface expression, or their overall protein expression. Graph shows geometric mean ± robust SD of the cellular population.

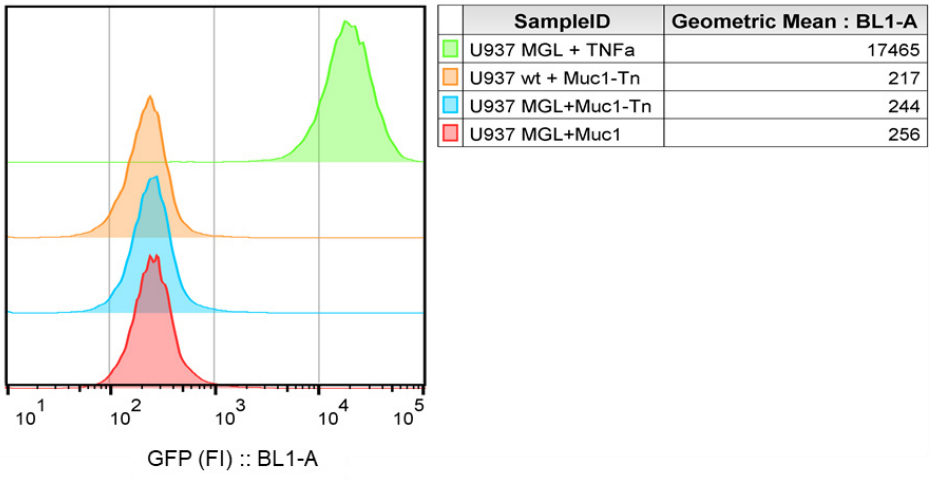

Figure 34: U937 MGL or wt cells stimulated for 16h with Mucine 1 with or without Tn antigen. Muc1 and Muc-Tn kindly provided by Hans Wandall, University of Copenhagen. TNF-α stimulation serves as positive control.

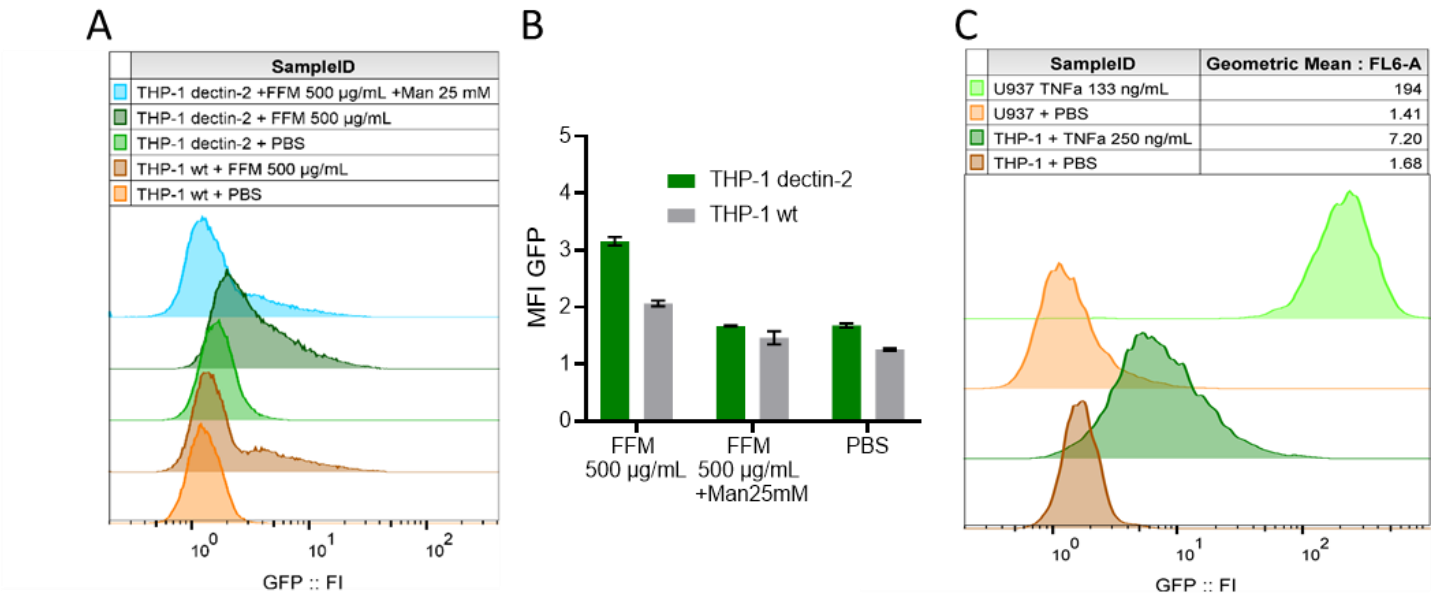

Figure 35: THP-1 NFκB reporter cells and U937 cells expressing dectin-2 or wt stimulated with FurFurMan or TNF-α. A) THP-1 reporter cells expressing dectin-2 or wt were stimulated for 48h with FurFurMan (FFM), unstimulated (PBS), or the FurFurMan stimulation was inhibited with 25 mM mannose. Graph shown representative histograms B) Geometric means of the experiment done in A in triplicates (n=3) with the error bar representing standard deviation. C) Representative histograms showing the TNF-a stimulation (16h) of U937 and THP-1 reporter cells. THP-1 cells stimulated for 48h with TNF-a gave less signal than at 16h (data not shown).

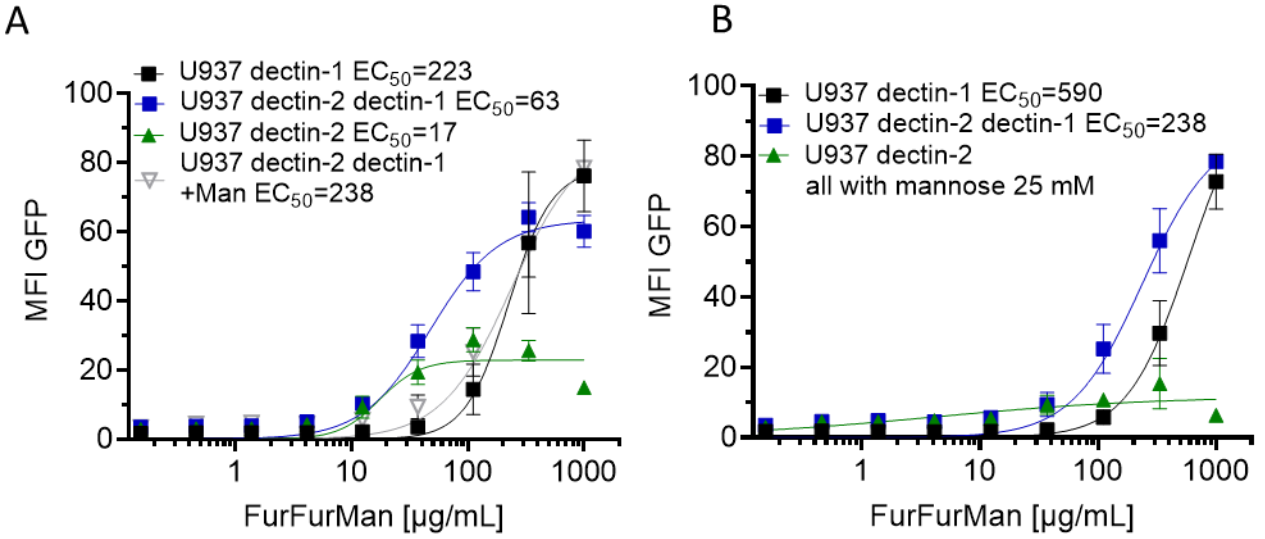

Figure 36: Signal integration between dectin-1 and dectin-2 with inhibition. A) and B) Monoclonal reporter cells either expressing dectin-2, dectin-1, or both dectin-2 and dectin-1, (n=3) were stimulated for 16h with various concentrations of FurFurMan. Cells were stimulated either with or without 25 mM mannose, shown are mean ± SD of n=3. Data were recorded on a MACSquant MQ16.

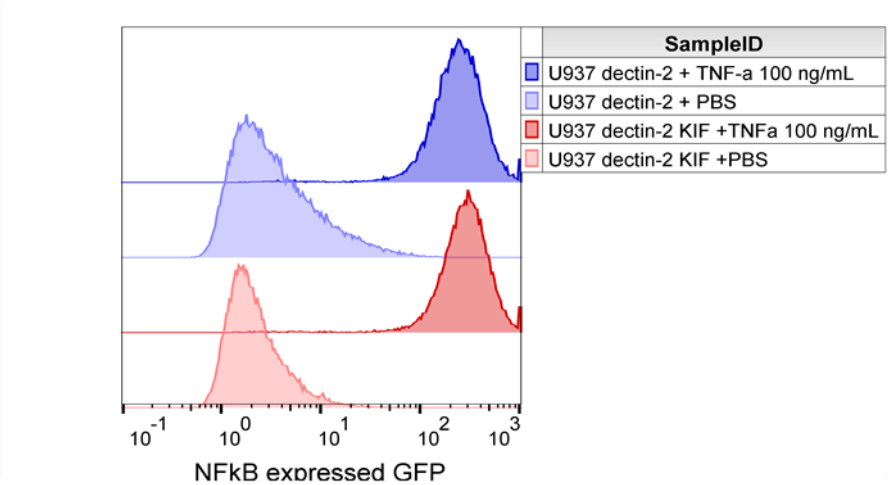

Figure 37: U937 cells cultivated with or without the inhibitor kifunensine (7.5 µM) for 48h, then stimulated with Invertase for 16h, shown is the mean ± SD of n=3.

9. References

Alston-Roberts, C. *et al.* (2010) 'Cell line misidentification: the beginning of the end', *Nature Reviews Cancer*, 10(6), pp. 441–448. doi: 10.1038/nrc2852.

An, H. J., Froehlich, J. W. and Lebrilla, C. B. (2009) 'Determination of glycosylation sites and site-specific heterogeneity in glycoproteins', *Current Opinion in Chemical Biology*, 13(4), pp. 421–426. doi: 10.1016/j.cbpa.2009.07.022.

Ariizumi, K., Shen, G.-L., Shikano, S., Ritter, R., *et al.* (2000) 'Cloning of a Second Dendritic Cell-associated C-type Lectin (Dectin-2) and Its Alternatively Spliced Isoforms', *Journal of Biological Chemistry*, 275(16), pp. 11957–11963. doi: 10.1074/jbc.275.16.11957.

Ariizumi, K., Shen, G.-L., Shikano, S., Xu, S., *et al.* (2000) 'Identification of a Novel, Dendritic Cell-associated Molecule, Dectin-1, by Subtractive cDNA Cloning', *Journal of Biological Chemistry*, 275(26), pp. 20157–20167. doi: 10.1074/jbc.M909512199.

Balch, S. G. *et al.* (1998) 'Cloning of a Novel C-type Lectin Expressed by Murine Macrophages', *Journal of Biological Chemistry*, 273(29), pp. 18656–18664. doi: 10.1074/jbc.273.29.18656.

Bates, E. E. *et al.* (1999) 'APCs express DCIR, a novel C-type lectin surface receptor containing an immunoreceptor tyrosine-based inhibitory motif.', *Journal of immunology (Baltimore, Md. : 1950)*, 163(4), pp. 1973–83. Available at: http://www.ncbi.nlm.nih.gov/pubmed/10438934.

Beltrán-Valero de Bernabé, D. *et al.* (2002) 'Mutations in the O-Mannosyltransferase Gene POMT1 Give Rise to the Severe Neuronal Migration Disorder Walker-Warburg Syndrome', *The American Journal of Human Genetics*, 71(5), pp. 1033–1043. doi: 10.1086/342975.

Bhattacherjee, A. *et al.* (2019) 'Repression of phagocytosis by human CD33 is not conserved with mouse CD33', *Communications Biology*, 2(1), p. 450. doi: 10.1038/s42003-019-0698-6.

Bi, L. *et al.* (2010) 'CARD9 Mediates Dectin-2-induced IκBα Kinase Ubiquitination Leading to Activation of NF-κB in Response to Stimulation by the Hyphal Form of Candida albicans*', *Journal of Biological Chemistry*, 285(34), pp. 25969–25977. doi: 10.1074/jbc.M110.131300.

Blanco-Menéndez, N. *et al.* (2015) 'SHIP-1 Couples to the Dectin-1 hemITAM and Selectively Modulates Reactive Oxygen Species Production in Dendritic Cells in Response to Candida albicans', *The Journal of Immunology*, 195(9), pp. 4466–4478. doi: 10.4049/jimmunol.1402874.

Bode, K. *et al.* (2019) 'Dectin-1 Binding to Annexins on Apoptotic Cells Induces Peripheral Immune Tolerance via NADPH Oxidase-2', *Cell Reports*, 29(13), pp. 4435-4446.e9. doi: 10.1016/j.celrep.2019.11.086.

Cheong, R. *et al.* (2011) 'Information Transduction Capacity of Noisy Biochemical Signaling Networks', *Science*, 334(6054), pp. 354–358. doi: 10.1126/science.1204553.

Clark, E. A. and Giltiay, N. V. (2018) 'CD22: A Regulator of Innate and Adaptive B Cell Responses and Autoimmunity', *Frontiers in Immunology*, 9. doi: 10.3389/fimmu.2018.02235.

Clausen, B. E. and Stoitzner, P. (2015) 'Functional Specialization of Skin Dendritic Cell Subsets in Regulating T Cell Responses', *Frontiers in Immunology*, 6(OCT), pp. 1–19. doi: 10.3389/fimmu.2015.00534.

Colman-Lerner, A. *et al.* (2005) 'Regulated cell-to-cell variation in a cell-fate decision system', *Nature*, 437(7059), pp. 699–706. doi: 10.1038/nature03998.

Corish, P. and Tyler-Smith, C. (1999) 'Attenuation of green fluorescent protein half-life in mammalian cells', *Protein Engineering, Design and Selection*, 12(12), pp. 1035–1040. doi: 10.1093/protein/12.12.1035.

Croci, D. O. *et al.* (2014) 'Glycosylation-Dependent Lectin-Receptor Interactions Preserve Angiogenesis in Anti-VEGF Refractory Tumors', *Cell*, 156(4), pp. 744–758. doi: 10.1016/j.cell.2014.01.043.

Cruz, L. J. *et al.* (2017) 'Controlled release of antigen and Toll-like receptor ligands from PLGA nanoparticles enhances immunogenicity', *Nanomedicine*, 12(5), pp. 491–510. doi: 10.2217/nnm-2016-0295.

Cummings, R. D. (2009) 'The repertoire of glycan determinants in the human glycome', *Molecular BioSystems*, 5(10), p. 1087. doi: 10.1039/b907931a.

Curtis, B. M., Scharnowske, S. and Watson, A. J. (1992) 'Sequence and expression of a membrane-associated C-type lectin that exhibits CD4-independent binding of human immunodeficiency virus envelope glycoprotein gp120.', *Proceedings of the National Academy of Sciences*, 89(17), pp. 8356–8360. doi: 10.1073/pnas.89.17.8356.

Daigneault, M. *et al.* (2010) 'The Identification of Markers of Macrophage Differentiation in PMA-Stimulated THP-1 Cells and Monocyte-Derived Macrophages', *PLoS ONE*. Edited by T. M. Doherty, 5(1), p. e8668. doi: 10.1371/journal.pone.0008668.

van Dalen, R. *et al.* (2019) 'Langerhans Cells Sense Staphylococcus aureus Wall Teichoic Acid through Langerin To Induce Inflammatory Responses', *mBio*. Edited by A. Gründling and T. Msadek, 10(3). doi: 10.1128/mBio.00330-19.

van Dalen, R. *et al.* (2020) 'A Common Genetic Variation in Langerin (CD207) Compromises Cellular Uptake of *Staphylococcus aureus*', *Journal of Innate Immunity*, 12(2), pp. 191–200. doi: 10.1159/000500547.

van Dalen, R., Peschel, A. and van Sorge, N. M. (2020) 'Wall Teichoic Acid in Staphylococcus aureus Host Interaction', *Trends in Microbiology*, 28(12), pp. 985–998. doi: 10.1016/j.tim.2020.05.017.

Decout, A. *et al.* (2017) 'Rational design of adjuvants targeting the C-type lectin Mincle', *Proceedings of the National Academy of Sciences*, 114(10), pp. 2675–2680. doi: 10.1073/pnas.1612421114.

Drickamer, K. (1988) 'Two distinct classes of carbohydrate-recognition domains in animal lectins.', *The Journal of biological chemistry*, 263(20), pp. 9557–60. Available at: http://www.ncbi.nlm.nih.gov/pubmed/3290208.

Dull, T. *et al.* (1998) 'A Third-Generation Lentivirus Vector with a Conditional Packaging System', *Journal of Virology*, 72(11), pp. 8463–8471. doi: 10.1128/JVI.72.11.8463-8471.1998.

Dustin, M. L. (2014) 'The Immunological Synapse', *Cancer Immunology Research*, 2(11), pp. 1023–1033. doi: 10.1158/2326-6066.CIR-14-0161.

Eberle, M. E. and Dalpke, A. H. (2012) 'Dectin-1 Stimulation Induces Suppressor of Cytokine Signaling 1, Thereby Modulating TLR Signaling and T Cell Responses', *The Journal of Immunology*, 188(11), pp. 5644–5654. doi: 10.4049/jimmunol.1103068.

Elowitz, M. B. (2002) 'Stochastic Gene Expression in a Single Cell', *Science*, 297(5584), pp. 1183–1186. doi: 10.1126/science.1070919.

Epstein, M. ., Achong, B. . and Barr, Y. . (1964) 'VIRUS PARTICLES IN CULTURED LYMPHOBLASTS FROM BURKITT'S LYMPHOMA', *The Lancet*, 283(7335), pp. 702–703. doi: 10.1016/S0140-6736(64)91524-7.

Epstein, M. A. and Barr, Y. M. (1965) 'Characteristics and Mode of Growth of a Tissue Culture Strain (EB1) of Human Lymphoblasts From Burkitt's Lymphoma2', *JNCI: Journal of the National Cancer Institute*, 34(2), pp. 231–240. doi: 10.1093/jnci/34.2.231.

Feinberg, H. *et al.* (2011) 'Structural Basis for Langerin Recognition of Diverse Pathogen and Mammalian Glycans through a Single Binding Site', *Journal of Molecular Biology*, 405(4), pp. 1027–1039. doi: 10.1016/j.jmb.2010.11.039.

Feinberg, H. *et al.* (2013) 'Common polymorphisms in human langerin change specificity for glycan ligands', *Journal of Biological Chemistry*, 288(52), pp. 36762–36771. doi: 10.1074/jbc.M113.528000.

Feinberg, H. *et al.* (2017) 'Mechanism of pathogen recognition by human dectin-2', *Journal of Biological Chemistry*, 292(32), pp. 13402–13414. doi: 10.1074/jbc.M117.799080.

Feng, S.-S. (2006) 'New-concept chemotherapy by nanoparticles of biodegradable polymers: where are we now?', *Nanomedicine*, 1(3), pp. 297–309. doi: 10.2217/17435889.1.3.297.

Fuster, M. M. and Esko, J. D. (2005) 'The sweet and sour of cancer: glycans as novel therapeutic targets', *Nature Reviews Cancer*, 5(7), pp. 526–542. doi: 10.1038/nrc1649.

Gabius, H.-J. (2015) 'The magic of the sugar code', *Trends in Biochemical Sciences*, 40(7), p. 341. doi: 10.1016/j.tibs.2015.04.003.

Garcia-Vallejo, J. J. and van Kooyk, Y. (2013) 'The physiological role of DC-SIGN: A tale of mice and men', *Trends in Immunology*, 34(10), pp. 482–486. doi: 10.1016/j.it.2013.03.001.

Geijtenbeek, T. B. H. *et al.* (2000) 'DC-SIGN, a Dendritic Cell–Specific HIV-1-Binding Protein that Enhances trans-Infection of T Cells', *Cell*, 100(5), pp. 587–597. doi: 10.1016/S0092-8674(00)80694-7.

Geijtenbeek, T. B. H. and Gringhuis, S. I. (2009) 'Signalling through C-type lectin receptors: shaping immune responses', *Nature Reviews Immunology*, 9(7), pp. 465–479. doi: 10.1038/nri2569.

Geijtenbeek, Teunis B. H. and Gringhuis, S. I. (2016) 'C-type lectin receptors in the control of T helper cell differentiation', *Nature Reviews Immunology*, 16(7), pp. 433–448. doi: 10.1038/nri.2016.55.

Geijtenbeek, Teunis B H and Gringhuis, S. I. (2016) 'C-type lectin receptors in the control of T helper cell differentiation', *Nature Reviews Immunology*, 16(7), pp. 433–448. doi: 10.1038/nri.2016.55.

Gerlach, D. *et al.* (2018) 'Methicillin-resistant Staphylococcus aureus alters cell wall glycosylation to evade immunity', *Nature*, 563(7733), pp. 705–709. doi: 10.1038/s41586-018-0730-x.

Girotti, M. R. *et al.* (2020) 'Sweetening the hallmarks of cancer: Galectins as multifunctional mediators of tumor progression', *Journal of Experimental Medicine*, 217(2). doi: 10.1084/jem.20182041.

Godwin, C. D., Gale, R. P. and Walter, R. B. (2017) 'Gemtuzumab ozogamicin in acute myeloid leukemia', *Leukemia*, 31(9), pp. 1855–1868. doi: 10.1038/leu.2017.187.

Goodridge, H. S. *et al.* (2011) 'Activation of the innate immune receptor Dectin-1 upon formation of a

"Phagocytic synapse"', *Nature*. doi: 10.1038/nature10071.

Goodridge, H. S., Wolf, A. J. and Underhill, D. M. (2009) 'β-glucan recognition by the innate immune system', *Immunological Reviews*, 230(1), pp. 38–50. doi: 10.1111/j.1600-065X.2009.00793.x.

Graham, L. M. *et al.* (2012) 'The C-type Lectin Receptor CLECSF8 (CLEC4D) Is Expressed by Myeloid Cells and Triggers Cellular Activation through Syk Kinase', *Journal of Biological Chemistry*, 287(31), pp. 25964–25974. doi: 10.1074/jbc.M112.384164.

Grell, M. *et al.* (1998) 'The type 1 receptor (CD120a) is the high-affinity receptor for soluble tumor necrosis factor', *Proceedings of the National Academy of Sciences*, 95(2), pp. 570–575. doi: 10.1073/pnas.95.2.570.

Gringhuis, S. I. *et al.* (2009) 'Carbohydrate-specific signaling through the DC-SIGN signalosome tailors immunity to Mycobacterium tuberculosis, HIV-1 and Helicobacter pylori', *Nature Immunology*, 10(10), pp. 1081–1088. doi: 10.1038/ni.1778.

Gringhuis, S. I. *et al.* (2014) 'Fucose-based PAMPs prime dendritic cells for follicular T helper cell polarization via DC-SIGN-dependent IL-27 production', *Nature Communications*, 5, p. 5074. doi: 10.1038/ncomms6074.

Gringhuis, S. I. and Geijtenbeek, T. B. H. (2010) 'Carbohydrate signaling by C-type lectin DC-SIGN affects NF-κB activity', *Methods in Enzymology*, 480(C), pp. 151–164. doi: 10.1016/S0076-6879(10)80008-4.

Gubin, A. N. *et al.* (1999) 'Stable expression of green fluorescent protein after liposomal transfection of K562 cells without selective growth conditions', *BioTechniques*, 27(6), pp. 1162–1170. doi: 10.2144/99276st02.

Guinn, M. T. *et al.* (2020) 'Observation and Control of Gene Expression Noise: Barrier Crossing Analogies Between Drug Resistance and Metastasis', *Frontiers in Genetics*, 11. doi: 10.3389/fgene.2020.586726.

Hanske, J. *et al.* (2016) 'Bacterial polysaccharide specificity of the pattern recognition receptor Langerin is highly species dependent', *Journal of Biological Chemistry* , 292(3), pp. 862–871. doi: 10.1074/jbc.M116.751750.

Hennet, T. and Cabalzar, J. (2015) 'Congenital disorders of glycosylation: a concise chart of glycocalyx dysfunction', *Trends in Biochemical Sciences*, 40(7), pp. 377–384. doi: 10.1016/j.tibs.2015.03.002.

Herre, J. (2004) 'Dectin-1 uses novel mechanisms for yeast phagocytosis in macrophages', *Blood*, 104(13), pp. 4038–4045. doi: 10.1182/blood-2004-03-1140.

Higashi, N. *et al.* (2002) 'The macrophage C-type lectin specific for galactose/N-acetylgalactosamine is an endocytic receptor expressed on monocyte-derived immature dendritic cells', *Journal of Biological Chemistry*, 277(23), pp. 20686–20693. doi: 10.1074/jbc.M202104200.

Hilfinger, A. and Paulsson, J. (2011) 'Separating intrinsic from extrinsic fluctuations in dynamic biological systems', *Proceedings of the National Academy of Sciences*, 108(29), pp. 12167–12172. doi: 10.1073/pnas.1018832108.

InvivoGen (2018) *Furfurman | Dectin-2 agonist from Malassezia | InvivoGen*. Available at: https://www.invivogen.com/furfurman (Accessed: 10 February 2021).

Ishikawa, E. *et al.* (2009) 'Direct recognition of the mycobacterial glycolipid, trehalose dimycolate, by C-type lectin Mincle', *Journal of Experimental Medicine*, 206(13), pp. 2879–2888. doi:

10.1084/jem.20091750.

Ishikawa, T. *et al.* (2013) 'Identification of Distinct Ligands for the C-type Lectin Receptors Mincle and Dectin-2 in the Pathogenic Fungus Malassezia', *Cell Host & Microbe*, 13(4), pp. 477–488. doi: 10.1016/j.chom.2013.03.008.

Jaiman, A. and Thattai, M. (2020) 'Golgi compartments enable controlled biomolecular assembly using promiscuous enzymes', *eLife*, 9. doi: 10.7554/eLife.49573.

de Jong, M. a W. P. *et al.* (2010) 'Herpes Simplex Virus Type 2 Enhances HIV-1 Susceptibility by Affecting Langerhans Cell Function', *The Journal of Immunology*, 185(3), pp. 1633–1641. doi: 10.4049/jimmunol.0904137.

Kawasaki, T. *et al.* (1986) 'Isolation and characterization of a receptor lectin specific for galactose/N-acetylgalactosamine from macrophages', *Carbohydrate Research*, 151(C), pp. 197–206. doi: 10.1016/S0008-6215(00)90340-9.

Kellogg, R. A. and Tay, S. (2015) 'Noise Facilitates Transcriptional Control under Dynamic Inputs', *Cell*, 160(3), pp. 381–392. doi: 10.1016/j.cell.2015.01.013.

Kerscher, B., Willment, J. A. and Brown, G. D. (2013) 'The Dectin-2 family of C-type lectin-like receptors: An update', *International Immunology*, pp. 271–277. doi: 10.1093/intimm/dxt006.

Khodarev, N. N., Roizman, B. and Weichselbaum, R. R. (2012) 'Molecular Pathways: Interferon/Stat1 Pathway: Role in the Tumor Resistance to Genotoxic Stress and Aggressive Growth', *Clinical Cancer Research*, 18(11), pp. 3015–3021. doi: 10.1158/1078-0432.CCR-11-3225.

Kissenpfennig, A. *et al.* (2005) 'Disruption of the langerin / CD207 Gene Abolishes Birbeck Granules without a Marked Loss of Langerhans Cell Function Disruption of the langerin / CD207 Gene Abolishes Birbeck Granules without a Marked Loss of Langerhans Cell Function', *Journal of Biological Chemistry*, 13(5), pp. 637–643. doi: 10.1128/MCB.25.1.88.

Kotler, M. and Steimle, S. (2018) *Ramot- Technology Transfer Company of Tel Aviv University*. Available at: https://ramot.org/news/2018/ramot-and-biontech-sign-license-agreement-to-use-novel-set-of-lipids-for-improved-mrna-delivery (Accessed: 16 February 2021).

Kranz, L. M. *et al.* (2016) 'Systemic RNA delivery to dendritic cells exploits antiviral defence for cancer immunotherapy', *Nature*, 534(7607), pp. 396–401. doi: 10.1038/nature18300.

Krutzik, P. O. and Nolan, G. P. (2003) 'Intracellular phospho-protein staining techniques for flow cytometry: Monitoring single cell signaling events', *Cytometry*, 55A(2), pp. 61–70. doi: 10.1002/cyto.a.10072.

Lambert, J.-C. *et al.* (2013) 'Meta-analysis of 74,046 individuals identifies 11 new susceptibility loci for Alzheimer's disease', *Nature Genetics*, 45(12), pp. 1452–1458. doi: 10.1038/ng.2802.

Levchenko, A. and Nemenman, I. (2014) 'Cellular noise and information transmission', *Current Opinion in Biotechnology*, 28, pp. 156–164. doi: 10.1016/j.copbio.2014.05.002.

Lombard, J. (2016) 'The multiple evolutionary origins of the eukaryotic N-glycosylation pathway', *Biology Direct*, 11(1), p. 36. doi: 10.1186/s13062-016-0137-2.

Lu, Q., Li, S. and Shao, F. (2015) 'Sweet Talk: Protein Glycosylation in Bacterial Interaction With the Host', *Trends in Microbiology*, 23(10), pp. 630–641. doi: 10.1016/j.tim.2015.07.003.

Magdanova, L. A. and Golyasnaya, N. V. (2013) 'Heterogeneity as an adaptive trait of microbial populations', *Microbiology*, 82(1), pp. 1–10. doi: 10.1134/S0026261713010074.

Matsumoto, M. *et al.* (1999) 'A novel LPS-inducible C-type lectin is a transcriptional target of NF-IL6 in macrophages.', *Journal of immunology (Baltimore, Md. : 1950)*, 163(9), pp. 5039–48. Available at: http://www.ncbi.nlm.nih.gov/pubmed/10528209.

McGreal, E. P. *et al.* (2006) 'The carbohydrate-recognition domain of Dectin-2 is a C-type lectin with specificity for high mannose', *Glycobiology*, 16(5), pp. 422–430. doi: 10.1093/glycob/cwj077.

Mehta, A. *et al.* (2012) 'Increased Levels of Tetra-antennary N -Linked Glycan but Not Core Fucosylation Are Associated with Hepatocellular Carcinoma Tissue', *Cancer Epidemiology Biomarkers & Prevention*, 21(6), pp. 925–933. doi: 10.1158/1055-9965.EPI-11-1183.

Mian, I. S. and Rose, C. (2011) 'Communication theory and multicellular biology', *Integrative Biology*, 3(4), p. 350. doi: 10.1039/c0ib00117a.

Mistretta, N. *et al.* (2019) 'Glycosylation of Staphylococcus aureus cell wall teichoic acid is influenced by environmental conditions', *Scientific Reports*, 9(1), p. 3212. doi: 10.1038/s41598-019-39929-1.

Miyake, Y. *et al.* (2013) 'C-type Lectin MCL Is an FcRγ-Coupled Receptor that Mediates the Adjuvanticity of Mycobacterial Cord Factor', *Immunity*, 38(5), pp. 1050–1062. doi: 10.1016/j.immuni.2013.03.010.

Miyake, Y., Oh-hora, M. and Yamasaki, S. (2015) 'C-Type Lectin Receptor MCL Facilitates Mincle Expression and Signaling through Complex Formation', *The Journal of Immunology*, 194(11), pp. 5366–5374. doi: 10.4049/jimmunol.1402429.

Mócsai, A., Ruland, J. and Tybulewicz, V. L. J. (2010) 'The SYK tyrosine kinase: a crucial player in diverse biological functions', *Nature Reviews Immunology*, 10(6), pp. 387–402. doi: 10.1038/nri2765.

Moran, A. (1996) 'Molecular mimicry of host structures by bacterial lipopolysaccharides and its contribution to disease', *FEMS Immunology and Medical Microbiology*, 16(2), pp. 105–115. doi: 10.1016/S0928-8244(96)00072-7.

Motulsky, H. (GraphPad P. (2019) *GraphPad Prism 8 Curve Fitting Guide - log(agonist) vs. normalized response -- Variable slope*. Available at: https://www.graphpad.com/guides/prism/latest/curve-fitting/REG_DR_stim_variable_2.htm (Accessed: 10 February 2021).

Napoletano, C. *et al.* (2007) 'Tumor-Associated Tn-MUC1 Glycoform Is Internalized through the Macrophage Galactose-Type C-Type Lectin and Delivered to the HLA Class I and II Compartments in Dendritic Cells', *Cancer Research*, 67(17), pp. 8358–8367. doi: 10.1158/0008-5472.CAN-07-1035.

Napoletano, C. *et al.* (2012) 'Targeting of macrophage galactose-type C-type lectin (MGL) induces DC signaling and activation', *European Journal of Immunology*, 42(4), pp. 936–945. doi: 10.1002/eji.201142086.

Negi, S. *et al.* (2019) 'Curdlan Limits Mycobacterium tuberculosis Survival Through STAT-1 Regulated Nitric Oxide Production', *Frontiers in Microbiology*, 10. doi: 10.3389/fmicb.2019.01173.

Ostrop, J. *et al.* (2015) 'Contribution of MINCLE–SYK Signaling to Activation of Primary Human APCs by Mycobacterial Cord Factor and the Novel Adjuvant TDB', *The Journal of Immunology*, 195(5), pp. 2417–2428. doi: 10.4049/jimmunol.1500102.

Ostrop, J. and Lang, R. (2017) 'Contact, Collaboration, and Conflict: Signal Integration of Syk-Coupled C-

Type Lectin Receptors', *The Journal of Immunology*, 198(4), pp. 1403–1414. doi: 10.4049/jimmunol.1601665.

Passos da Silva, D. *et al.* (2019) 'The Pseudomonas aeruginosa lectin LecB binds to the exopolysaccharide Psl and stabilizes the biofilm matrix', *Nature Communications*, 10(1), p. 2183. doi: 10.1038/s41467-019-10201-4.

Paternoster, L. *et al.* (2015) 'Multi-ancestry genome-wide association study of 21,000 cases and 95,000 controls identifies new risk loci for atopic dermatitis', *Nature Genetics*, 47(12), pp. 1449–1456. doi: 10.1038/ng.3424.

Patin, E. C., Thompson, A. and Orr, S. J. (2019) 'Pattern recognition receptors in fungal immunity', *Seminars in Cell & Developmental Biology*, 89, pp. 24–33. doi: 10.1016/j.semcdb.2018.03.003.

Paulsen, S. M. *et al.* (2003) 'In vivo effects of β-glucan and LPS on regulation of lysozyme activity and mRNA expression in Atlantic salmon (Salmo salar L.)', *Fish & Shellfish Immunology*, 14(1), pp. 39–54. doi: 10.1006/fsim.2002.0416.

van der Peet, P. L. *et al.* (2015) 'Corynomycolic acid-containing glycolipids signal through the pattern recognition receptor Mincle', *Chemical Communications*, 51(24), pp. 5100–5103. doi: 10.1039/C5CC00085H.

Pinho, S. S. and Reis, C. A. (2015) 'Glycosylation in cancer: mechanisms and clinical implications', *Nature Reviews Cancer*, 15(9), pp. 540–555. doi: 10.1038/nrc3982.

Poole, J. *et al.* (2018) 'Glycointeractions in bacterial pathogenesis', *Nature Reviews Microbiology*, 16(7), pp. 440–452. doi: 10.1038/s41579-018-0007-2.

Qin, F., Aachmann, F. L. and Christensen, B. E. (2012) 'Chain length distribution and aggregation of branched (1→3)-β-d-glucans from Saccharomyces cerevisae', *Carbohydrate Polymers*, 90(2), pp. 1092–1099. doi: 10.1016/j.carbpol.2012.06.048.

Raetz, C. R. H. and Whitfield, C. (2002) 'Lipopolysaccharide Endotoxins', *Annual Review of Biochemistry*, 71(1), pp. 635–700. doi: 10.1146/annurev.biochem.71.110601.135414.

Raj, A. and van Oudenaarden, A. (2008) 'Nature, Nurture, or Chance: Stochastic Gene Expression and Its Consequences', *Cell*, 135(2), pp. 216–226. doi: 10.1016/j.cell.2008.09.050.

van Reeuwijk, J. (2005) 'POMT2 mutations cause -dystroglycan hypoglycosylation and Walker-Warburg syndrome', *Journal of Medical Genetics*, 42(12), pp. 907–912. doi: 10.1136/jmg.2005.031963.

Reitz, C. (2014) 'Genetic loci associated with Alzheimer's disease', *Future Neurology*, 9(2), pp. 119–122. doi: 10.2217/fnl.14.1.

Rhee, A., Cheong, R. and Levchenko, A. (2012) 'The application of information theory to biochemical signaling systems', *Physical Biology*, 9(4), p. 045011. doi: 10.1088/1478-3975/9/4/045011.

Ribet, D. and Cossart, P. (2010) 'Post-translational modifications in host cells during bacterial infection', *FEBS Letters*, 584(13), pp. 2748–2758. doi: 10.1016/j.febslet.2010.05.012.

Richardson, M. B. and Williams, S. J. (2014) 'MCL and Mincle: C-Type Lectin Receptors That Sense Damaged Self and Pathogen-Associated Molecular Patterns', *Frontiers in Immunology*, 5. doi: 10.3389/fimmu.2014.00288.

Riddy, D. M. *et al.* (2018) 'Comparative genotypic and phenotypic analysis of human peripheral blood monocytes and surrogate monocyte-like cell lines commonly used in metabolic disease research', *PLOS ONE*. Edited by G. Zissel, 13(5), p. e0197177. doi: 10.1371/journal.pone.0197177.

Robinson, M. J. *et al.* (2009) 'Dectin-2 is a Syk-coupled pattern recognition receptor crucial for Th17 responses to fungal infection', *Journal of Experimental Medicine*, 206(9), pp. 2037–2051. doi: 10.1084/jem.20082818.

RodrÍguez, E., Schetters, S. T. T. and van Kooyk, Y. (2018) 'The tumour glyco-code as a novel immune checkpoint for immunotherapy', *Nature Reviews Immunology*, 18(3), pp. 204–211. doi: 10.1038/nri.2018.3.

Rogers, N. C. *et al.* (2005) 'Syk-Dependent Cytokine Induction by Dectin-1 Reveals a Novel Pattern Recognition Pathway for C Type Lectins', *Immunity*, 22(4), pp. 507–517. doi: 10.1016/j.immuni.2005.03.004.

Roscioli, T. *et al.* (2012) 'Mutations in ISPD cause Walker-Warburg syndrome and defective glycosylation of α-dystroglycan', *Nature Genetics*, 44(5), pp. 581–585. doi: 10.1038/ng.2253.

Russell, W. C. *et al.* (1977) 'Characteristics of a Human Cell Line Transformed by DNA from Human Adenovirus Type 5', *Journal of General Virology*, 36(1), pp. 59–72. doi: 10.1099/0022-1317-36-1-59.

Sahin, U., Karikó, K. and Türeci, Ö. (2014) 'mRNA-based therapeutics — developing a new class of drugs', *Nature Reviews Drug Discovery*, 13(10), pp. 759–780. doi: 10.1038/nrd4278.

Sancho, D. and Reis e Sousa, C. (2012) 'Signaling by Myeloid C-Type Lectin Receptors in Immunity and Homeostasis', *Annual Review of Immunology*, 30(1), pp. 491–529. doi: 10.1146/annurev-immunol-031210-101352.

dos Santos, L. R. *et al.* (2017) 'Validating GWAS Variants from Microglial Genes Implicated in Alzheimer's Disease', *Journal of Molecular Neuroscience*, 62(2), pp. 215–221. doi: 10.1007/s12031-017-0928-7.

Sato, K. *et al.* (2006) 'Dectin-2 is a pattern recognition receptor for fungi that couples with the Fc receptor γ chain to induce innate immune responses', *Journal of Biological Chemistry*, 281(50), pp. 38854–38866. doi: 10.1074/jbc.M606542200.

Schäffer, C. and Messner, P. (2016) 'Emerging facets of prokaryotic glycosylation', *FEMS Microbiology Reviews*. Edited by M. Pohlschroder, 41(1), pp. 49–91. doi: 10.1093/femsre/fuw036.

Schulze, J. *et al.* (2019) 'A Liposomal Platform for Delivery of a Protein Antigen to Langerin-Expressing Cells.', *Biochemistry*, 58(21), pp. 2576–2580. doi: 10.1021/acs.biochem.9b00402.

Schwarz, F. and Aebi, M. (2011) 'Mechanisms and principles of N-linked protein glycosylation', *Current Opinion in Structural Biology*, pp. 576–582. doi: 10.1016/j.sbi.2011.08.005.

Šebestík, J., Reiniš, M. and Ježek, J. (2012) 'Sugar Code (Glycocode)', in *Biomedical Applications of Peptide-, Glyco- and Glycopeptide Dendrimers, and Analogous Dendrimeric Structures*. Vienna: Springer Vienna, pp. 23–27. doi: 10.1007/978-3-7091-1206-9_3.

Selimkhanov, J. *et al.* (2014) 'Accurate information transmission through dynamic biochemical signaling networks', *Science*, 346(6215), pp. 1370–1373. doi: 10.1126/science.1254933.

Shannon, C. E. (1948) 'A Mathematical Theory of Communication', *Bell System Technical Journal*, 27(3), pp. 379–423. doi: 10.1002/j.1538-7305.1948.tb01338.x.

Shannon, C. E. (1949) 'Communication in the Presence of Noise', *Proceedings of the IRE*, 37(1), pp. 10–21. doi: 10.1109/JRPROC.1949.232969.

Shcherbakova, D. M. *et al.* (2012) 'An Orange Fluorescent Protein with a Large Stokes Shift for Single-Excitation Multicolor FCCS and FRET Imaging', *Journal of the American Chemical Society*, 134(18), pp. 7913–7923. doi: 10.1021/ja3018972.

Singh, A. and Soltani, M. (2013) 'Quantifying Intrinsic and Extrinsic Variability in Stochastic Gene Expression Models', *PLoS ONE*. Edited by J. Vera, 8(12), p. e84301. doi: 10.1371/journal.pone.0084301.

Spaulding, C. N. *et al.* (2017) 'Selective depletion of uropathogenic E. coli from the gut by a FimH antagonist', *Nature*, 546(7659), pp. 528–532. doi: 10.1038/nature22972.

Stambach, N. S. and Taylor, M. E. (2003) 'Characterization of carbohydrate recognition by langerin, a C-type lectin of Langerhans cell', *Glycobiology*, 13(5), pp. 401–410. doi: 10.1093/glycob/cwg045.

Stavenhagen, K. *et al.* (2019) 'Site-specific N- and O-glycosylation analysis of atacicept', *mAbs*. doi: 10.1080/19420862.2019.1630218.

Suderman, R. *et al.* (2017) 'Fundamental trade-offs between information flow in single cells and cellular populations', *Proceedings of the National Academy of Sciences*, 114(22), pp. 5755–5760. doi: 10.1073/pnas.1615660114.

Sundström, C. and Nilsson, K. (1976) 'Establishment and characterization of a human histiocytic lymphoma cell line (U-937)', *International Journal of Cancer*, 17(5), pp. 565–577. doi: 10.1002/ijc.2910170504.

Szymanski, C. M. *et al.* (1999) 'Evidence for a system of general protein glycosylation in Campylobacter jejuni.', *Molecular microbiology*, 32(5), pp. 1022–1030. Available at: http://www.ncbi.nlm.nih.gov/pubmed/10361304.

Tacken, P. J. *et al.* (2012) 'Antibodies and carbohydrate ligands binding to DC-SIGN differentially modulate receptor trafficking', *European Journal of Immunology*, 42(8), pp. 1989–1998. doi: 10.1002/eji.201142258.

Tacken, P. J. and Figdor, C. G. (2011) 'Targeted antigen delivery and activation of dendritic cells in vivo: Steps towards cost effective vaccines', *Seminars in Immunology*, pp. 12–20. doi: 10.1016/j.smim.2011.01.001.

Taylor, P. R. *et al.* (2002) 'The β-Glucan Receptor, Dectin-1, Is Predominantly Expressed on the Surface of Cells of the Monocyte/Macrophage and Neutrophil Lineages', *The Journal of Immunology*, 169(7), pp. 3876–3882. doi: 10.4049/jimmunol.169.7.3876.

Thépaut, M. *et al.* (2020) 'DC/L-SIGN recognition of spike glycoprotein promotes SARS-CoV-2 trans-infection and can be inhibited by a glycomimetic antagonist', *bioRxiv*, p. 2020.08.09.242917. doi: 10.1101/2020.08.09.242917.

Thomas, P. J. (2011) 'Every Bit Counts', *Science*, 334(6054), pp. 321–322. doi: 10.1126/science.1213834.

Thomas, P. and Smart, T. G. (2005) 'HEK293 cell line: A vehicle for the expression of recombinant proteins', *Journal of Pharmacological and Toxicological Methods*, 51(3), pp. 187–200. doi: 10.1016/j.vascn.2004.08.014.

Totté, J. E. E. *et al.* (2016) 'Prevalence and odds of Staphylococcus aureus carriage in atopic dermatitis: a

systematic review and meta-analysis', *British Journal of Dermatology*. doi: 10.1111/bjd.14566.

Toyonaga, K., Miyake, Y. and Yamasaki, S. (2014) 'Characterization of the Receptors for Mycobacterial Cord Factor in Guinea Pig', *PLoS ONE*. Edited by Y. Hoshino, 9(2), p. e88747. doi: 10.1371/journal.pone.0088747.

Tsuchiya, S. *et al.* (1980) 'Establishment and characterization of a human acute monocytic leukemia cell line (THP-1)', *International Journal of Cancer*, 26(2), pp. 171–176. doi: 10.1002/ijc.2910260208.

Tsuchiya, S. *et al.* (1982) 'Induction of maturation in cultured human monocytic leukemia cells by a phorbol diester.', *Cancer research*, 42(4), pp. 1530–6. Available at: http://www.ncbi.nlm.nih.gov/pubmed/6949641.

Underhill, D. M. and Goodridge, H. S. (2007) 'The many faces of ITAMs', *Trends in Immunology*, 28(2), pp. 66–73. doi: 10.1016/j.it.2006.12.004.

Valladeau, J. *et al.* (2000) 'Langerin, a Novel C-Type Lectin Specific to Langerhans Cells, Is an Endocytic Receptor that Induces the Formation of Birbeck Granules', *Immunity*, 12(1), pp. 71–81. doi: 10.1016/S1074-7613(00)80160-0.

Varki, A. *et al.* (2017) *Essentials of glycobiology, third edition*, *Cold Spring Harbor Laboratory Press*.

Varki, A., Schnaar, R. L. and Schauer, R. (2015) *Sialic Acids and Other Nonulosonic Acids*, *Essentials of Glycobiology*.

Veiga, N. *et al.* (2018) 'Cell specific delivery of modified mRNA expressing therapeutic proteins to leukocytes', *Nature Communications*, 9(1), p. 4493. doi: 10.1038/s41467-018-06936-1.

Wadhwa, A. *et al.* (2020) 'Opportunities and Challenges in the Delivery of mRNA-Based Vaccines', *Pharmaceutics*, 12(2), p. 102. doi: 10.3390/pharmaceutics12020102.

Wamhoff, E. C. *et al.* (2019) 'A Specific, Glycomimetic Langerin Ligand for Human Langerhans Cell Targeting', *ACS Central Science*, 5(5), pp. 808–820. doi: 10.1021/acscentsci.9b00093.

Ward, E. M. *et al.* (2006) 'Polymorphisms in Human Langerin Affect Stability and Sugar Binding Activity', *Journal of Biological Chemistry*, 281(22), pp. 15450–15456. doi: 10.1074/jbc.M511502200.

Werninghaus, K. *et al.* (2009) 'Adjuvanticity of a synthetic cord factor analogue for subunit Mycobacterium tuberculosis vaccination requires FcRγ–Syk–Card9–dependent innate immune activation', *Journal of Experimental Medicine*, 206(1), pp. 89–97. doi: 10.1084/jem.20081445.

Werz, D. B. *et al.* (2007) 'Exploring the Structural Diversity of Mammalian Carbohydrates ("Glycospace") by Statistical Databank Analysis', *ACS Chemical Biology*, 2(10), pp. 685–691. doi: 10.1021/cb700178s.

Williams, S. J. (2017) 'Sensing lipids with Mincle: Structure and function', *Frontiers in Immunology*, 8(NOV). doi: 10.3389/fimmu.2017.01662.

de Witte, L. *et al.* (2007) 'Langerin is a natural barrier to HIV-1 transmission by Langerhans cells.', *Nature medicine*, 13(3), pp. 367–371. doi: 10.1038/nm1541.

Woods, E. C. *et al.* (2017) 'A bulky glycocalyx fosters metastasis formation by promoting G1 cell cycle progression', *eLife*, 6. doi: 10.7554/eLife.25752.

Wortzel, I. and Seger, R. (2011) 'The ERK Cascade: Distinct Functions within Various Subcellular

Organelles', *Genes & Cancer*, 2(3), pp. 195–209. doi: 10.1177/1947601911407328.

Wu, D. *et al.* (2018) 'N-glycan microheterogeneity regulates interactions of plasma proteins', *Proceedings of the National Academy of Sciences*, 115(35), pp. 8763–8768. doi: 10.1073/pnas.1807439115.

Wu, S. (2020) 'Progress and Concept for COVID-19 Vaccine Development', *Biotechnology Journal*, 15(6), p. 2000147. doi: 10.1002/biot.202000147.

Xu, X. *et al.* (2019) 'Delivery of CRISPR/Cas9 for therapeutic genome editing', *The Journal of Gene Medicine*, 21(7), p. e3107. doi: 10.1002/jgm.3107.

Yamasaki, S. *et al.* (2008) 'Mincle is an ITAM-coupled activating receptor that senses damaged cells', *Nature Immunology*, 9(10), pp. 1179–1188. doi: 10.1038/ni.1651.

Yamasaki, S. *et al.* (2009) 'C-type lectin Mincle is an activating receptor for pathogenic fungus, Malassezia', *Proceedings of the National Academy of Sciences*, 106(6), pp. 1897–1902. doi: 10.1073/pnas.0805177106.

Yonekawa, A. *et al.* (2014) 'Dectin-2 is a direct receptor for mannose-capped lipoarabinomannan of mycobacteria', *Immunity*, 41(3), pp. 402–413. doi: 10.1016/j.immuni.2014.08.005.

Yuki, N. and Koga, M. (2006) 'Bacterial infections in Guillain-Barré and Fisher syndromes', *Current Opinion in Neurology*, 19(5), pp. 451–457. doi: 10.1097/01.wco.0000245367.36576.e9.

Zelensky, A. N. and Gready, J. E. (2005) 'The C-type lectin-like domain superfamily', *FEBS Journal*, 272(24), pp. 6179–6217. doi: 10.1111/j.1742-4658.2005.05031.x.

Zeng, C. and Biemann, K. (1999) 'Determination of N-linked glycosylation of yeast external invertase by matrix-assisted laser desorption/ionization time-of-flight mass spectrometry', *Journal of Mass Spectrometry*, 34(4), pp. 311–329. doi: 10.1002/(SICI)1096-9888(199904)34:4<311::AID-JMS773>3.0.CO;2-F.

Zhang, Q. *et al.* (2017) 'NF-κB Dynamics Discriminate between TNF Doses in Single Cells', *Cell Systems*, 5(6), pp. 638-645.e5. doi: 10.1016/j.cels.2017.10.011.

Zhao, L. (2019) 'CD33 in Alzheimer's Disease – Biology, Pathogenesis, and Therapeutics: A Mini-Review', *Gerontology*, 65(4), pp. 323–331. doi: 10.1159/000492596.

Zhong, X.-P. *et al.* (2011) 'Receptor signaling in immune cell development and function', *Immunologic Research*, 49(1–3), pp. 109–123. doi: 10.1007/s12026-010-8175-9.

Zhou, M. N. *et al.* (2018) 'N -Carboxyanhydride Polymerization of Glycopolypeptides That Activate Antigen-Presenting Cells through Dectin-1 and Dectin-2', *Angewandte Chemie International Edition*, 57(12), pp. 3137–3142. doi: 10.1002/anie.201713075.

Zhu, L.-L. *et al.* (2013) 'C-Type Lectin Receptors Dectin-3 and Dectin-2 Form a Heterodimeric Pattern-Recognition Receptor for Host Defense against Fungal Infection', *Immunity*, 39(2), pp. 324–334. doi: 10.1016/j.immuni.2013.05.017.

Zufferey, R. *et al.* (1998) 'Self-inactivating lentivirus vector for safe and efficient in vivo gene delivery.', *Journal of virology*, 72(12), pp. 9873–9880. doi: 99030895.